OAK RIDGE NATIONAL LABORATORY

operated by

UNION CARBIDE CORPORATION

for the

U.S. ATOMIC ENERGY COMMISSION

ORNL - TM - 65

135

UNIT OPERATIONS SECTION MONTHLY PROGRESS REPORT

AUGUST 1961

ORNL-TM-65

UNIT OPERATIONS SECTION MONTHLY PROGRESS REPORT

August 1961

CHEMICAL TECHNOLOGY DIVISION

M. E. Whatley

P. A. Haas
R. W. Horton
A. D. Ryon
J. C. Suddath
C. D. Watson

Date Issued

MAR - 1 1962

OAK RIDGE NATIONAL LABORATORY
Oak Ridge, Tennessee
Operated By
UNION CARBIDE CORPORATION
for the
U. S. Atomic Energy Commission

ABSTRACT

Engineering studies of a 6-in.-ID countercurrent foam column were started. The capacity of Mark II Stacked Clone Contactor was found to be limited by gradually increasing entrainment. Thoria sols were prepared from trough denitrator products in a conical bottom tank agitated by circulation through an external centrifugal pump. Experimental results agreed favorably with predicted results for the reaction of CO with CuO and for the simultaneous reactions of H_2 and CO with CuO. In a 2-in. dissolver, Modified Zirflex dissolution rates of Zircaloy-2 increased non-linearly with F/S. The 250 ton prototype shear has been received and installed. Priorities were established for development work on graphite fuels. A total of 5 SRE Core I fuel clusters were mechanically dejacketed from the second carrier shipment of SRE Core I fuel. Degradation of NaK to a solid or waxy form required that the slugs be ejected by the jackscrew. The NaK disposal system operated satisfactorily for the last ~3,000 ml of NaK. A procedure for estimating the temperature rise of spent reactor fuels during shipping gives reasonably good results. A pulse column was operated with the light phase continuous using an external phase separator. Zirconium oxide plates were dissolved by HF in molten salt at rates at least twice as great as for Zircaloy-2 metal in the same system. Magnesium additive to high sulfate Purex waste was tested.

CONTENTS

Previous Reports in this Series for the Year 1961

January	ORNL CF 61-1-27
February	ORNL CF 61-2-65
March	ORNL CF 61-3-67
April	ORNL-TM-32
May	ORNL-TM-33
June	ORNL-TM-34
July	ORNL-TM-35

All previous reports in this series are listed in the June 1961 report, ORNL-TM-34, from the beginning, December 1954.

SUMMARY

1.0 CHEMICAL ENGINEERING STUDIES

Foam Separation

Engineering studies of a 6-in.-ID countercurrent foam-liquid column were started using isotopic exchange between Sr-89 tracer and inactive Sr. Dodecyl benzene sulfonate in 10^{-3} M NaOH was used as the surfactant complexing agent and foaming agent. Surfactant material balances from analyses by ultraviolet absorption were excellent, but gross β material balances were only 60-70%. Based on the liquid phase, and considering the bottom of the column as one theoretical stage, 3.2 to 4.3 transfer units were obtained for 18 inches of countercurrent foam-liquid contact. These values are uncertain due to the poor tracer balance and a non-optimum flow ratio resulting in pinching of the operating and equilibrium line.

2.0 FISSION PRODUCT RECOVERY

The capacity limit of Mark II Stacked Clone Contactor processing 17% TBP in Amsco against 1 M $NaNO_3$ was found to be determined by gradually increasing entrainment of organic in the aqueous rather than by a sudden onset of flooding. The per cent of the organic fed which entrained with the aqueous followed the relation: $D = 0.21\ A/O\ (A + O)^{1.5}$ where A and O are feed rates of aqueous and organic in liter/min. For example, the organic entrainment is 3% at a total flow of 2.0 liter/min and A/O of 5.

3.0 FUEL CYCLE DEVELOPMENT

A conical bottom tank with recycle by a centrifugal pump appears adequate for dispersion of trough denitrator products into thoria sols. Sampling and analyses of both powders and thoria sols were reproducible within the 1% limit necessary for a fabrication facility. Losses during routine transfers of one batch through dispersion, drying, and firing steps totaled 2.37%.

4.0 GCR COOLANT PURIFICATION STUDIES

Experimental results agreed favorably with predicted results for the reaction of CO with CuO and for the simultaneous reactions of H_2 and CO with CuO. The predicted results were based on a finite difference solution of the mathematical model for external and internal diffusion of H_2 and CO controlling.

5.0 POWER REACTOR FUEL PROCESSING

5.1 Continuous Modified Zirflex

Efforts are being made to adapt the Modified Zirflex process for continuous dissolution in order to take advantage of the increased throughputs made possible by this method of operation. In a 2-in. dissolver, dissolution rates of Zircaloy-2 increased non-linearly with F/S (feed rate/surface area) ratio such that lower Zr loadings were obtained as reaction rates increased.

Desirable loadings of $\geq$ 80 g Zircaloy-2/liter were obtained only with F/S $\leq$ 0.06 which produced reaction rates $\leq$ 5 mg/cm^2-min. One run, in 6-in. equipment, having a 1 hr period of steady-state operation used as dissolvent 6.5 M NH_4F-0.6 M NH_4NO_3-0.1 M H_2O_2 and gave an average reaction rate of 5.6 mg/cm^2-min (specimen area constant throughout the run) at F/S = 0.08 producing an effluent containing 70 g Zircaloy-2/liter.

5.2 Shear and Leach

The 250 ton prototype shear has been received and installed on the third floor of Bldg. 4505. The shear has been checked out and operated.

Scouting tests operating the modified leacher as a conveyor feeder at ~2 rpm and 15 degrees of inclination resulted in less than 5% backmixing when using a 2.5 liter batch of stainless steel rods per flight and no backmixing with a 2.0 liter batch.

A single batch dissolution of ~600 g of crushed UO_2-ThO_2 pellets resulted in 73% dissolution in 6-1/2 hrs.

5.3 U-C Fuel Processing

Priorities established for Unit Operations development work on graphite fuels were (1) demonstration of a semicontinuous aqueous flowsheet for graphite fuels containing uncoated UC_2 or UO_2, (2) combustion-dissolution studies on elements fueled with pyrolytic carbon-coated particles, and (3) fine grinding work on fuel containing alumina-coated or pyrolytic carbon-coated particles.

5.4 SRE Dejacketing Studies

A total of 5 SRE Core I fuel clusters were mechanically dejacketed from the second carrier shipment of SRE Core I fuel. An average dejacketing rate of 4.8 kg U/hr was attained ignoring down time for repairs. An overall rate of ~2.4 kg U/hr was maintained despite the loss of 3.5 shifts, 28 hrs, for repairs and adjustment. One cluster of 7 fuel rods contained 4 rods that required tedious auxiliary dejacketing methods because of waxy, oxidized NaK and swollen slugs. One of these slugs, originally 3/4-in.-OD x 6-in.-long, had grown 6.25% in length and 1.47 to 5.2% in diameter.

Micrometer measurements made of 5 jackets show an expansion of from 7 to 20 mils in diameter occurs by an applied internal hydraulic pressure of 1500 psig. This expansion should free the slugs so that they could be flushed out easily by hydraulic pressure. However, due to degradation of NaK to a solid or waxy form, the slugs could be ejected only by the jackscrew or cutting the jacket at the slug junctures, followed by slitting and prying of the jackets from the uranium slugs.

The down time for repair of equipment, slug canner, crane, General Mills manipulator and pusher cylinder was 28 hrs, or 3.5 shifts. The slug canning machine required ~16 hrs for decontamination, removal from the cell and necessary adjustments and repairs. The crane, General Mills manipulator and pusher cylinder were repaired in a single campaign over a period of 12 hrs.

The NaK disposal system operated satisfactorily while reacting ~3,000 ml of NaK eutectic bonding agent discharged during the dejacketing operations.

6.0 REACTOR EVALUATION STUDIES

Heat Transfer from Spent Reactor Fuels during Shipping

Experimental measurements of temperature rises in electrically heated mock fuel elements in a horizontal simulated shipping carrier have been continued. A procedure for estimating the temperature rise based upon radiant heat transfer has been shown to give answers having average differences from measured temperatures of less than 15°C for fuel bundles containing up to 64 tubes and heat generation rates up to 0.0514 watts/tube-cm.

7.0 SOLVENT EXTRACTION STUDIES

Operation of a pulse column with the light phase continuous using an external phase separator and an air lift to recycle the light phase to the column was successfully demonstrated. The main problem was a tendency for the flows to cycle; this was minimized by increased light phase recycle rate and selection of slow control modes of reset and gain.

8.0 VOLATILITY

Zirconium oxide plates were dissolved by HF in molten salt at rates of 1.24 mg/(cm^2)(min) and 3.13 mg/(cm^2)(min). The corresponding HF rates were 0.25 lbs/hr and 1.5 lbs/hr. These rates are at least twice as great as for Zircaloy-2 metal dissolution in the same system.

9.0 WASTE PROCESSING

Magnesium additive to high sulfate Purex waste was tested as a simulated feed to the close-coupled evaporator-calciner complex. Although high corrosion had occurred previously (R-37), only a little pitting was observed on the inside pot wall after this test. Both ruthenium and sulfate were confined to the evaporator-calciner complex, with less than 1% escaping with the evaporator condensate.

1.0 CHEMICAL ENGINEERING STUDIES

1.1 Foam Separation - P. A. Haas, W. W. Wall, Jr.

Experimental studies were started on an engineering development program for countercurrent foam columns (as outlined in February 1961 Unit Operations Monthly Progress Report). The immediate objective is to study the engineering variables controlling the performance of a countercurrent foam-liquid separation. A future objective will be to decontaminate dilute wastes by using foam columns with complexing surfactants to remove Sr, Cs, or other radioactive elements.

Interpretation of foam column performance is complicated by the chemical and physical characteristics of the system. The "surface phase" flow rates are estimated from gas flow and bubble size and tend to decrease up the column as bubbles collapse. Some of the liquid phase always leaves the column with the "surface phase" removed as product or samples. Surface-liquid equilibrium is complicated by the effects of pH, concentrations, and equilibrium between the surfactant and the ion to be complexed. The initial experiments and calculations were aimed at selecting conditions and procedures to eliminate chemical effects and control physical effects in order to simplify the interpretation of results.

Selection of Chemical Conditions. Chemical effects on foam column performance may be avoided by having pH and chemical concentrations which are not a function of column position. This is possible for isotopic exchange between radioactive and non-radioactive surfactant. An isotopic equilibrium factor of unity may be assumed; i.e., radioactive surfactant/non-radioactive surfactant mole ratios at equilibrium are equal in the liquid and at the surface.

Radioactively traced surfactants satisfactory in all respects are not available. Neutron activation of non-active molecules is not practical because of bond ruptures from the capture γ recoils. Compounds containing S-35 are available (for example, sodium lauryl sulfate), but the costs would be appreciable and the 0.17 Mev β requires special counting techniques. Use of a radioactive ion complexed by the surfactant requires a knowledge of the complexing equilibrium.

Use of Sr-89 tracer with a purified dodecylbenzenesulfonate was selected as the best compromise system. By using a large excess of the surfactant, essentially 100% complexing of the Sr may be assumed.* The Sr tracer is carrier free and relatively cheap ($2.00/mc). The 1.46 Mev β of 51 day half life gives an easy activity to count. One disadvantage is the presence of 1 to 10% of Sr-90 and Y-90 activity.

The liquid concentrations selected for initial runs were:

10^{-3} M NaOH

10^{-3} to 10^{-4} M dodecylbenzenesulfulate as the sodium salt

Sr/surfactant ratio of 5×10^{-3} g/g or about 1/45 mole/mole

---

* Personal communication with Ernesto Schonfeld, ORNL, June 1961.

Complexing of the Sr is poor at low pH and the NaOH was added to give a pH of 9.5 for 5×10^{-4} M surfactant. The Sr concentrations are a compromise since low concentrations result in excessive surface adsorption effects while high concentrations result in significant amounts of uncomplexed Sr.

Methods of Analyses. The concentrations of surfactant-radioactive Sr complexes are obtained from gross β counts. The total surfactant concentrations may be calculated from liquid-surface equilibrium data if surfactant concentrations are not functions of column position. The dodecylbenzenesulfonate surfactant was selected* in order to use ultraviolet absorption of the benzene ring as a measure of concentrations. The calibration curve for 2230 A (Figure 1.1) gave excellent material balance for the initial two flow ratios for which analyses were made. An initial attempt to use the smaller peak at 2610 A with variable NaOH concentrations did not give usable results.

Several refinements of the gross β counting may be necessary. Special low level counting will be necessary for accurate results below 10^2 c/min cc. Recounts after a decay period should show if separation of the Sr and the Y radioactivity occurs. Chemical separation of the Sr and Y is possible although the Y-90 will grow back from the Sr-90.

Gas Dispersion Methods. Results with the sintered stainless steel gas dispersion spargers along with laboratory results show excessive variations in the bubble sizes and smaller than optimum bubbles. Bubble size distributions from photographs (Figure 1.2) are point values at the column walls since increasing bubble size up the column and variations around the circumference were observed at all times. Bubble sizes were smaller for F and E porosity sintered stainless (20μ and 35μ dia pores) than for the D porosity (65μ dia pores), but size distributions were not measured. Both sintered glass and spinerette (sheet Pt alloy with drilled holes) gas dispersers have been ordered for testing.

Liquid Feed Distribution. Channeling in the 6-in.-dia column was greatly reduced by altering the feed distributor to give well distributed liquid feed at low velocities and with no liquid flow directed to the wall. The initial distributor was a ring of tubing drilled with 1/32-in.-dia holes. The jets of liquid from these holes resulted in severe foam collapse and jets which reached the wall caused severe channeling at these points. The holes directed at the wall were plugged and the other holes enlarged to give low liquid velocities. The flow distribution through the open holes varied by factors of two or more at low rates and severe channeling continued. A feed "spider" was fabricated using 0.048-in.-ID capillary tubing with one nozzle in the column center and six ending on a 4-in.-dia circle. These were bent and soldered into holes drilled in a 1/8-in. pipe cap. This arrangement appeared to give uniform flow to within ± 10% for 20 to 400 cc/min with low enough liquid velocities to avoid foam collapse. Downflow of foam is not noticeable with this feed distributor, but variations in the upward foam velocity can be seen.

---

* Recommended by Ernesto Schonfeld, personal communication in July 1961.

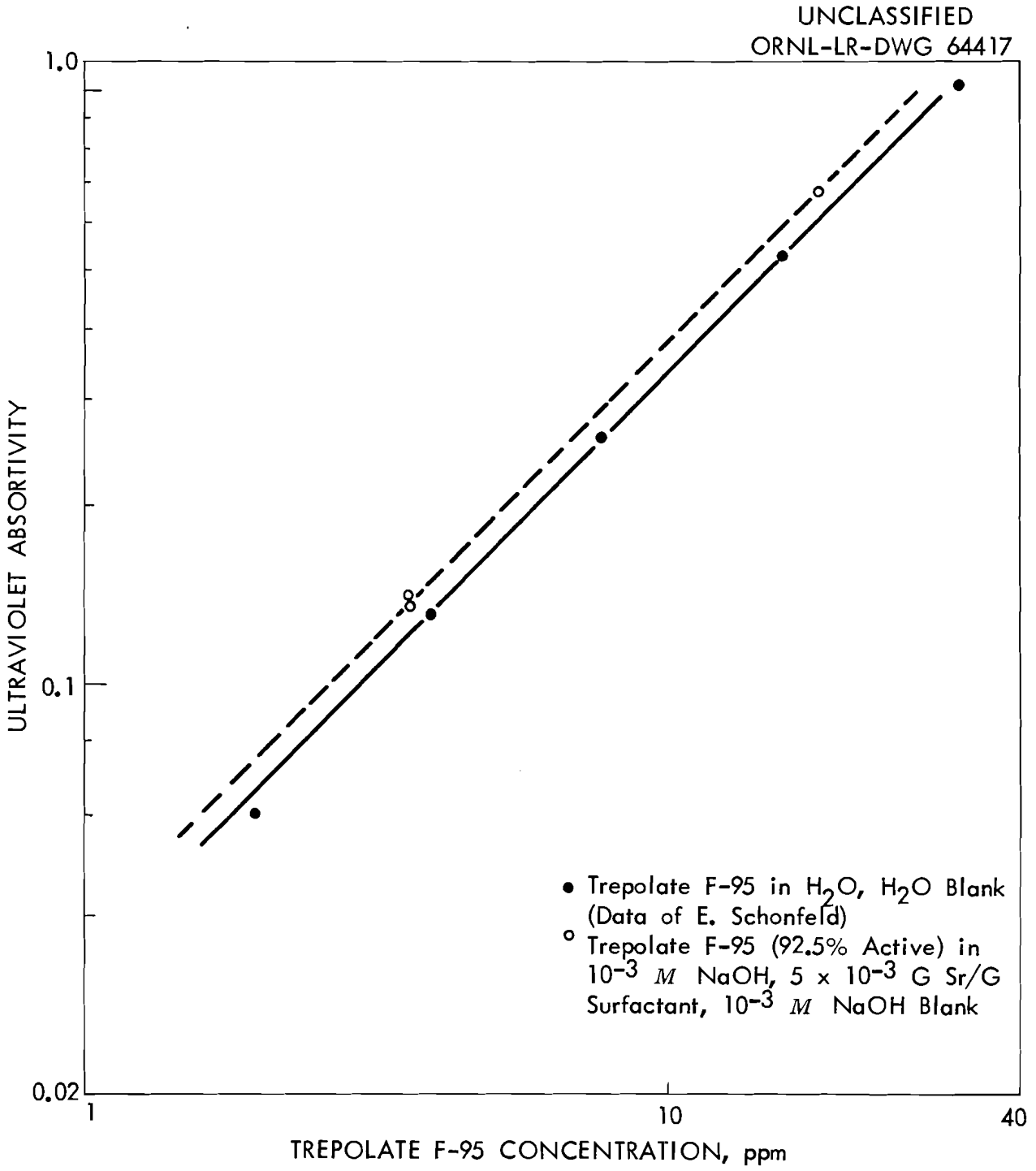

Fig. 1.1. Ultraviolet absorption by dodecyl benzene sulfonate solutions for 2230 A.

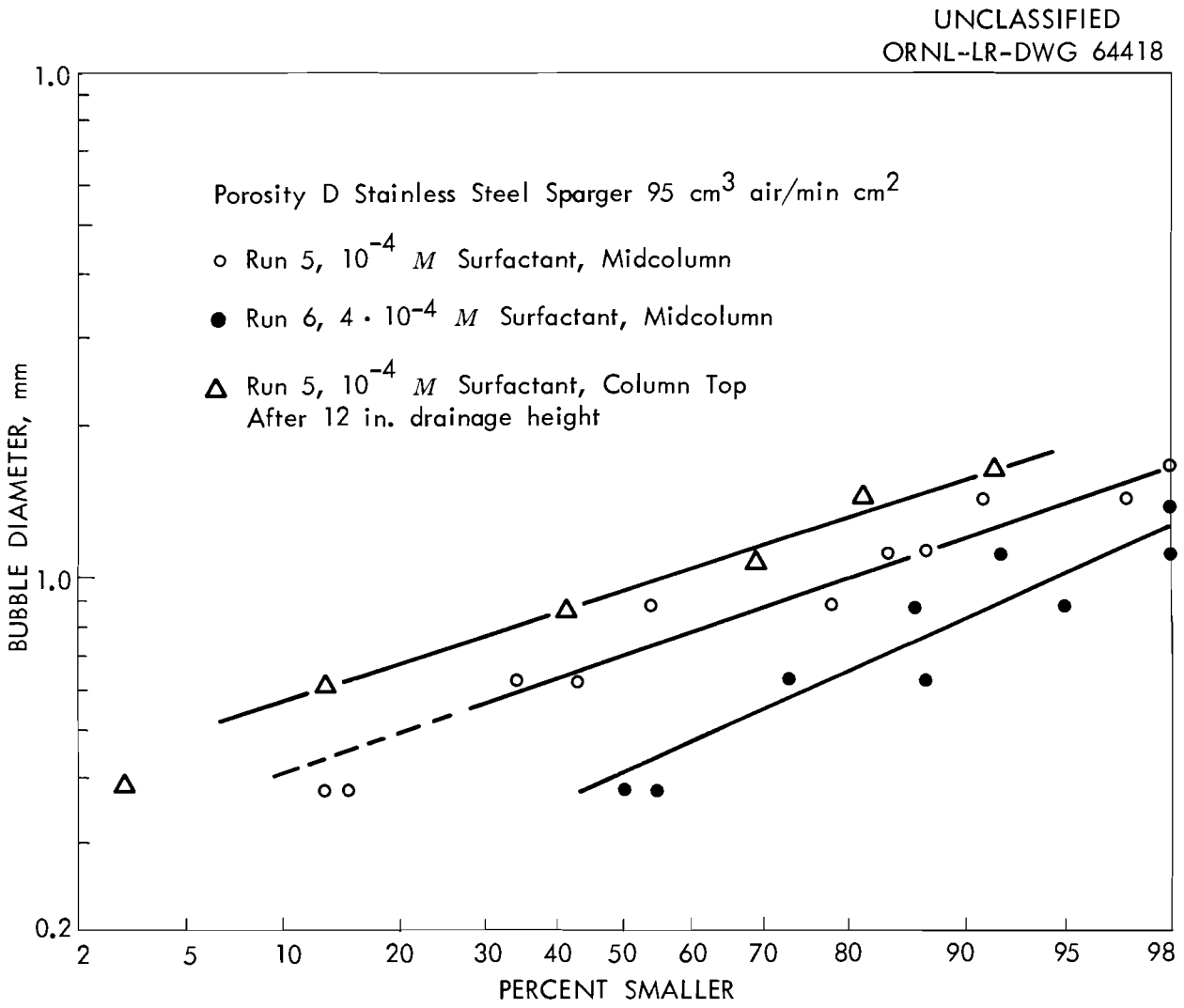

Fig. 1.2. Estimated bubble size distributions.

Countercurrent Run Results. Analytical results for run 5 show excellent material balances for the surfactant and 60-70% recovery of the tracer activity. The number of transfer units based on the liquid phase and assuming one theoretical stage for the liquid pool were 3.2 to 4.3 in 18 inches. All three flow ratios resulted in pinching of the operating and equilibrium lines at the bottom and the pinching was increased by the loss of tracer.

The column as originally installed (June 1961 Unit Operations Monthly Progress Report) was altered as a result of the first three runs. Gas and liquid feed alterations were mentioned. The drainage section was reduced to 18 in. of 6-in.-ID column. This gave a wet foam which was easier to pump from the cyclone foam condenser pot and which minimized evaporation, sampling, and precipitation problems. Small portable vacuum pumps discharging to the hot off-gas were used for the foam breaker vacuum supply in order to avoid any discharge of entrained Sr-89 to the house vacuum. Minor changes were made to facilitate sampling and feed preparation.

Measured flow rates and concentrations for the three parts of run 5 (Table 1.1) were used to calculate material balances and tracer activities (Table 1.2). The number of transfer units based on the liquid phase, N_x, were calculated as follows by assuming straight operating and equilibrium lines: i.e., V and L constant where:

x is the tracer activity in the liquid, cpm/cc

y is the tracer activity in the condensed foam, cpm/sq cm

x^* and y^* are equilibrium tracer activities, note that $x^* = y/(\Gamma/c)$ and $y^* = x(\Gamma/c)$ where Γ/c is the Sr distribution coefficient.

subscript 2 refers to the top of the column

subscript 1 refers to the bottom of the region of countercurrent flow

L is the net liquid flow down the column, cc/min

V is surface flow, sq cm/min

$$N_x = \int_{x_1}^{x_2} \frac{dx}{x - x^*} = \int_{x_1}^{x_2} \frac{dx}{x - y/(\Gamma/c)}$$

$$V(y - y_1) = L(x - x_1)$$

$$\left(\frac{\Gamma}{c}\right) x_2^* = y_2 = y_1 + \frac{L}{V}(x_2 - x_1)$$

$$N_x = \int_{x_1}^{x_2} \frac{dx}{\left[1 - \left(\frac{c}{\Gamma}\right)\frac{L}{V}\right] x + \left(\frac{c}{\Gamma}\right)\left(\frac{L}{V} x_1 - y_1\right)}$$

Table 1.1. Foam Column Concentrations and Flow Rates - Run 5

Gas Flow Rates: 3000 cm^3/min

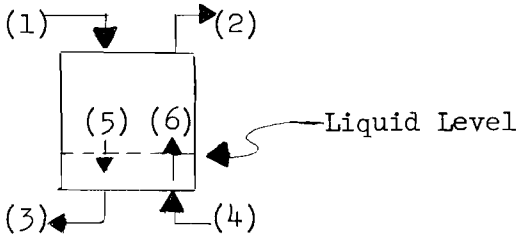

Quantity	Units	Value for Stream: (1)	(2)[a]	(3)	(4)
Run 5C					
Liquid flow rate	cm^3/min	200	10.4	290	100
Liquid surfactant conc.	ppm	36	763	60	180
Liquid tracer conc.[b]	c/min·cc	9,100	109,000	80	0
Run 5B					
Liquid flow rate	cm^3/min	50	9.5	90.5	50
Liquid surfactant conc.	ppm	36	650	51	180
Liquid tracer conc.	c/min·cc	9,100	33,200	40	0
Run 5A					
Liquid flow rate	cm^3/min	100	12.7	137	50
Liquid surfactant conc.	ppm	36	530	40[c]	180
Liquid tracer conc.	c/min·cc	9,100	40,600	30	0

[a] For condensed foam

[b] Multiple samples taken, averages for end of run samples used

[c] Estimated, analyses not available

Table 1.2. Surfactant and Tracer Material Balances - Run 5

Concentrations and Flow Rates: see Table 1.1
Stream Identification: see Table 1.1

Quantity	Stream No.	Units	Run 5C	Run 5B	Run 5A
Surfactant in liquid feed	1	mg/min	7.20	1.80	3.60
Surfactant in bottom feed	4	mg/min	18.00	9.00	9.00
Total surfactant in	1 + 4	mg/min	25.20	10.80	12.60
Surfactant in condensed foam	2	mg/min	7.94	6.17	6.74
Surfactant in exit liquid	3	mg/min	17.40	4.61	-
Total surfactant out	2 + 3	mg/min	25.34	10.78	-
Recovery of surfactant	-	%	101	100	-
Tracer in liquid feed	1	10^3c/min	1820	455	910
Tracer in bottom feed	4	10^3c/min	0	0	0
Total tracer in	1 + 4	10^3c/min	1820	455	910
Tracer in condensed foam	2	10^3c/min	1133	316	516
Tracer in exit liquid	3	10^3c/min	23	4	4
Total tracer out	2 + 3	10^3c/min	1156	320	520
Recovery of tracer	-	%	64	70	58
Inlet tracer conc., x_2	1	cpm/cc	9100	9100	9100
Foam tracer conc., y_2[a]	2	cpm/sq cm	7.6	2.14	3.5
Liquid in equil. with y_2[b], x_2*	-	cpm/cc	1900	535	870
Exit liquid tracer conc., x_1*	3	cpm/cc	80	40	30
x_1 from material balance	5	cpm/cc	320	520	210
$x_2 - x_1$	-	cpm/cc	8880	8580	8890
$(x - x^*)_{\text{ln mean}}$	-	cpm/cc	2050	2690	2110
Number of transfer units based on liquid phase, N_x	-	-	4.3	3.2	4.2
HTU_x	-	in.	4.2	5.6	4.3

[a] Based on an area of 50 sq cm/cc foam

[b] Based on an assumed value of $\Gamma/c = 4 \times 10^{-3}$

$$N_x = \frac{1}{1 - \left(\frac{c}{\Gamma}\right)\frac{L}{V}} \ln \left[\frac{\frac{L}{V} x_1 - y_1 + \left(\frac{\Gamma}{c} - \frac{L}{V}\right) x_2}{\frac{L}{V} x_1 - y_1 + \left(\frac{\Gamma}{c} - \frac{L}{V}\right) x_1} \right]$$

Substituting for $1 - \left(\frac{c}{\Gamma}\right)\left(\frac{L}{V}\right)$ and y_1:

$$N_x = \frac{x_2 - x_1}{(x_2 - x_1) - (c/\Gamma)(y_2 - y_1)} \ln \frac{x_2 - x_2^*}{x_1 - x_1^*} = \frac{x_2 - x_1}{(x - x^*)_{\ln \text{ mean}}}$$

$$N_x = (x_2 - x_1) \Big/ \frac{(x_2 - x_2^*) - (x_1 - x_1^*)}{\ln \frac{x_2 - x_2^*}{x_1 - x_1^*}}$$

A similar expression is obtained for N_y in terms of $(y^* - y)_{\ln \text{ mean}}$. Values of x_2 and y_2 are obtained directly from the analyses of tracer and surfactant concentrations. Values of x_1 and y_1 are calculated assuming that the liquid pool in which the foam is generated is one theoretical stage. Then y_1 is in equilibrium with the liquid leaving the column. Values of x_1 are calculated from a material balance for this theoretical stage.

The validity of the calculated HTU values of 4.2 to 5.6 inches is doubtful because of:

1. The loss of tracer activity makes the operating line uncertain; the line may be curved.

2. The low activity in the exit liquid results in poor analytical accuracy.

3. The operating line may be curved due to a varying value of L/V or Γ/c.

The results for run 6 with larger values of V/L will help determine the importance of the first two factors.

The bubble size distribution for run 5 (Figure 1.2) gives a surface area of about 50 cm^2/cm^3 foam. The surfactant leaving the condensed form corresponds to about 1.1×10^{-10} moles/cm^2 based on this surface; however, much less surface reaches the foam breaker because of foam collapse in the drainage section.

Preliminary operation of the column with sodium lauryl sulfate as the surfactant (runs 1, 2, and 3) were without tracer for the purposes of checking the feed distributors, foam breaker, and other details of mechanical operation. Use of Na analyses as a measure of surfactant concentrations during these runs indicated this was an unpromising procedure. Run 4 was a practice run at run 5 conditions with the exception of no Sr-89 tracer. Run 6 was with four times the surfactant concentration of run 5 in the liquid feed and with liquid feed flow rates to give surfactant liquid/surface flow ratios of 100 to 220% of those of 5C. Analyses for this run are not complete.

2.0 FISSION PRODUCT RECOVERY

A. D. Ryon

Processing of highly radioactive solutions by solvent extraction calls for a contactor with low solvent exposure time per theoretical stage. Some promising new solvent extraction systems require extreme values of A/O, up to 10 or 20, where conventional contactors generally behave poorly. The Stacked Clone Contactor program is an attempt to develop a contactor meeting these needs. The present progress report describes the entrainment behavior of Mark II contactor with two polishing stages below the organic feed inlet, and operating on the system 17% TBP in Amsco, 1 M $NaNO_3$.

2.1 Organic Entrainment from Stacked Clone Contactor - W. M. Woods

A Mark II contactor stage consists of a 1-1/2-in.-dia x 2-in.-high hydroclone with 0.5-in. underflow and overflow ports. Each stage was driven by an Eastern D-11 pump. The contactor consisted of seven of these stages, two of which were below the organic feed point, i.e., the feed port of No. 5 clone counting down. Figure 2.1 shows the assembled apparatus.

Aqueous and organic rates were adjusted and held steady for a few minutes and samples of raffinate were then withdrawn into 250 cc volumetric flasks. After these had settled overnight the amount of entrained organic was determined by adding water from a burette to bring the aqueous meniscies to the mark on the flask.

Figure 2.2 shows that the amount of organic entrained in the raffinate increases exponentially with total flow rate. With the exception of some scatter at low entrainment and low A/O ratios the entrainment data are well correlated by $E = 0.21\ A/O\ (A + O)^{1.5}$ in which E = % of organic fed which was entrained, A = aqueous flow rate, and O = organic flow rate.

Figure 2.3 shows a plot of per cent entrainment of organic vs A/O with superimposed lines of constant A + O and constant A calculated from the above correlation.

UNCLASSIFIED
PHOTO 53549

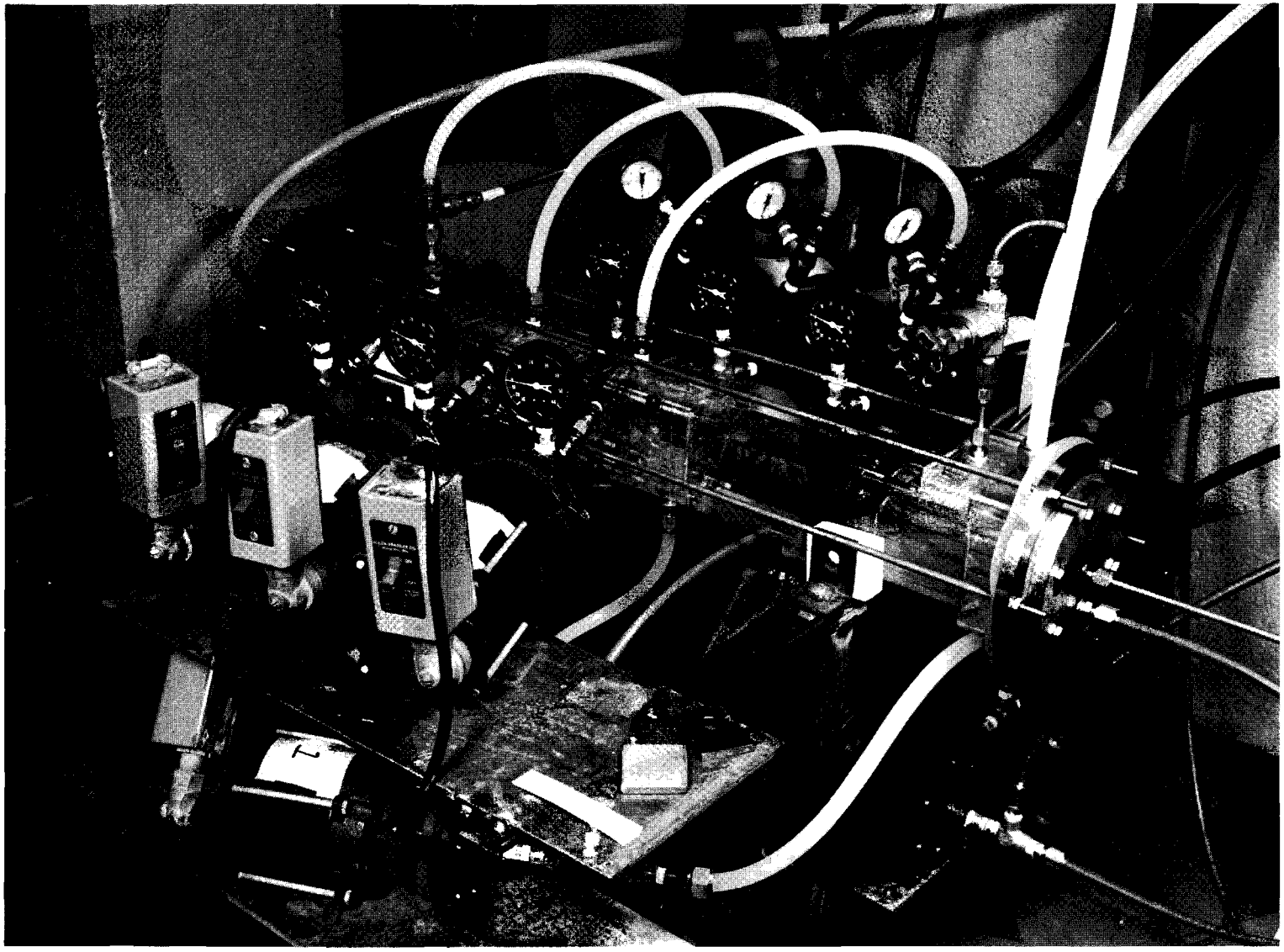

Fig. 2.1. Mark II Stacked Clone Contactor.

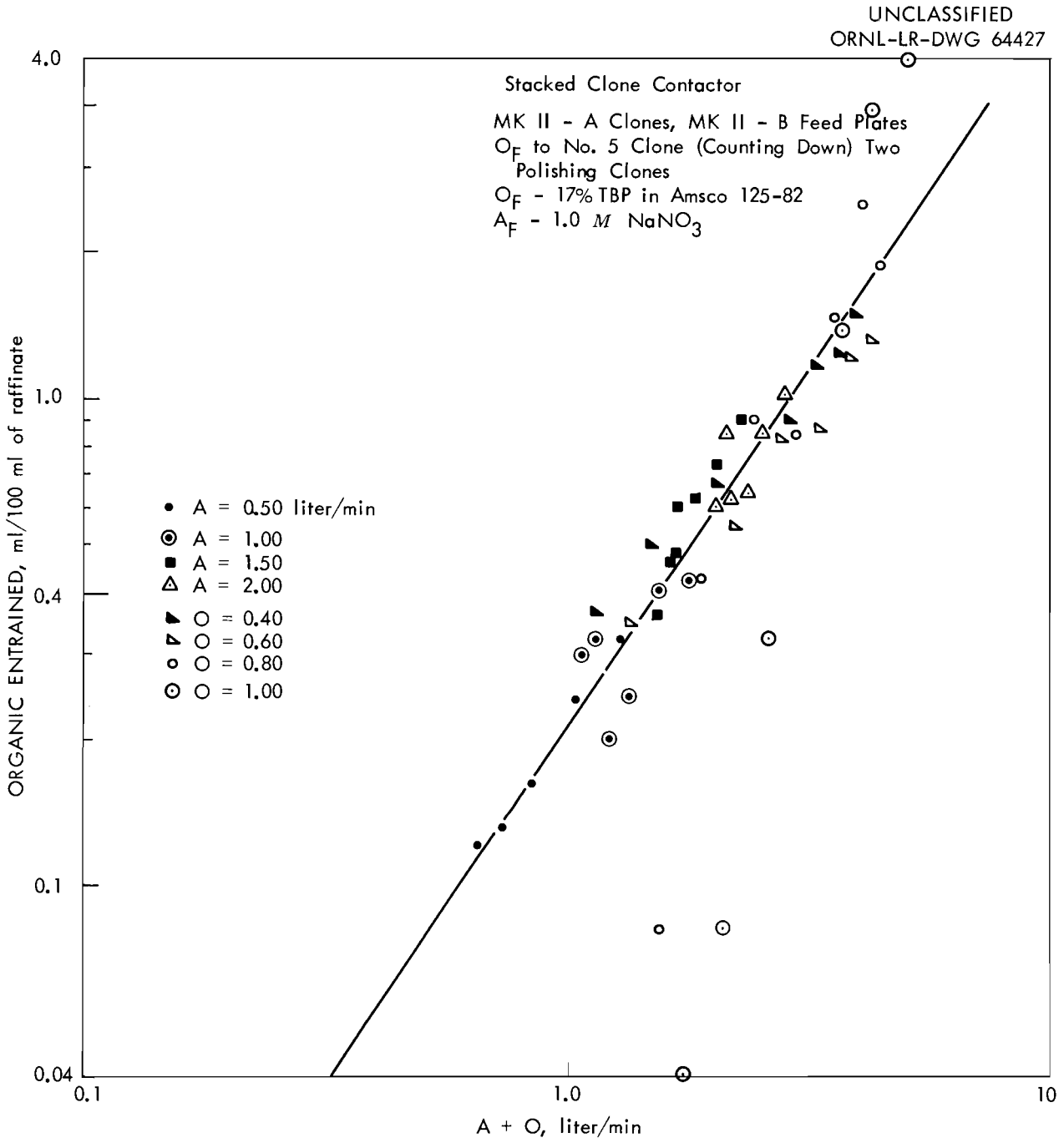

Fig. 2.2. Organic entrainment in stacked clone contactor.

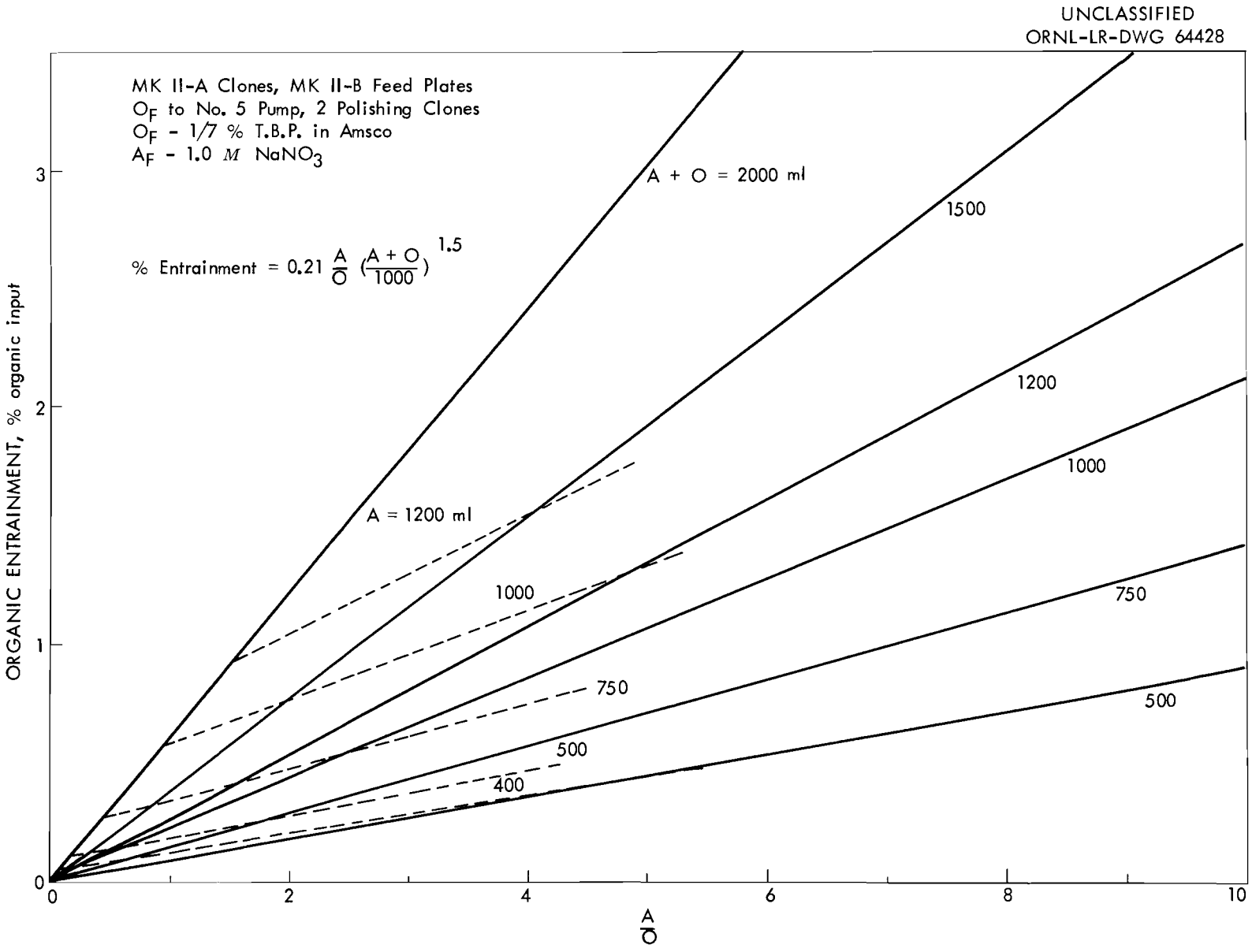

Fig. 2.3. Effect of $\frac{A}{O}$ on organic entrainment.

3.0 FUEL CYCLE DEVELOPMENT

P. A. Haas

The fuel cycle program is a study of fuel materials preparation and element fabrication procedures economically adaptable to remote operation for the recycle of fissile and fertile materials. The immediate objective is to develop to the pilot plant stage the process for ThO_2-U(233)O_2 in cladding tubes. The unit operations studies are on denitration of $Th(NO_3)_4$ in steam atmospheres followed by dispersion into thoria sols, uranium addition, drying, and calcination to give high density oxide particles. Test elements of vibratorily compacted oxides are being fabricated or irradiated.

3.1 Sol Dispersion and Inventory Studies - J. W. Snider, C. C. Haws, Jr., R. D. Arthur

The methods of thoria dispersion and inventory control important to design of a virgin Th-U(233) fabrication facility (July 1961 Unit Operations Monthly Report) were studied. A pump loop and tank were tested for sol dispersion and mixing. Reproducibility of powder and sol sampling and analyses were determined.

A centrifugal pump with a 6 or 9.25-in.-ID conical bottom tank was tested for dispersion of denitrated thoria powders with HNO_3 addition, and for mixing of uranium with the sol. Flow at about 7 liter/min was either into or out of the conical bottom with the tank as part of a loop. A lot of denitrated thoria powder containing 1934 g of ThO_2 was dispersed using the 6-in.-dia tank at a N/Th ratio of 0.09. The flow rate of the water was such that a Reynold's Number of 2,460 prevailed prior to powder addition within the 6-in.-dia tank. After dispersion and heel removal (1.45% removed as undispersed heel) the sol was recharged to the tank and sufficient uranium added to give a U/Th ratio of 0.0417.

The larger tank, 9.25-in.-dia, was used to disperse a second lot of denitrated powder containing 7.25 kg of ThO_2 at a N/Th ratio of 0.10. A Reynold's Number of 1,590 prevailed within the 9.25-in.-dia section prior to powder addition. After powder addition, sufficient 1 N HNO_3 was added as a peptizing agent to give the desired N/Th ratio.

The run made with the 6-in.-dia dispersion tank was sampled in duplicate before and after dispersion. The two samples taken before acid addition were 39.86% and 39.91% ThO_2 by weight or a difference of 0.17%. The two samples taken after acid addition were 42.27% and 42.36 wt % ThO_2 or a difference of 0.21%. The increase in concentration is due to evaporation of H_2O from the tank at 80°C.

To test reproducibility of sampling the sol, one lot of steam denitrated powder containing 4430 g of ThO_2 was dispersed at a N/Th ratio of 0.11. The dispersion was done in the rotating-baffled cylinder used previously. Over a period of 15 days a heel amounting to 3.25% was removed. The remaining sol was then separated into 7 equal volumes with no agitation other than that associated with pouring. After standing for 48 hrs at 80°C these portions were shaken and a 25 cc sample of each taken. These samples were analyzed

for ThO_2 by drying and firing to 1000°C. The ThO_2 concentrations were: 45.95%, 45.85%, 45.85%, 45.89%, 45.99%, 45.98%, and 45.85% or a spread of 0.31%.

Duplicate samples of denitrated powder were taken and analyzed for ThO_2. They were 97.17% and 96.78% ThO_2 or a difference of 0.40%.

If one used powder sampling procedures to control the U/Th ratio, the thorium inventory would have to be controlled to prevent losses during transfer. A careful material balance was made during the transfer of material for one set of weighing, dispersing, drying, and firing steps. The thoria loss based on a single powder analysis was 2.37%.

From these studies the following conclusions were drawn:

1. Either powder or dispersed sol sampling can be done within the 1% allowable limit. Duplicate samples varied by 0.40% and duplicate dispersed sol samples varied by 0.21%.

2. It is doubtful if ThO_2 inventory can be controlled to less than 1% in plant operation without posing excessive design limitations on all tanks, pumps, and piping. A 2.37% ThO_2 loss occurred on a batch during dispersing, drying, and firing.

3. Lots of Th sol may be withdrawn from a large batch and be uniform in thoria concentration. The spread in seven lots was 0.31%.

4. A conical bottom tank and a centrifugal pump loop would suffice for a sol dispersion and uranium adsorber tank. Two steam denitrated batches were dispersed in such a tank with Reynold's Numbers of 2,460 and 1,590 in the tanks. The same system was used to add uranium to the thoria sol at a Reynold's Number of 2,460. The system ran well with no evidence of pump plugging.

4.0 GCR COOLANT PURIFICATION STUDIES

J. C. Suddath

Contamination of coolant gases by chemical impurities and release of fission products from fuel elements are major problems in gas-cooled reactors and in-pile experimental loops. Investigations are being made to determine the best methods to reduce the impurities, both radioactive and non-radioactive, with emphasis on the kinetics of the fixed bed oxidation of hydrogen, carbon monoxide, and methane by copper oxide.

An attempt is being made to fit experimental data from the study of the H_2-CuO and CO-CuO reactions to a mathematical model of external diffusion and internal diffusion of the H_2 or CO controlling a rapid, irreversible reaction.

4.1 Comparison of Predicted Results and Experimental Data for the CO-CuO Reaction - C. D. Scott

The mathematical model used to predict the CO effluent concentration history curves was external diffusion and internal diffusion of CO controlling a rapid irreversible reaction between CO and CuO (Unit Operations Monthly Report, May 1961). A finite difference solution of the differential equations describing this model has been set up for computation by the IBM 7090 computer. The predicted curves from the mathematical model can then be compared to experimental data from tests on deep beds of CuO pellets.

A total of seven such tests were made for the CO-CuO system. The tests covered the following ranges of operating conditions:

System pressure - 10.2 - 30.0 atm
System temperature - 400 - 600°C
Gas mass flow rate - 0.084 - 0.255 g-moles/cm^2-min
Initial CO concentration in He stream - 0.44 - 1.25 vol %
CuO pellet bed volume - 48.5 - 97.0 cc

The experimental CO effluent concentrations appear to agree with the predicted curves within experimental error (Figures 4.1 - 4.7). The largest error appears to be in the apparent effective porosity of the CuO pellets. The shape of the experimental curve suggests that the value of the effective porosity used in the finite difference calculations should be about 25% higher. The effective porosity of these tests was determined to be 0.057 (effective void volume/total void volume of CuO pellet) from differential bed tests.

4.2 Comparison of Predicted Results and Experimental Data for Reaction of Both H_2 and CO with CuO

An IBM 7090 computer code was written for the finite difference solution of the mathematical model of simultaneous reaction of H_2 and CO in a flowing stream of helium with fixed beds of CuO pellets. The model assumed a rapid and irreversible reaction of both H_2 and CO with CuO controlled by both external diffusion and internal diffusion of H_2 and CO.

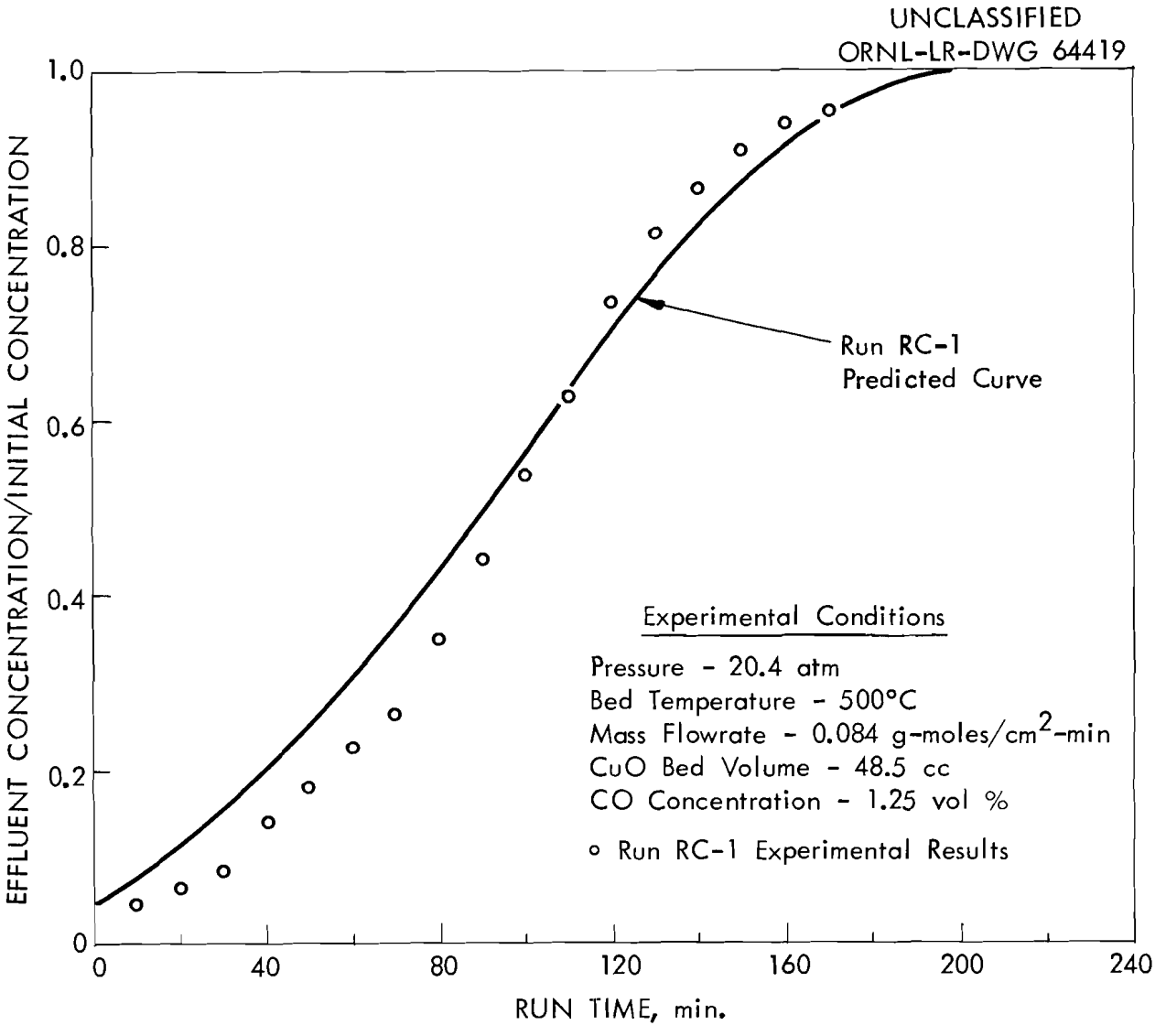

Fig. 4.1. Comparison between experimental results from Run RC-1 and predicted results from the mathematical model of external diffusion and internal diffusion of carbon monoxide controlling a rapid, irreversible reaction of carbon monoxide with porous pellets of CuO.

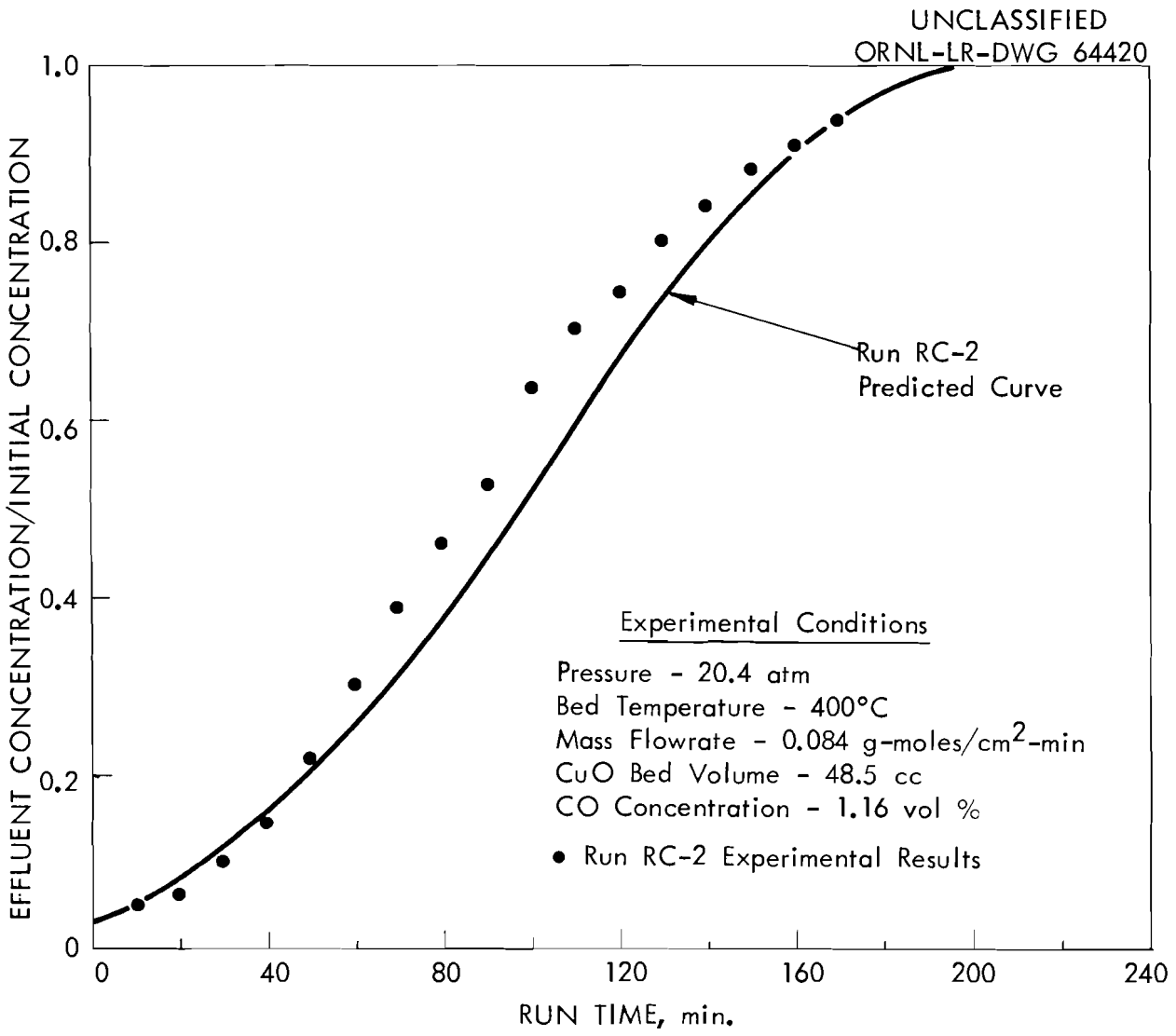

Fig. 4.2. Comparison between experimental results from Run RC-2 and predicted results from the mathematical model of external diffusion and internal diffusion of carbon monoxide controlling a rapid, irreversible reaction of carbon monoxide with porous pellets of CuO.

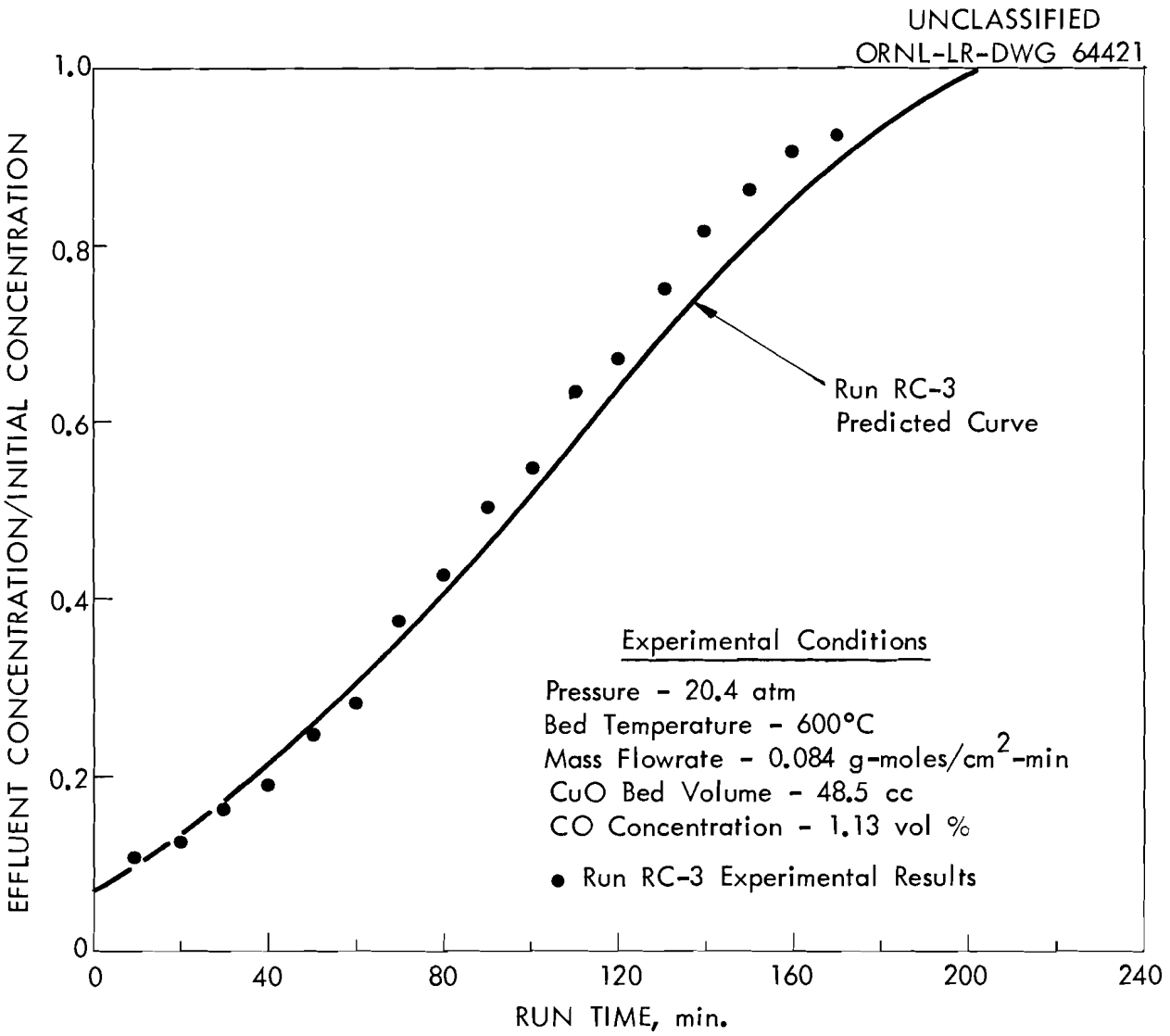

Fig. 4.3. Comparison between experimental results from Run RC-3 and predicted results from the mathematical model of external diffusion and internal diffusion of carbon monoxide controlling a rapid, irreversible reaction of carbon monoxide with porous pellets of CuO.

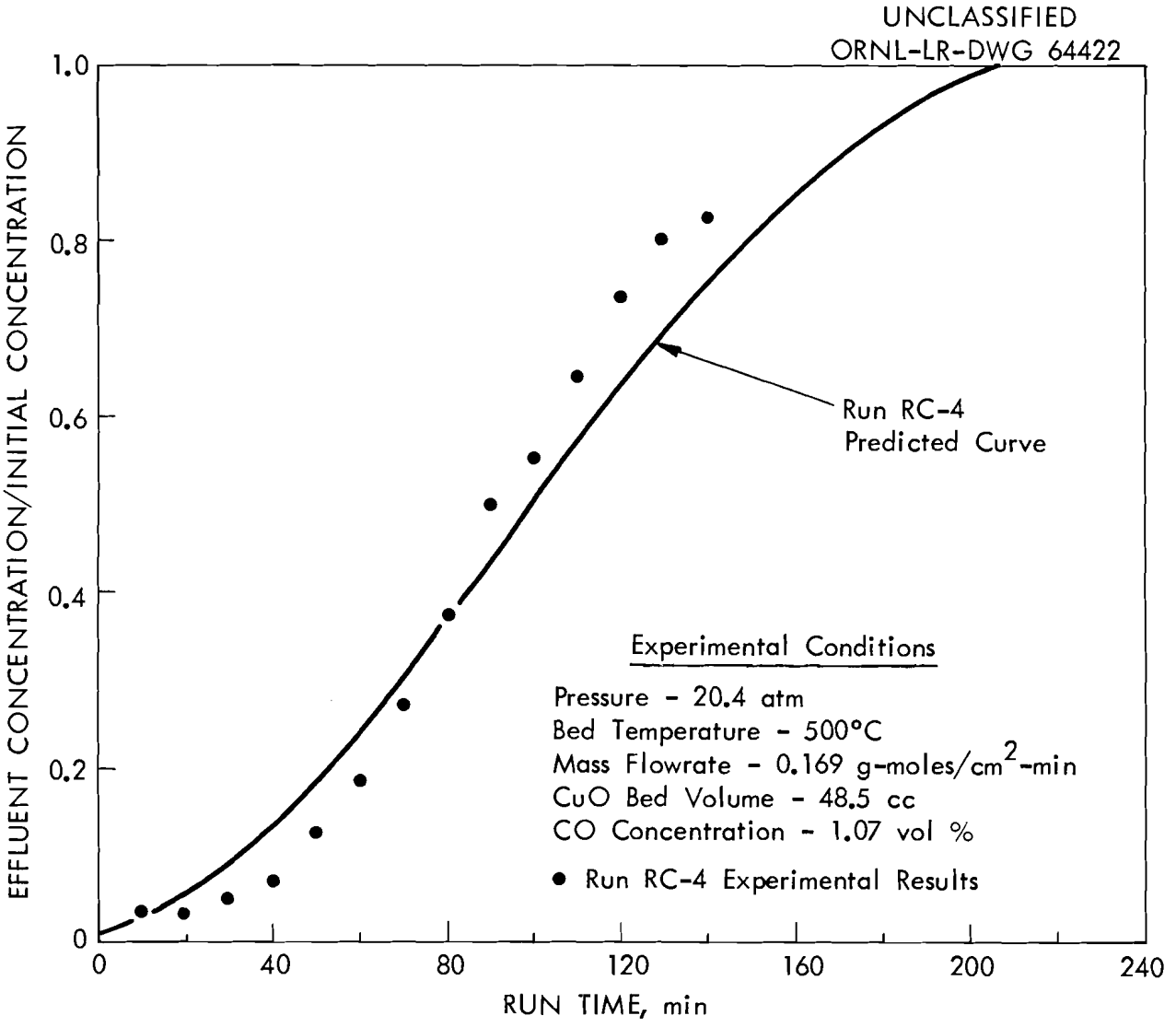

Fig. 4.4. Comparison between experimental results from Run RC-4 and predicted results from the mathematical model of external diffusion and internal diffusion of carbon monoxide controlling a rapid, irreversible reaction of carbon monoxide with porous pellets of CuO.

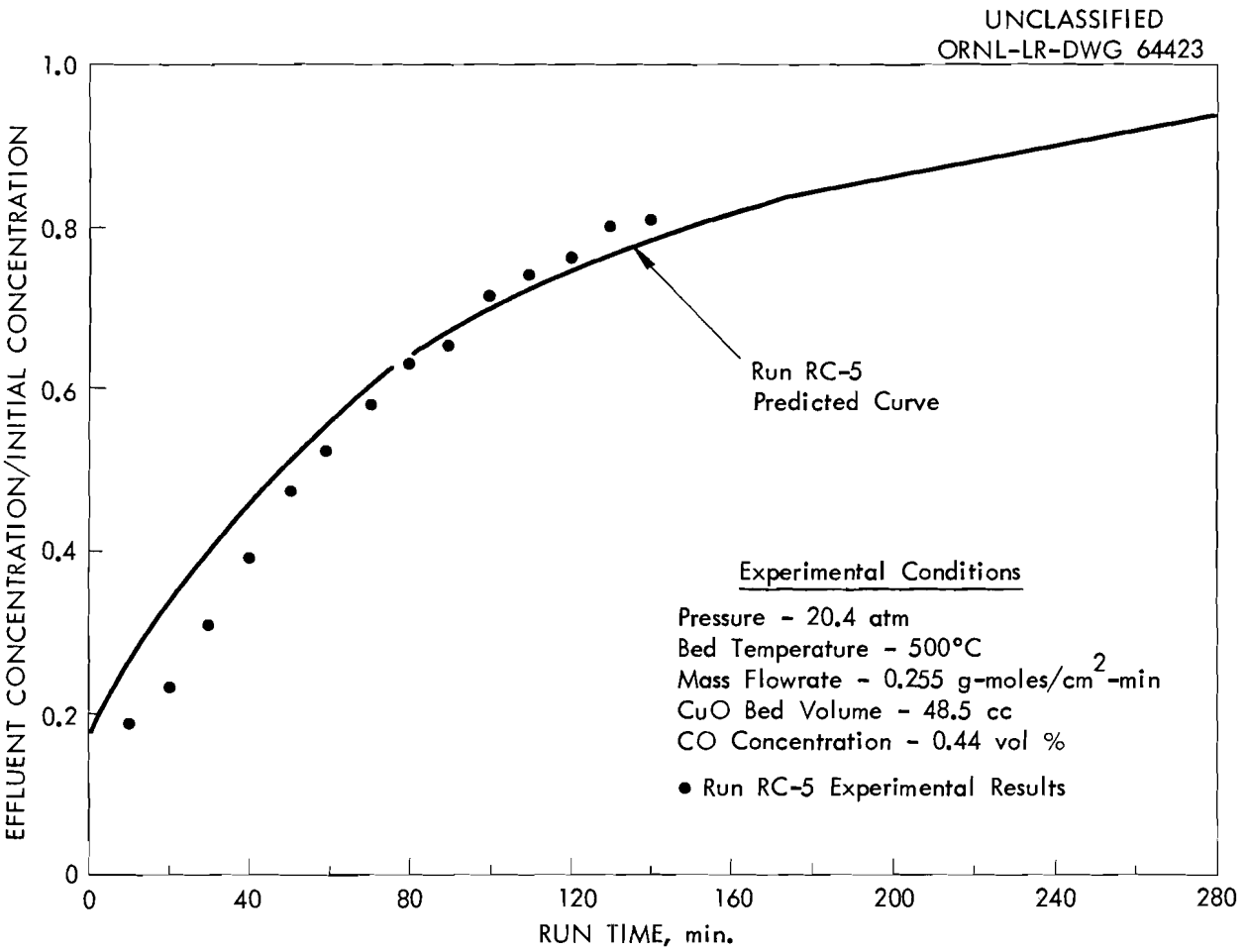

Fig. 4.5. Comparison between experimental results from Run RC-5 and predicted results from the mathematical model of external diffusion and internal diffusion of carbon monoxide controlling a rapid, irreversible reaction of carbon monoxide with porous pellets of CuO.

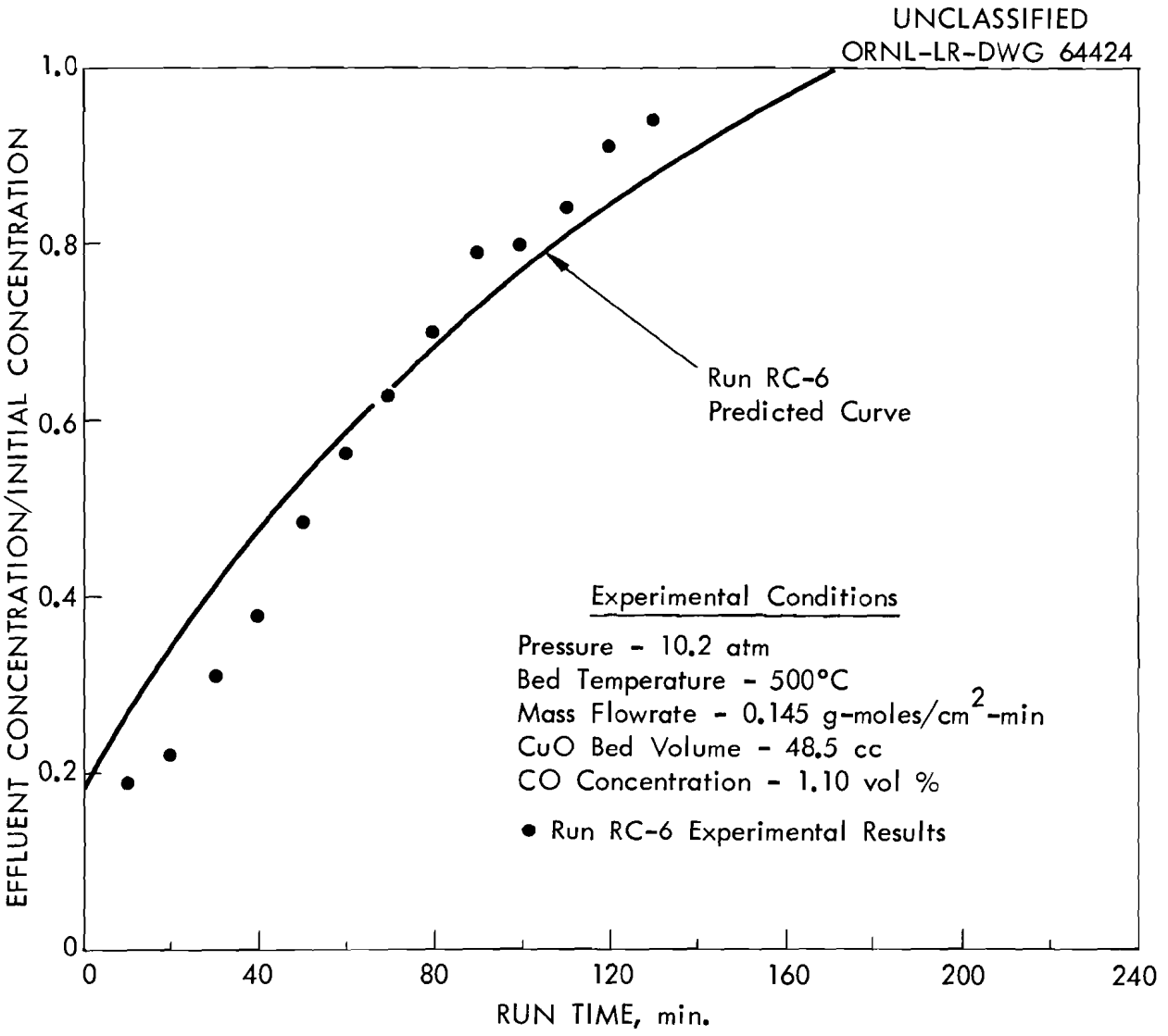

Fig. 4.6. Comparison between experimental results from Run RC-6 and predicted results from the mathematical model to external diffusion and internal diffusion of carbon monoxide controlling a rapid, irreversible reaction of carbon monoxide with porous pellets of CuO.

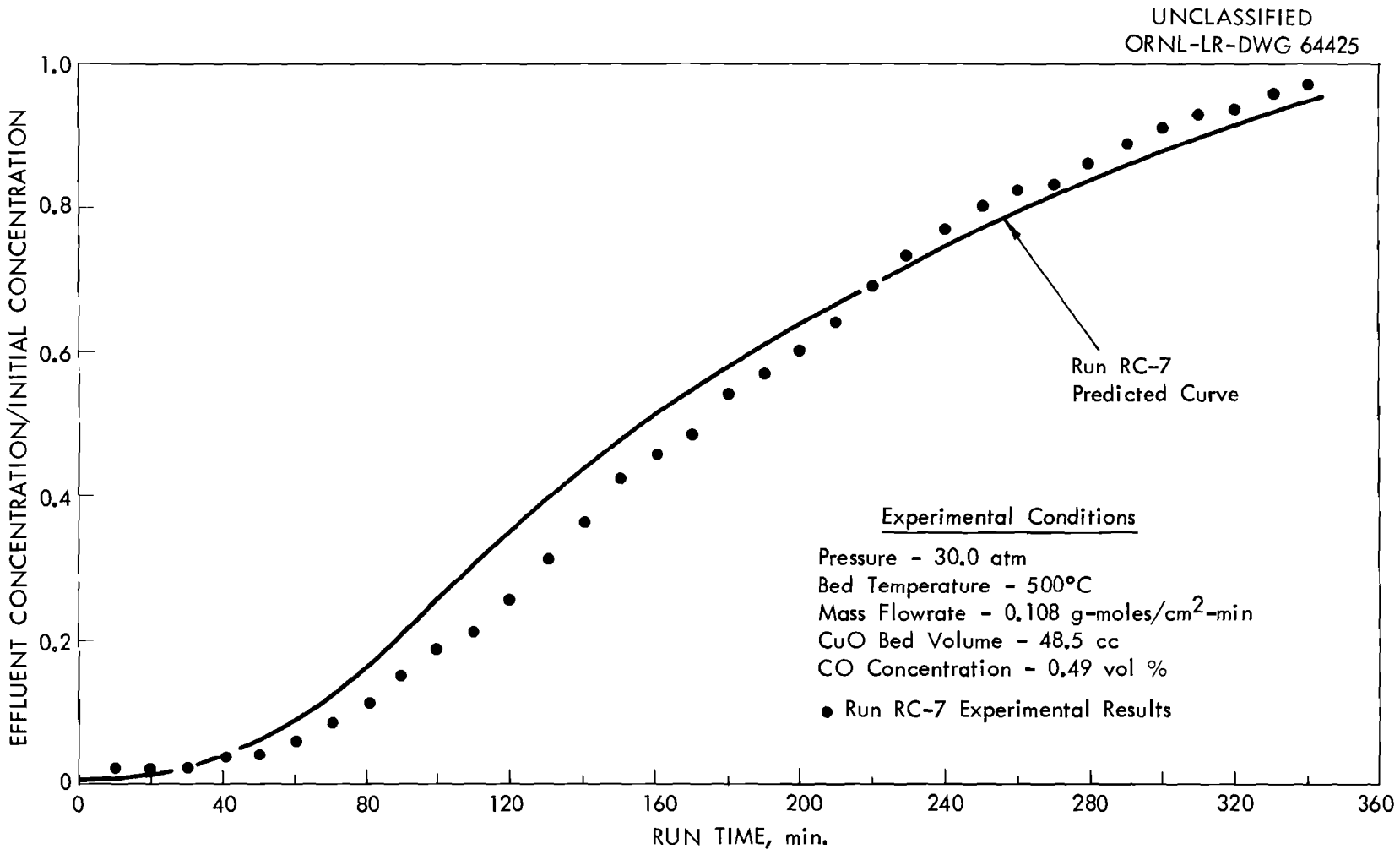

Fig. 4.7. Comparison between experimental results from Run RC-7 and predicted results from the mathematical model of external diffusion and internal diffusion of carbon monoxide controlling a rapid, irreversible reaction of carbon monoxide with porous pellets of CuO.

The results from this assumed model have been compared with an experimental test in which both H_2 and CO were removed from a flowing stream of He by reaction with a fixed bed of CuO. The comparison was between predicted values of the effluent concentration of H_2 and CO and experimental values of these concentrations as a function of time (Figure 4.8). Agreement between predicted and experimental values was probably within experimental error.

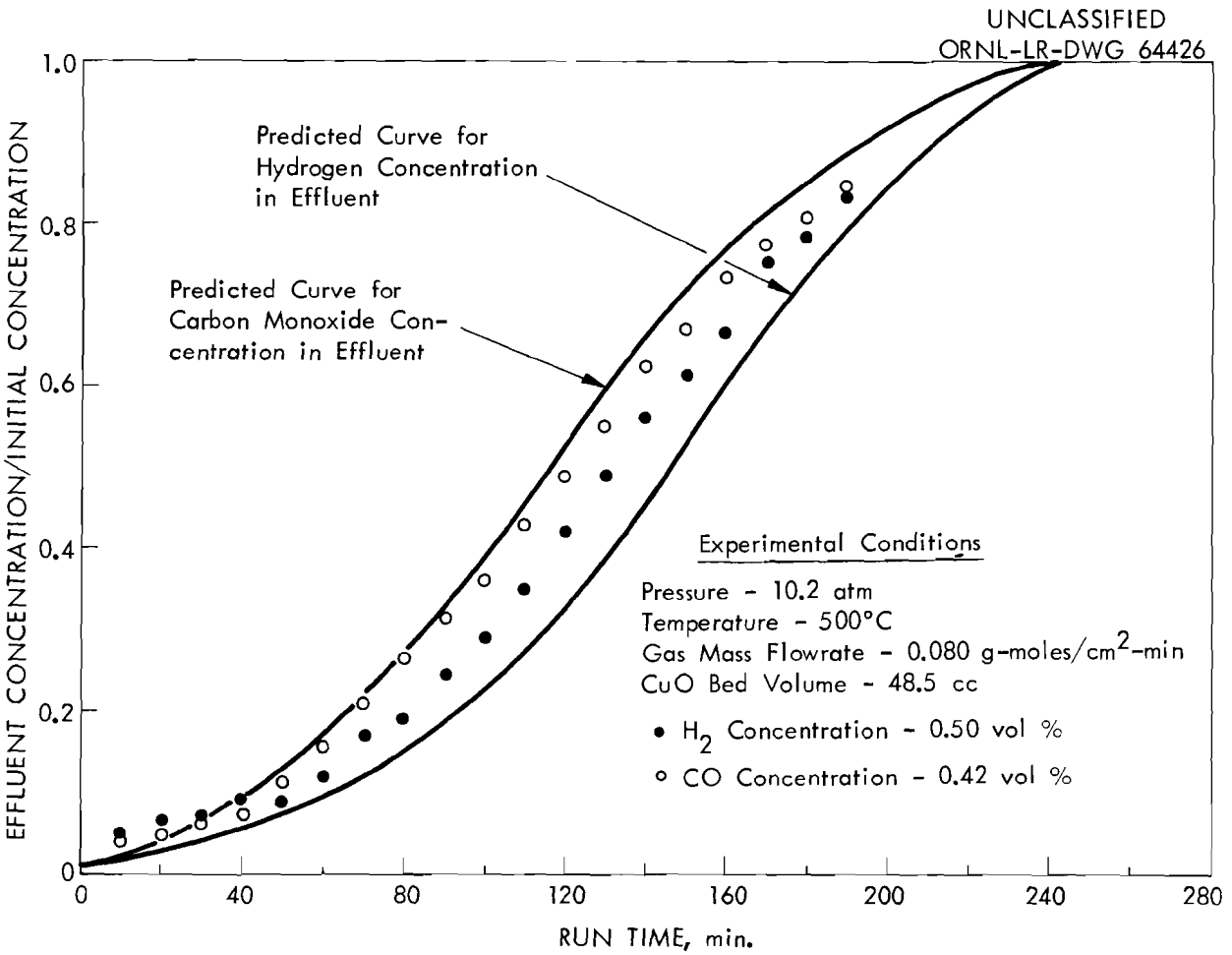

Fig. 4.8. Comparison between experimental results from Run HC-1 and predicted results from the mathematical model of external diffusion and internal diffusion of H_2 and CO controlling rapid, irreversible reactions of H_2 and CO with porous pellets of CuO.

5.0 POWER REACTOR FUEL PROCESSING

C. D. Watson

5.1 Continuous Modified Zirflex - F. G. Kitts

Modified Zirflex denotes a process for the recovery of uranium from U-Zr-Sn fuels by dissolution in NH_4F-NH_4NO_3-H_2O_2 solutions, stabilization with HNO_3-$Al(NO_3)_3$, and TBP extraction. H_2O_2 is added to the dissolvent to oxidize U^{IV} to the more soluble U^{VI} so that fuels containing higher per centages of U (up to 10%) can be processed without the intermediate precipitation of UF_4 which would occur if this oxidant were not added. Presently attempts are being made to adapt the process for continuous dissolution to take advantage of the increased throughputs made possible by this method of operation.

Twenty-three runs in a 2-in. dissolver and one run in a 6-in. dissolver were made to determine the effect on reaction rate of F/S (feed rate/surface area) ratio, oxidant concentration and boil-up rate in continuous dissolution. It was found that reaction rate increased with F/S but the relationship was non-linear (Figure 5.1) so that lower loadings (calculated from the relationship L = reaction rate/(F/S)) resulted at conditions which gave high dissolution rates. Oxidant concentrations of 1.0 M NH_4NO_3 and/or 0.1 M H_2O_2 in the dissolvent gave comparable results (Figure 5.1) while rates obtained with 1.5 M NH_4NO_3 were quite erratic (Table 5.1). The higher boil-up rate produced higher reaction rates (Figure 5.1).

The first rate determinations were made under static conditions using short exposure times and dissolvents which represented continuous dissolution with 3 levels of loading and hence 3 different free F^- concentrations. These results (Table 5.2) were higher than those found under flowing conditions probably due to the shorter exposure which dissolved only the more reactive surface of the Zircalloy-2 specimens.

The runs reported in Table 5.1 were made under reflux conditions with dissolvent feeding into an overflowing 2-in. pyrex dissolver heated through a stainless steel flanged bottom by a hot plate. A strip of Zircalloy-2 the same length and width as the specimen (~0.9-in. x 9.5-in. x 0.068-in.) was dissolved under controlled conditions of feed rate and heat input until a steady-state operation had been achieved; the strip was removed and the weighed specimen was inserted simultaneously and the run was continued without disturbing dissolver operation. Reproducible steady-state conditions were achieved as can be seen by comparing runs made under similar conditions such as 7 and 8, and 16 and 17 (Table 5.1). Reaction rates were calculated from weight loss, exposure time and initial area, which did not change appreciably during a run (~10 mils uniform attack). Loading was calculated from L = R/(F/S). The column headed solvent extraction feed (Table 5.1) indicates the Zr concentration which would result from adding 0.8 volume of stabilizer per volume of dissolver effluent.

The run in the 6-in. equipment (the Modified Zirflex batch dissolver reworked to permit continuous operation) was made in much the same way as the smaller scale runs except the estimated steady-state dissolver charge

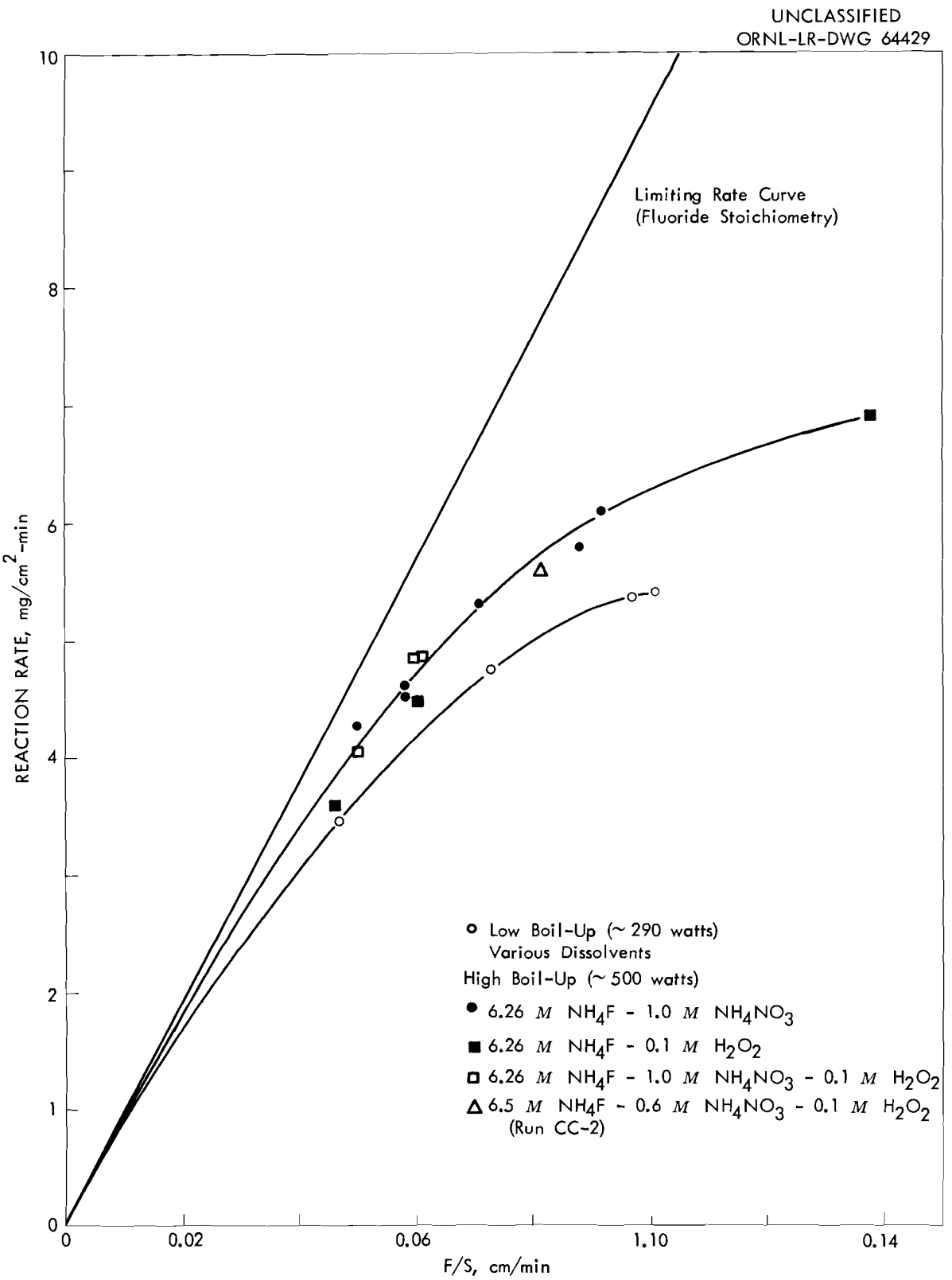

Fig. 5.1. Reaction rate as a function of feed rate/specimen area ratio.

Table 5.1. Continuous Modified Zirflex Dissolution Rates

Run No.	Dissolvent NH_4F M	Dissolvent NH_4NO_3 M	Dissolvent H_2O_2 M	Feed Rate cm^3/min	Surface cm^2	F/S	Weight Loss g	Dissol Time min	Reaction Rate mg/cm^2-min	Loading Zly-2 g/ℓ	Loading Zr M	SX Feed Zr M
1[a]	6.5	-	0.01	12.0	124	0.097	22.177	33.3	5.37	55.4	0.60	0.34
2	6.0	0.6	-	12.2	121	0.101	21.453	32.7	5.42	53.7	0.58	0.33
3	6.0	0.6	-	6.0	128	0.047	14.723	33.3	3.45	73.4	0.79	0.44
4	6.26	1.0	-	6.33	127	0.050	17.134	31.6	4.27	85.7	0.92	0.52
5	6.26	1.0	-	9.43	133	0.071	22.468	31.8	5.31	74.8	0.80	0.45
6	6.26	1.0	-	9.26	126	0.073	19.405	32.4	4.75	64.6	0.69	0.39
7	6.26	1.0	-	6.65	115	0.058	15.830	30.1	4.58	79.2	0.85	0.48
8[b]	6.26	1.0	-	6.61	115	0.058	15.575	30.3	4.48	77.9	0.84	0.47
9	6.26	1.0	-	11.66	127	0.092	19.864	25.7	6.08	66.2	0.71	0.40
10	6.26	1.0	-	11.59	131	0.088	19.713	25.9	5.79	65.8	0.71	0.40
11	6.26	-	0.1	7.13	120	0.060	14.979	28.1	4.46	74.9	0.81	0.45
12	6.26	-	0.1	5.45	119	0.046	15.657	36.7	3.58	78.3	0.84	0.47
13	6.26	-	0.1	16.40	119	0.138	25.197	30.5	6.94	50.3	0.54	0.31
14	6.26	1.5	-	7.15	234	0.030	29.781	28.0	4.54	149[c]	1.60	0.89
15	6.26	1.5	-	7.02	119	0.059	23.945	28.5	7.07	120[c]	1.29	0.72
16	6.26	1.0	0.1	7.19	119	0.060	16.020	27.8	4.84	80.1	0.86	0.48
17	6.26	1.0	0.1	7.30	119	0.061	15.828	27.4	4.85	79.1	0.85	0.48
18	6.26	1.0	0.1	5.99	121	0.050	16.406	33.4	4.06	82.0	0.88	0.49
19	6.26	1.5	0.17	9.72	119	0.082	8.048	30.9	2.19	26.8	0.29	0.16
20	6.26	1.5	0.1	9.19	122	0.075	8.530	32.6	2.14	28.4	0.31	0.17
21	6.26	1.5	0.04	9.58	121	0.079	8.615	31.3	2.27	28.7	0.31	0.18
22	6.26	1.5	-	9.06	119	0.076	12.312	33.1	3.13	41.1	0.44	0.25
23	6.26	1.5	-	9.43	119	0.079	23.149	31.8	6.12	77.3	0.83	0.47
CC-1	6.5	0.6	0.1	330	4046	0.0816	1,244.5	55.0	5.60	68.6	0.74	0.42

[a] Runs 1-3, and 6 were made with a heat input of ~280 watts; all others except CC-1 were made at ~500 watts.

[b] Rerun of 7 using same specimen.

[c] Steady-state conditions did not prevail as loadings are considerably above those allowed by F^- stoichiometry.

Table 5.2. Instantaneous Dissolution Rates Under Static Conditions

Dissolvent		Weight Loss	Specimen Area	Exposure Time	Reaction Rate
Zr M	Free F^- M	g	cm^2	min	mg/cm^2-min
0.75	2	0.0560	6.48	1.0	8.64
0.75	2	0.1172	6.41	2.0	9.14
0.83	1.5	0.1142	6.48	2.5	7.05
0.83	1.5	0.1119	6.39	2.5	7.00
0.92	1.0	0.1307	6.15	3.0	7.08
0.92	1.0	0.1143	6.21	3.0	6.14

was made by a batch dissolution of a weighed amount of Zircaloy-2. When this had dissolved, the element (15 plates, 7-13/16-in. x 2-11/16-in. x 0.068-in.) was lowered into the solution and dissolvent feed was begun. The reaction rate reported was calculated from the element weight-loss; samples of dissolver contents were taken every 5 min to check the "steady-state" operation, but results have not yet been received. The equipment will be modified and additional runs will be made to try to get higher rates and increase throughput.

5.2 Shear and Leach - B. C. Finney

A shear and leach program to determine the economic and technological feasibility of continuously leaching the core material (UO_2 or UO_2-ThO_2) from relatively short sections (1-in. long) of fuel elements produced by shearing is continuing. This processing method has the apparent advantage of recovering fissile and fertile material from spent power reactor fuel elements without dissolution of the inert jacketing material and end adapters. These unfueled portions are stored directly in a minimum volume form as solid waste. A "cold" chop-leach complex consisting of a shear, conveyor-feeder, and leacher is being evaluated prior to "hot" runs.

A 250 ton prototype shear including the feed mechanism and hydraulic (oil) system was received from the Birdsboro Steel Foundry and Machine Company and installed on the third floor of Bldg. 4505. The shear has been checked out and operated.

In operability demonstration tests, a porcelain filled Mark I fuel assembly was sheared. Rubber inserts were used on the outer and inner gags which hold the fuel bundle during the shearing operation. Although the rubber facing on the inner gag was badly deformed and torn away by the moving blade, the fuel assembly was sheared to less than 3 inches of the end. To date, eight porcelain filled Mark I fuel assemblies (7 at Birdsboro and 1 at ORNL) have been sheared with the present blade and the blade edges show essentially no signs of wear. However, there are some scored places on the side of the blade resulting from rubbing against the fuel bundle on the backward stroke. This is caused by the fuel bundle being moved forward in preparation for the next cut before the blade reaches the full open position. This situation can be remedied by improving the timing of the shear cycle.

Scouting tests operating the modified leacher as a conveyor feeder at ~2 rpm and at 15 degrees of inclination indicate less than 5% backmixing using a 2.5 liter batch per flight (1/2-in.-OD x 1-in. long stainless steel rod) and no backmixing occurs when charging a 2.0 liter batch. The results are based on a throughput of 20 batch charges of color coded stainless steel rods.

A single batch dissolution of ~600 g of crushed UO_2-ThO_2 pellets (Davison Chemical Company) using 13 $\underline{M}$ HNO_3, 0.04 $\underline{M}$ F^-, and 0.10 $\underline{M}$ Al^{+++} as the dissolvent at a feed rate of ~10 ml/min resulted in 73% dissolution in 6-1/2 hours.

5.3 U-C Fuel Processing - B. A. Hannaford

Proposed reactor fuels of the uranium-graphite type contain compounds (UO_2, UO_2-ThO_2, UC_2, UC_2-ThC_2) generally in the form of 100-200 μ particles, dispersed in a graphite matrix. The fuel particles may be uncoated, or coated with a refractory (Al_2O_3, pyrolytic carbon); fuel elements may be coated with a carbide compound - such as siliconized SiC - or may contain cylindrical cores of unfueled graphite.

As suggested by their descriptions, the fuel types vary considerably in processing difficulty. While all graphite fuels could be processed by the grind-leach method, other processes offer potential advantages for certain classes of graphite fuel - such as the 90% HNO_3 process for graphite containing uncoated fuel particles, and combustion-dissolution for graphite containing pyrolytic carbon-coated fuel particles. Since all three processes require engineering development work, some order or priority is required. Accordingly, priorities must be based on answers to: (1) which graphite fuels would first be available for processing in any significant quantity, (2) which fuel type shows the greatest promise and what is the corresponding best processing method, (3) what work could be done on the most universal process: grind-leach.

Priorities established were:

1. Demonstration of a process for graphite fuels containing uncoated UC_2 or UO_2. The 90% HNO_3 process appears to be suitable for this fuel type, if a portion of the reagent is modified to provide for recovery of uranium from uranium-containing carbide element coatings, which are not leached by 90% HNO_3 alone. Work would continue on the semicontinuous 90% HNO_3 flowsheet to establish the best range of flow rates, temperature, time, acid/wash water ratio, etc.

2. Combustion-Dissolution. All the graphite fuels can be burned in oxygen, following at least a rough crushing operation to destroy the integrity of any fuel element coating. After combustion, dissolution in HNO_3 or HNO_3-HF solution recovers U and Th from fuels which contained uncoated or pyrolytic carbon-coated particles. Engineering-scale work will be done to determine the optimum degree of crushing, suitable combustion chamber geometry with respect to criticality and heat transfer, procedure for controlling the rate of combustion, methods for transfer of ash to a dissolution tank for dissolving uranium and thorium, etc.

3. Fine Grinding. Graphite fuel containing alumina-coated fuel particles apparently can be processed only by grind-leach; fuel compacts containing pyrolytic carbon-coated fuel particles are amenable to aqueous processing only if the fuel has been ground fine enough to fracture each fuel particle coating. However, fine grinding work was given third priority because indications are that alumina-coated fuels may never become important due to their temperature limitation in graphite, and because combustion-dissolution can possibly be employed for pyrolytic carbon-coated fuel.

The principal problems to be solved are: (1) demonstration of a machine for fine-grinding fuel compacts having a coating of highly abrasive material, e.g., silicon carbide, present

in concentrations as high as 20 wt %, and (2) size classification of the product to produce -200 mesh powder with a minimum of dusting. The standard fine-grinding device for abrasive material - the ball mill - probably cannot be used because of criticality considerations. The feasibility of using some type of hammer mill or fluid energy mill will be determined and some method of continuous size classification and dust collection will be investigated.

5.4 SRE Dejacketing Studies - G. A. West

Mechanical dejacketing techniques are being demonstrated and evaluated in the ORNL High Level Segmenting Facility, Bldg. 3026-D, by processing NaK bonded, stainless steel clad uranium fuel from the Sodium Reactor Experiment, Core I, burned to about 675 MWD/ton and decayed approximately 2 years. Fifteen fuel clusters have now been mechanically dejacketed. The processing campaign will be completed upon dejacketing the remaining 11 clusters.

A total of 5 fuel clusters (345 kg U) from the second carrier shipment of 10 clusters, 7 rods per cluster, 12 slugs per rod, were dejacketed at an average rate of 4.8 kg U/hr, and ~2.4 kg U/hr when including equipment maintenance time. Uranium and plutonium were not found in the NaK discharged during the dejacketing operation but cesium was detected in significant amounts.

A pictorial presentation of receiving a fuel shipment, charging fuel to the dejacketing facility and stepwise processing of an irradiated fuel cluster and rod is presented in Figures 5.2 through 5.20. Figures 5.7 through 5.20 were photographed through the shield windows consisting of 6 inches of glass and ~5 ft of zinc bromide solution (3.2 g/cc).

The slugs from only 2 rods of the 5 clusters were expelled by hydraulic flushing, 28 rods were dejacketed by forcing a jackscrew through the length of the jacket and 5 rods were cut near the 12 slug junctures and individual slug jackets slit longitudionally in an auxiliary dejacketing die and the jacket pried from the slugs.

Growth and warpage of the slugs from the 675 MWD/ton burnup was evidenced by measurements made which show a maximum elongation of 6.25% and 5.2% increase in diameter, an original slug is 0.75-in.-OD x 6-in. long. Profile measurements show that most slugs are cambered from 7 to 20 mils. A typical profile measurement is shown on a slug from the center rod of a cluster:

Distance from End of 6-in. long Slug in.	Camber mils
1/4	7.15
1	17.2
2	20.75
3	17.7
4	12.35
5	7.25
5-3/4	3.6

UNCLASSIFIED
PHOTO 53627

Fig. 5.2. SRE core I fuel shipment in 30 ton carrier (38" dia x 12'-7" long). Received at Y-12 spur track of Oak Ridge National Laboratory from Atomics International, Conoga Park, California.

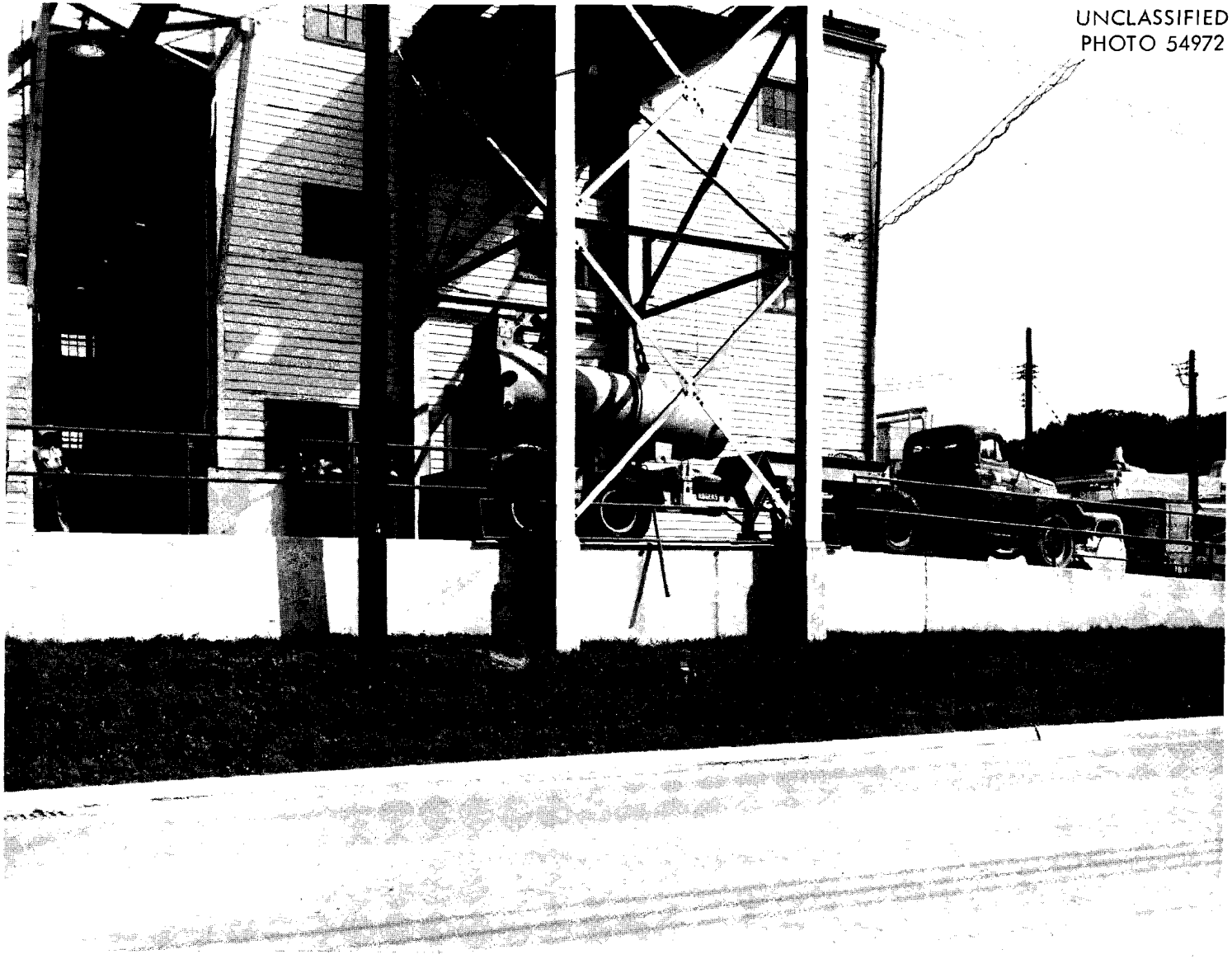

Fig. 5.3. SRE core I fuel shipment in 30 ton carrier arriving at the Oak Ridge National Laboratory Segmenting Facility, X-10 Area, Building 3026-D.

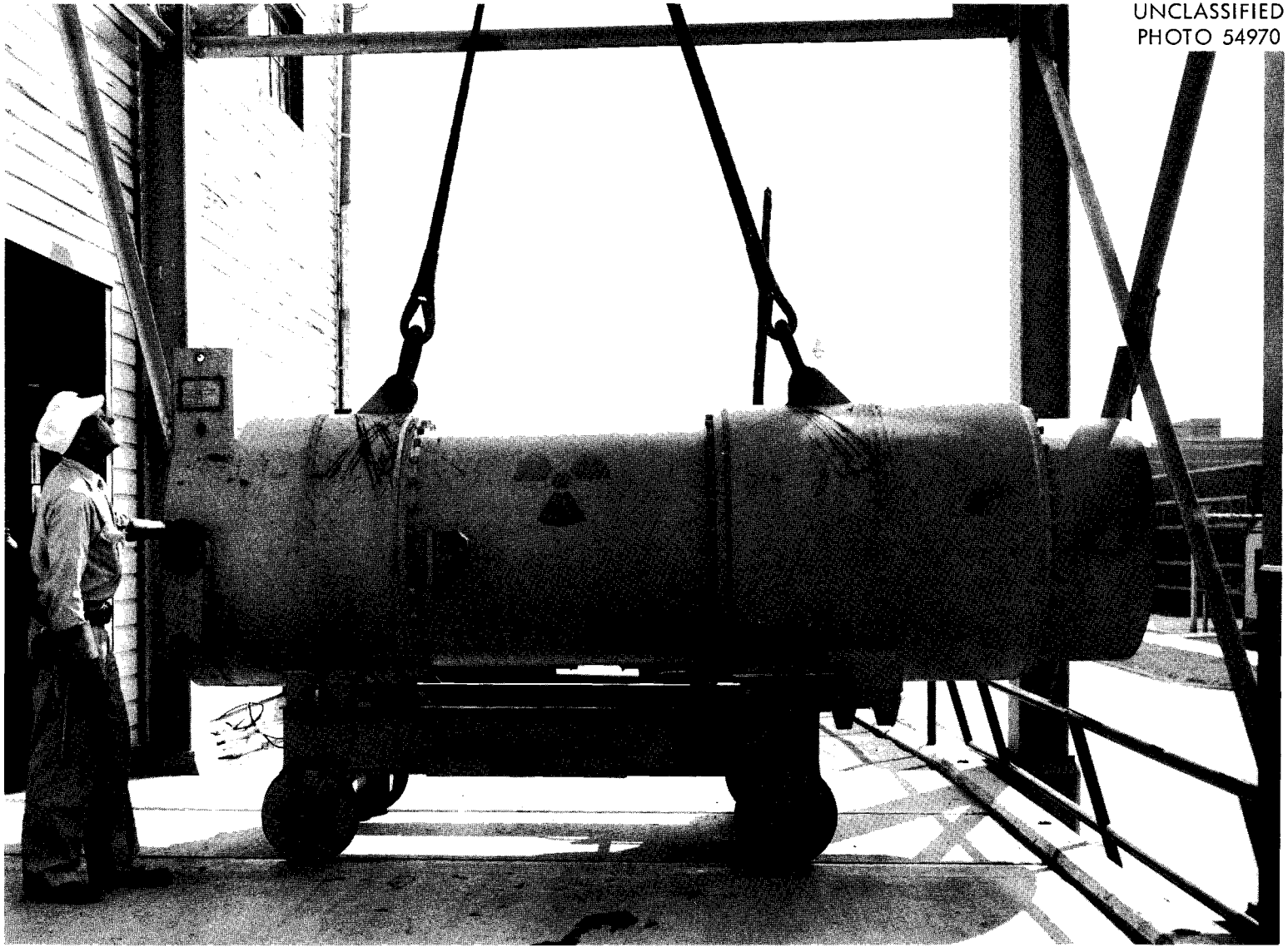

Fig. 5.4. 30 Ton boral poisoned carrier on tracks leading to charging face of dejacketing cell – Building 3026-D Oak Ridge National Laboratory.

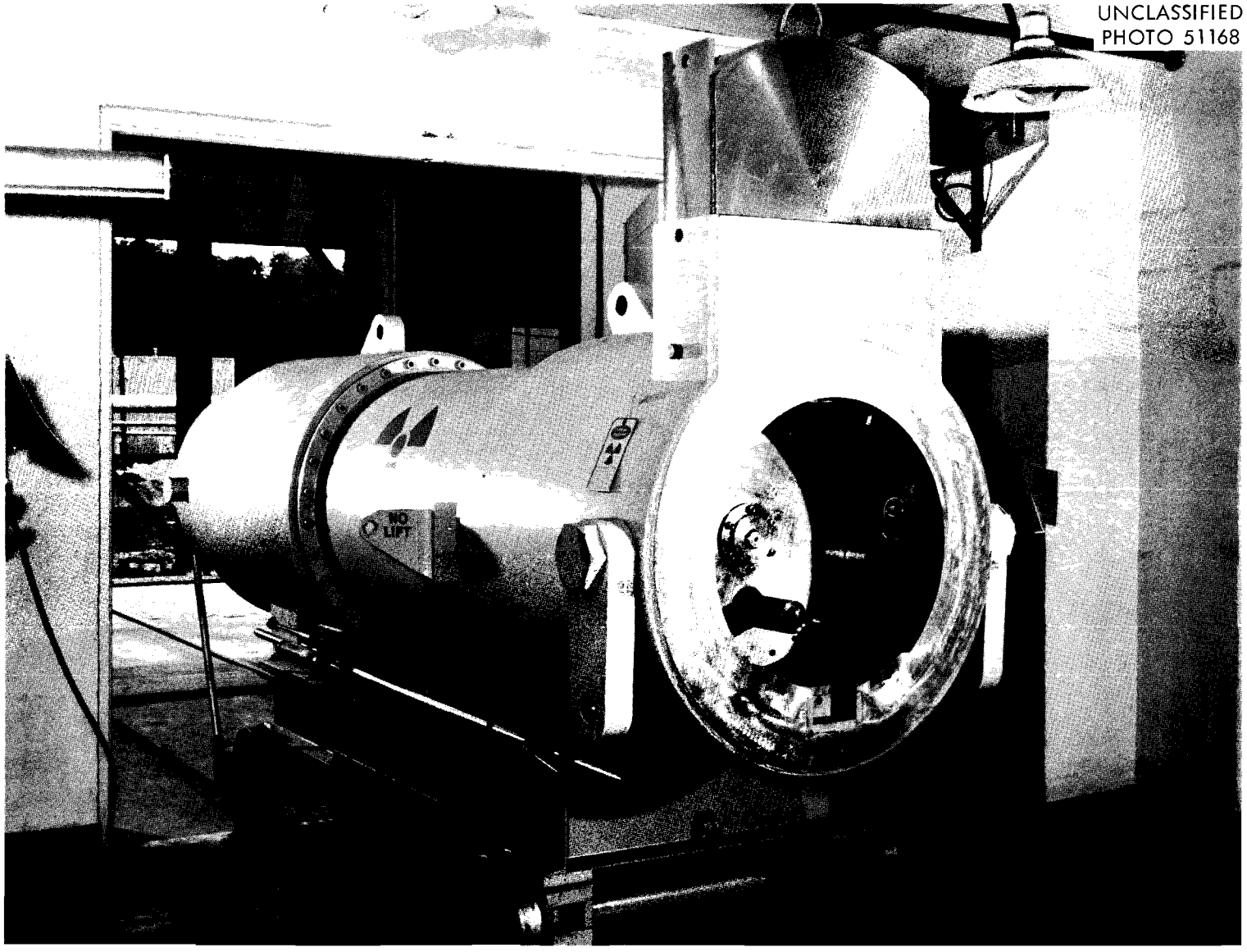

Fig. 5.5. Carrier containing prototype canisters showing method of discharging single canister containing unirradiated fuel cluster forward into cell.

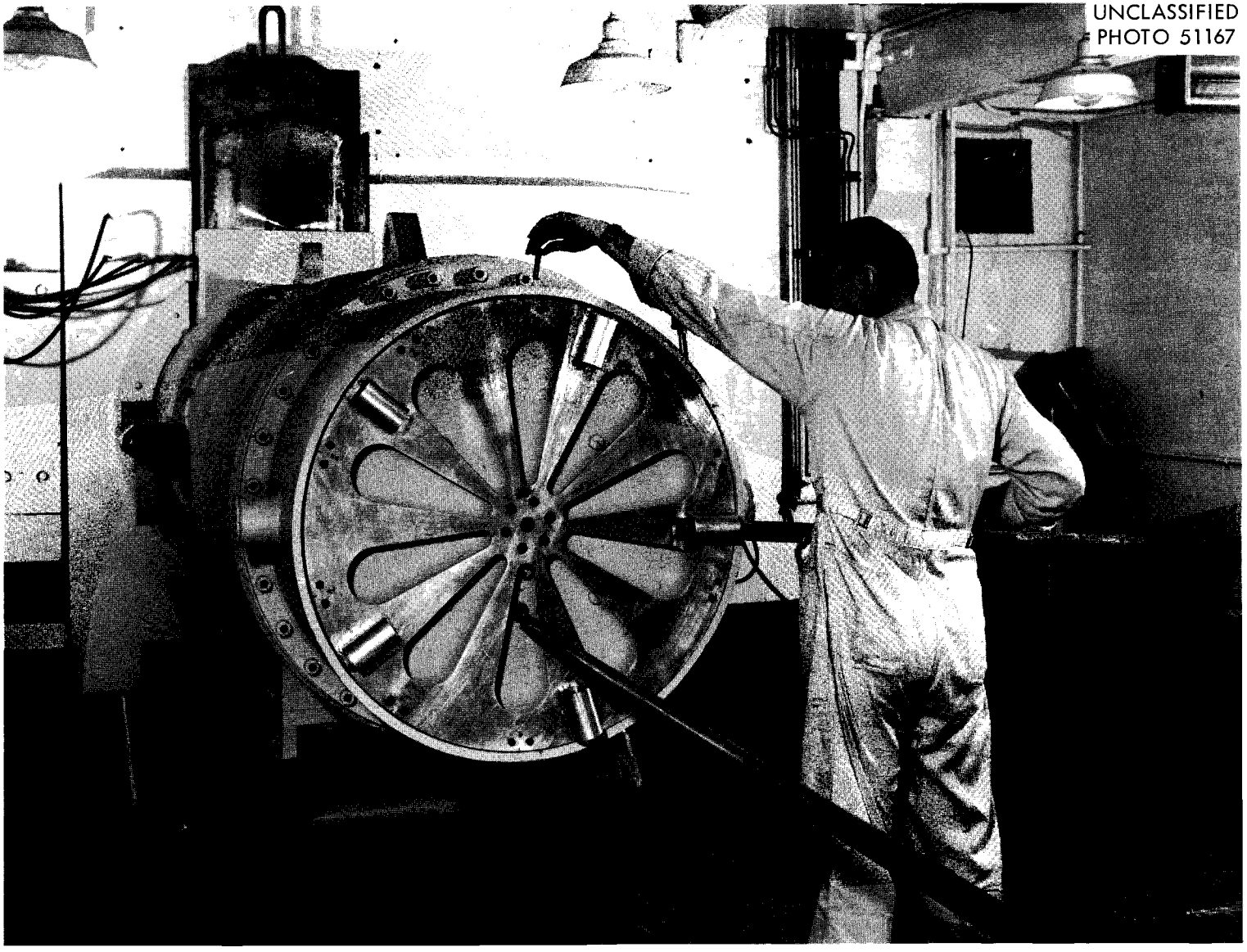

Fig. 5.6. Carrier against charging face of dejacketing cell – wheel at rear permits selection of canister from one of ten boral poisoned compartments.

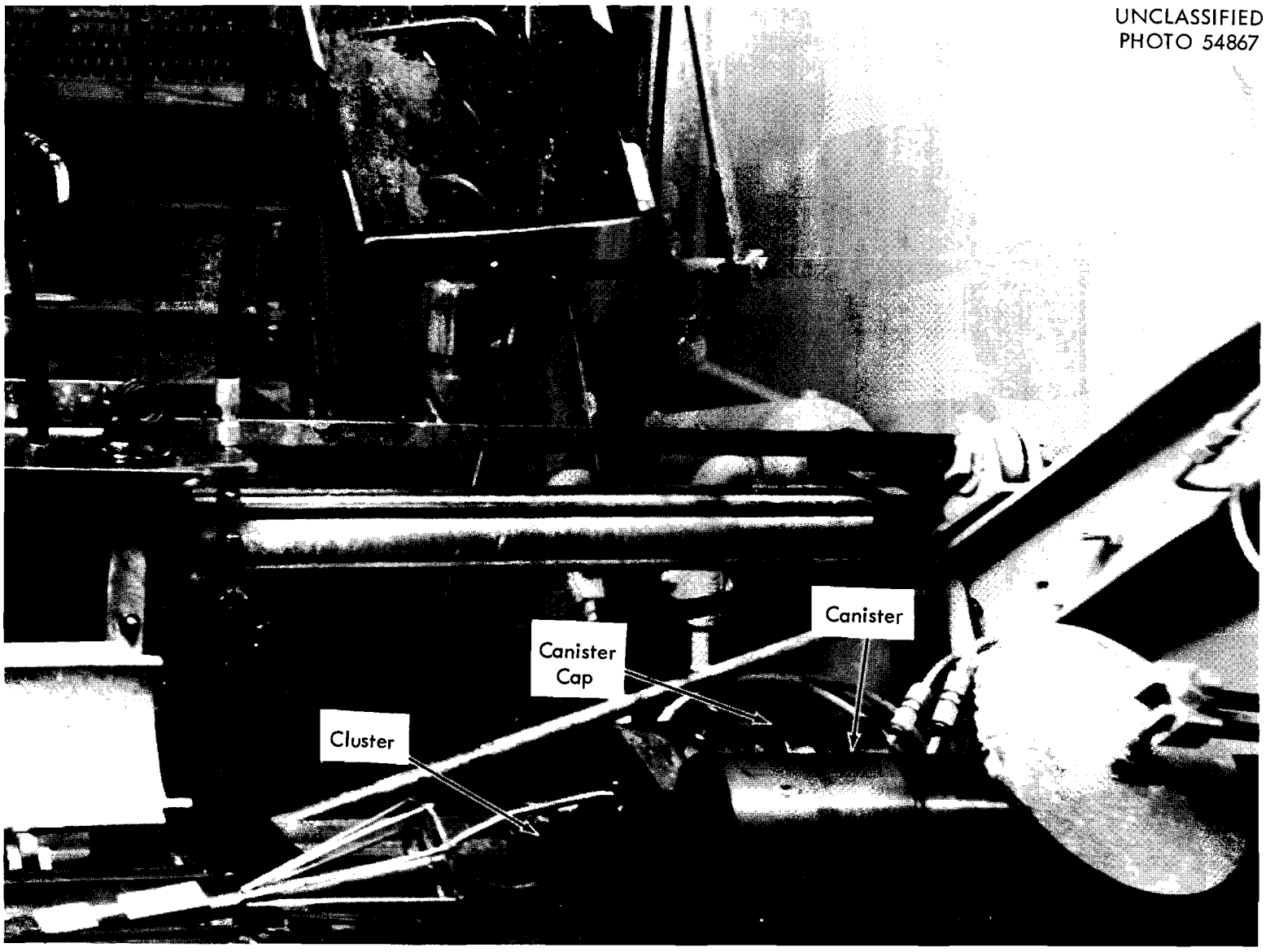

Fig. 5.7. Cluster of SRE core I fuel being withdrawn by grappling hook from canister pushed from carrier into dejacketing cell.

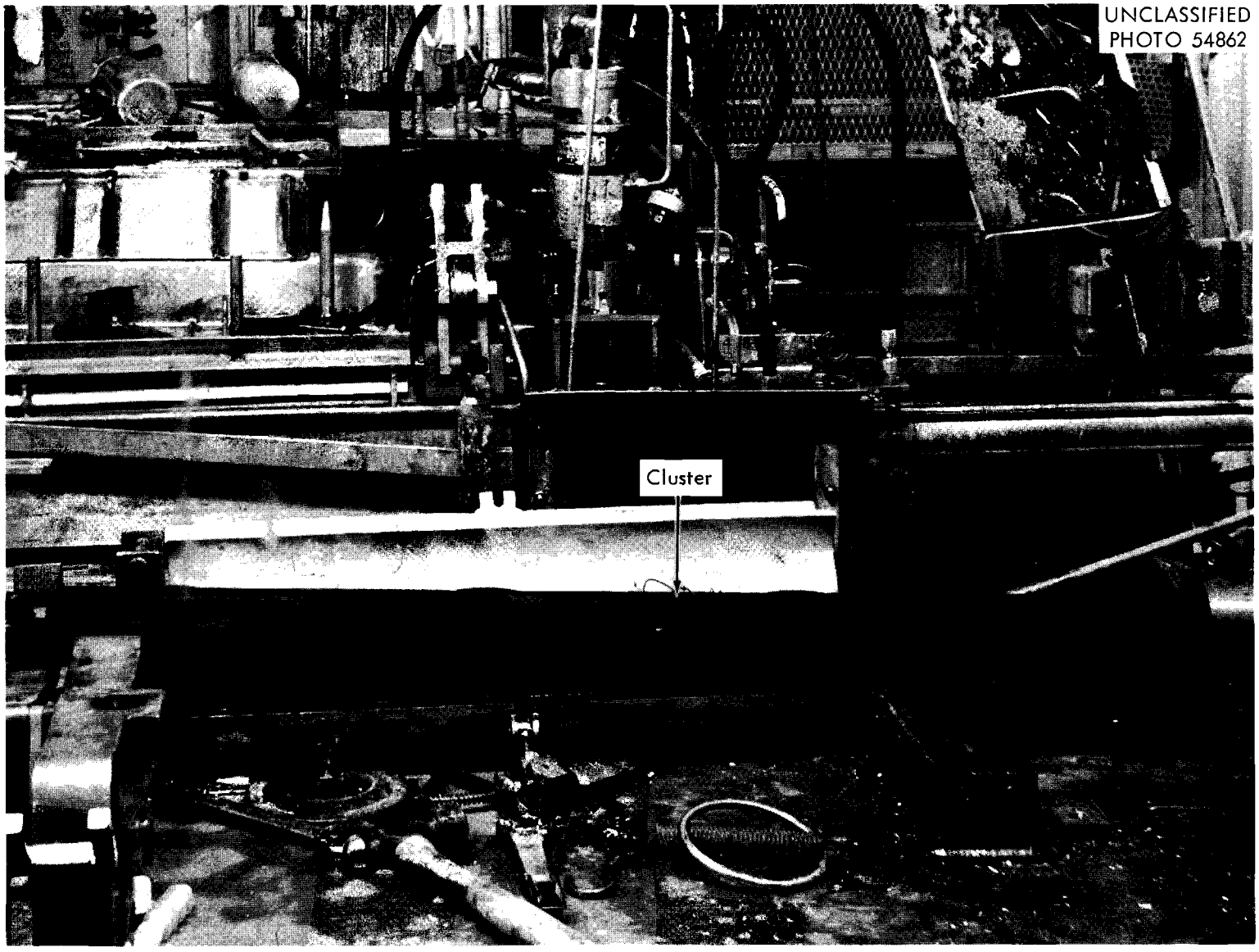

Fig. 5.8. SRE core I cluster in saw trough preparatory to removal of inert ends by abrasive disc sawing. Hydraulic dejacketing unit in background.

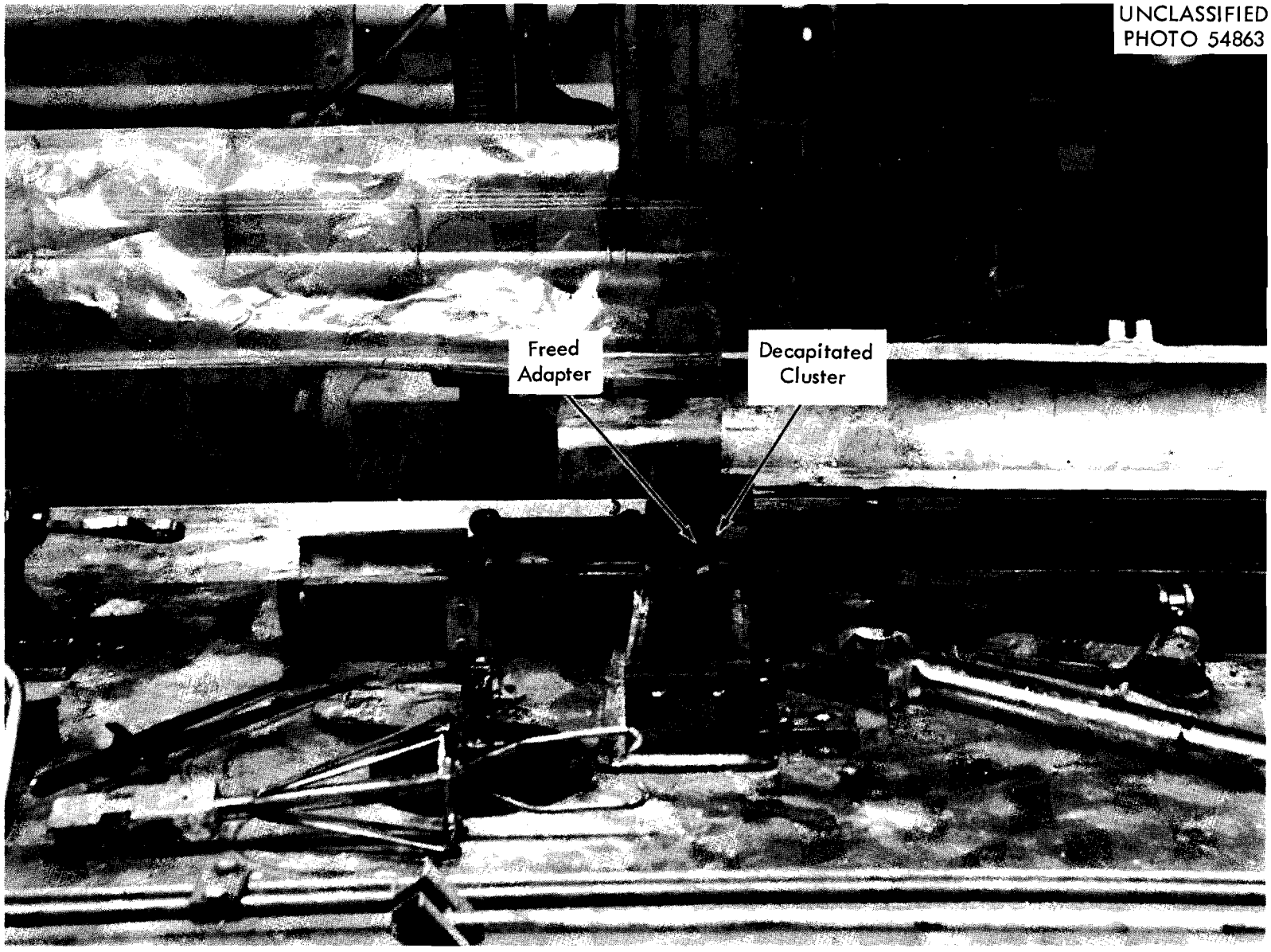

Fig. 5.9. Top adapter of SRE core I fuel cluster freed by sawing.

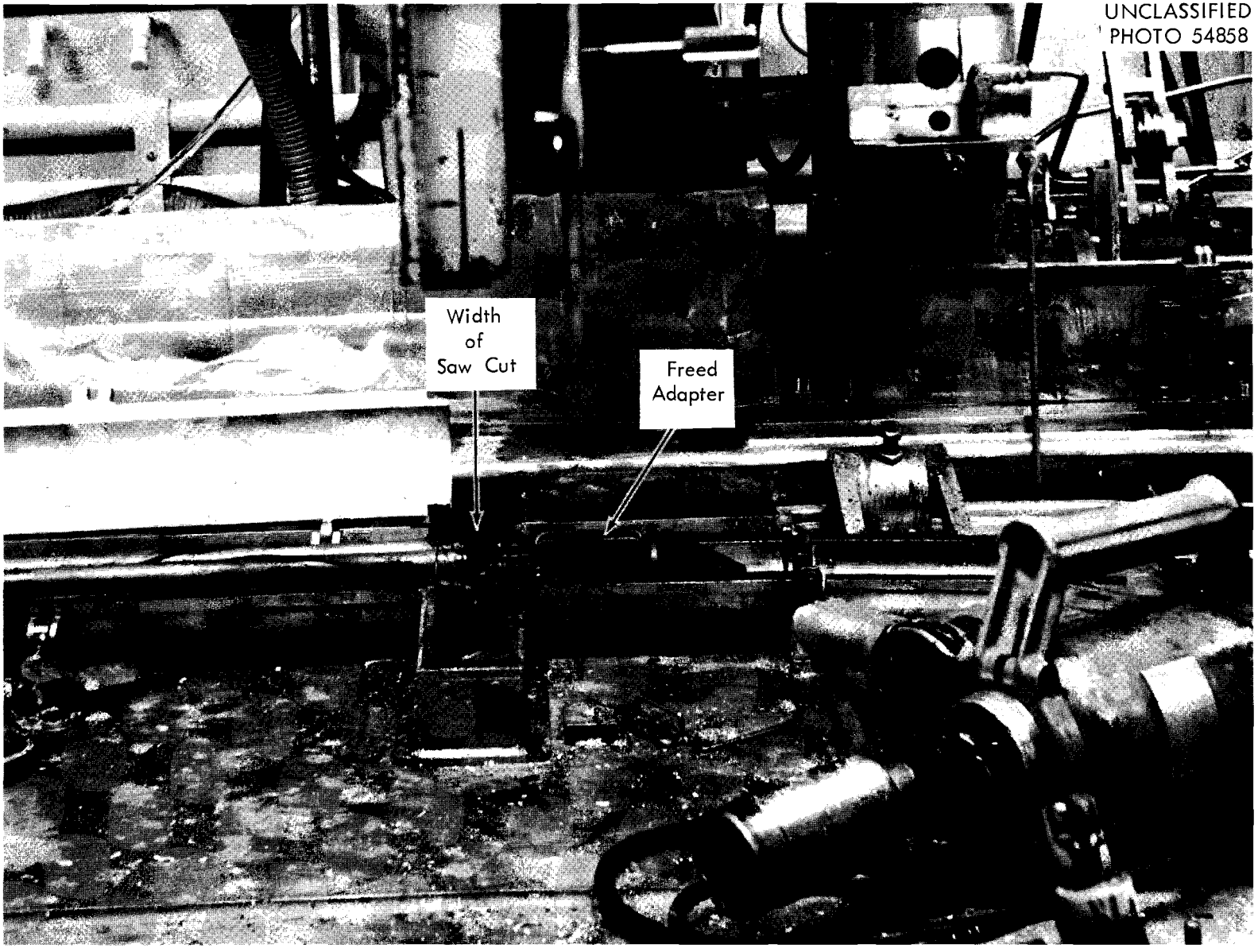

Fig. 5.10. Bottom adapter of SRE core I fuel cluster freed by sawing.

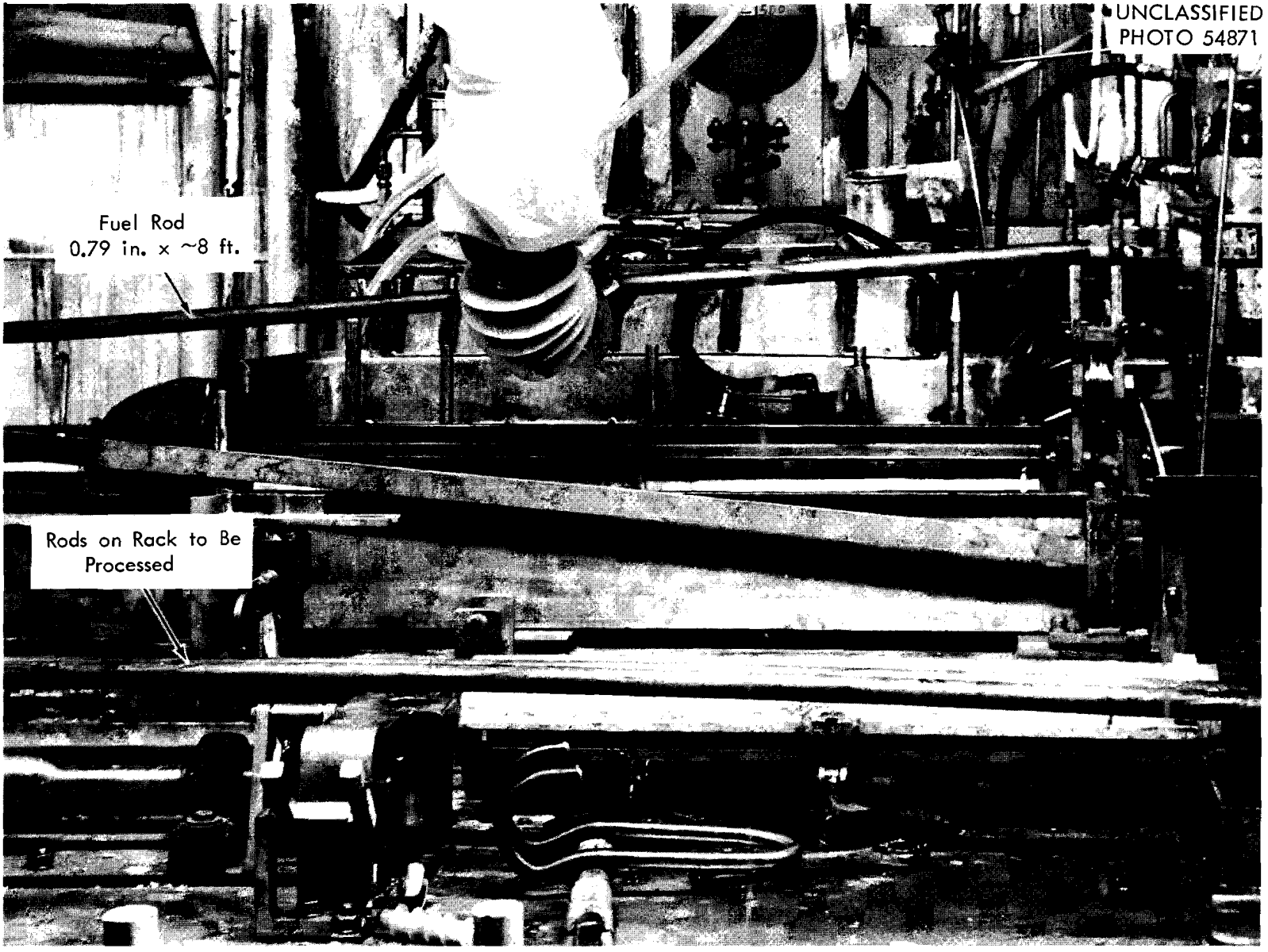

Fig. 5.11. One of seven fuel rods freed by sawing being laid into dejacketer trough.

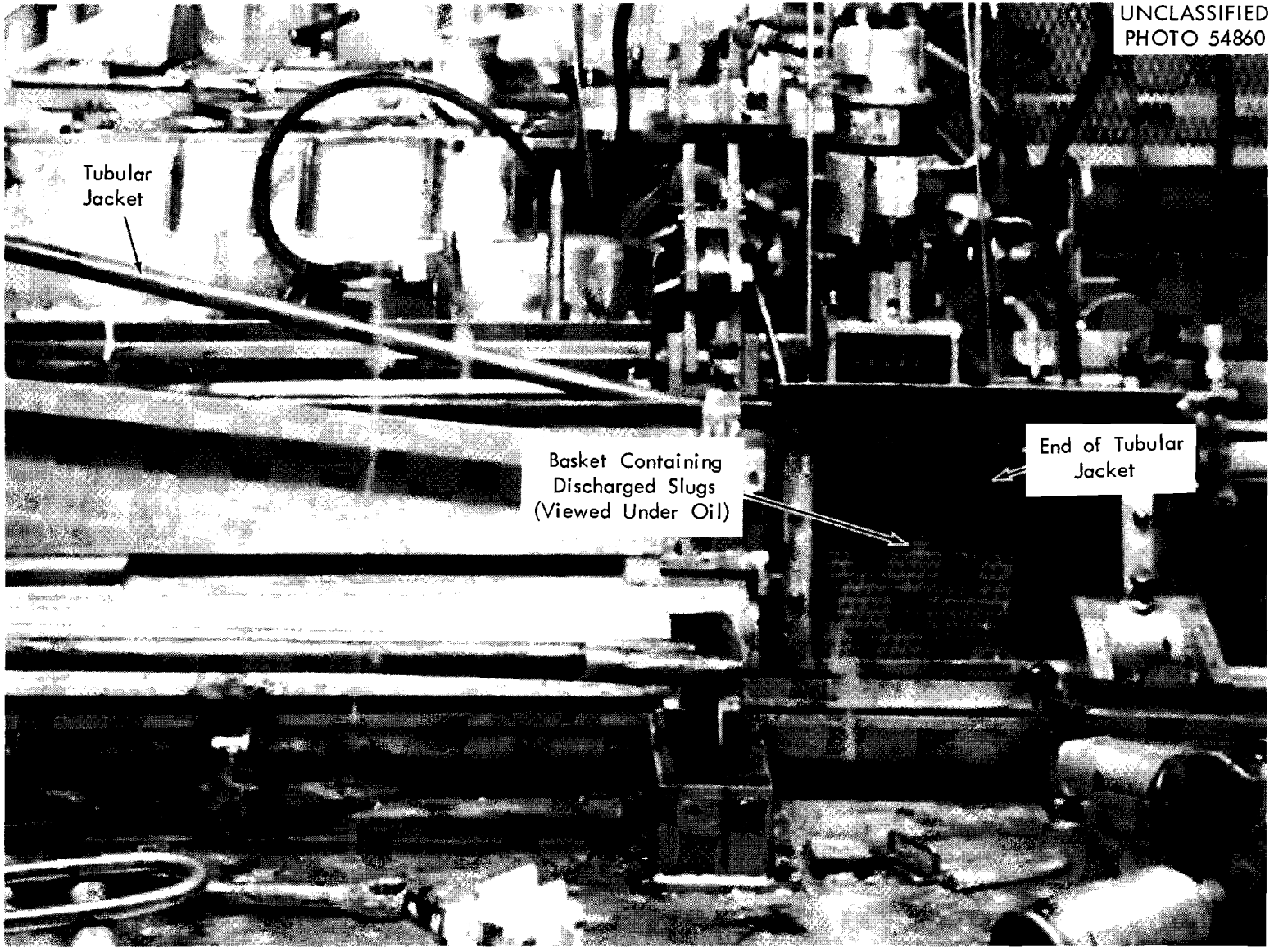

Fig. 5.12. Stainless steel jacket emptied of slugs being inserted in split shaft for flattening and winding into a coil under Bayol D blanketing oil.

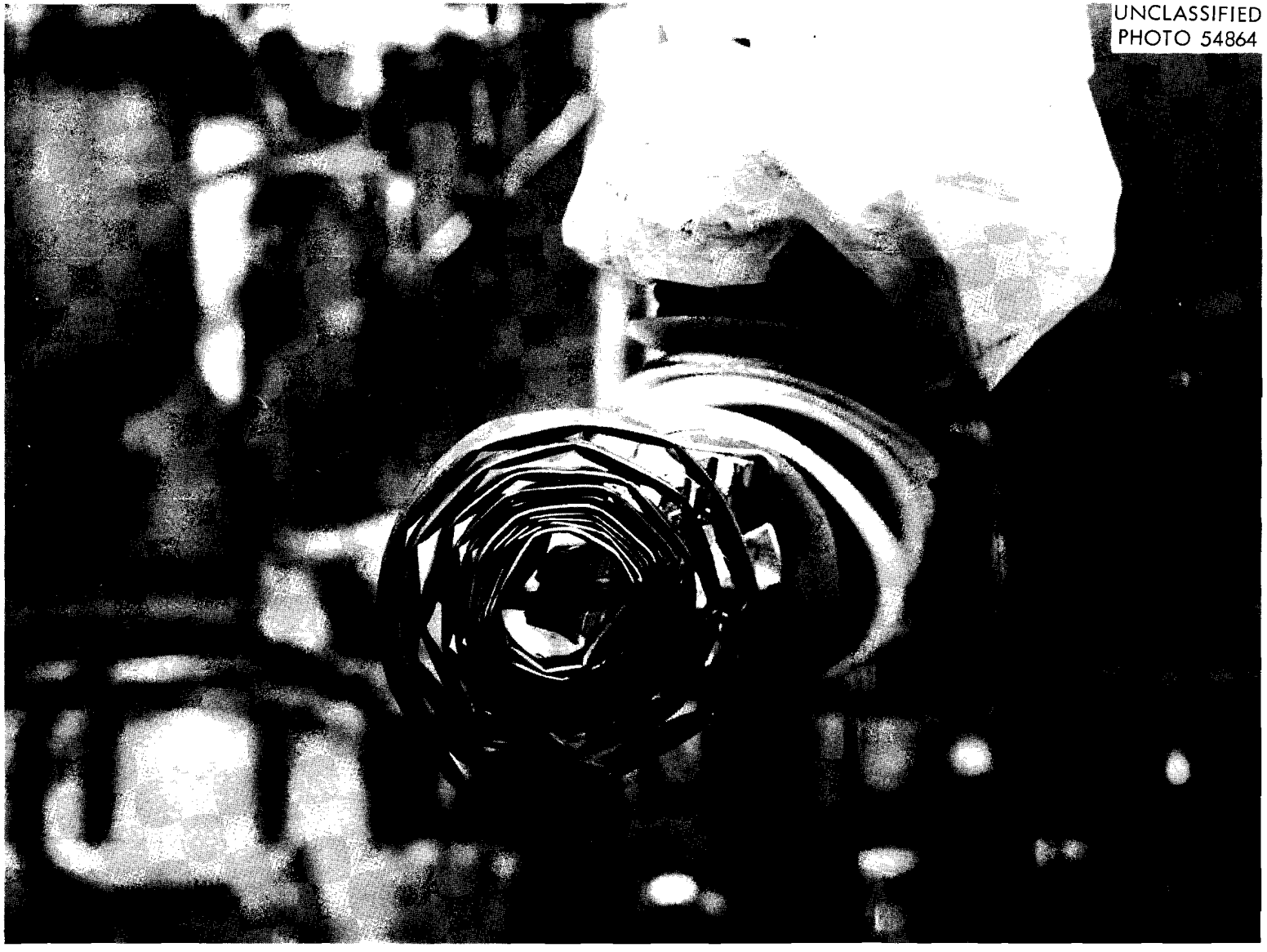

Fig. 5.13. Flattened and coiled stainless steel jacket approximately 8 in. diameter. Note: crumpling and spring back of tubular jacket indicating embrittlement.

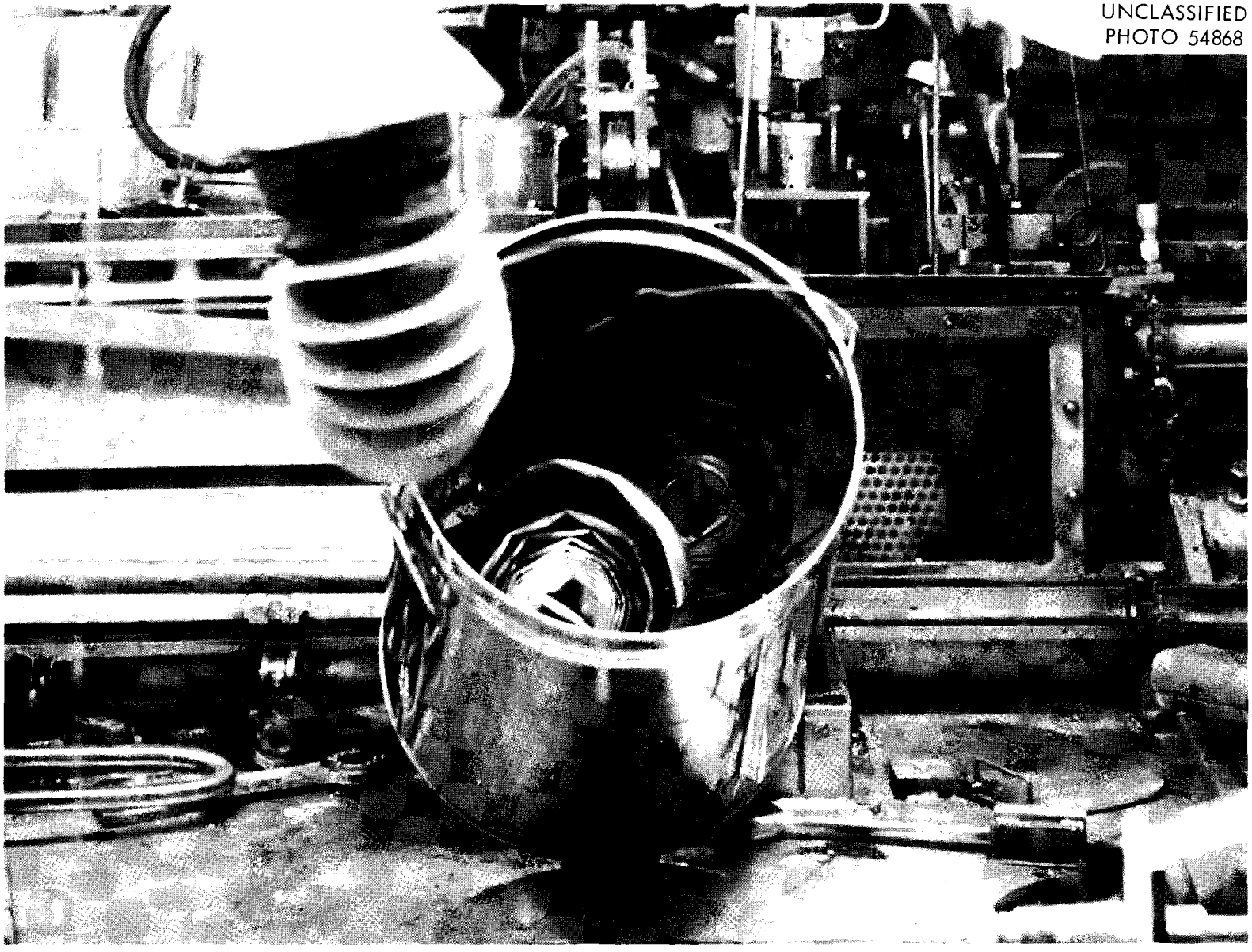

Fig. 5.14. Jackets and spacer wires in 3 gallon can used for disposal of inert metal by burial in the ground.

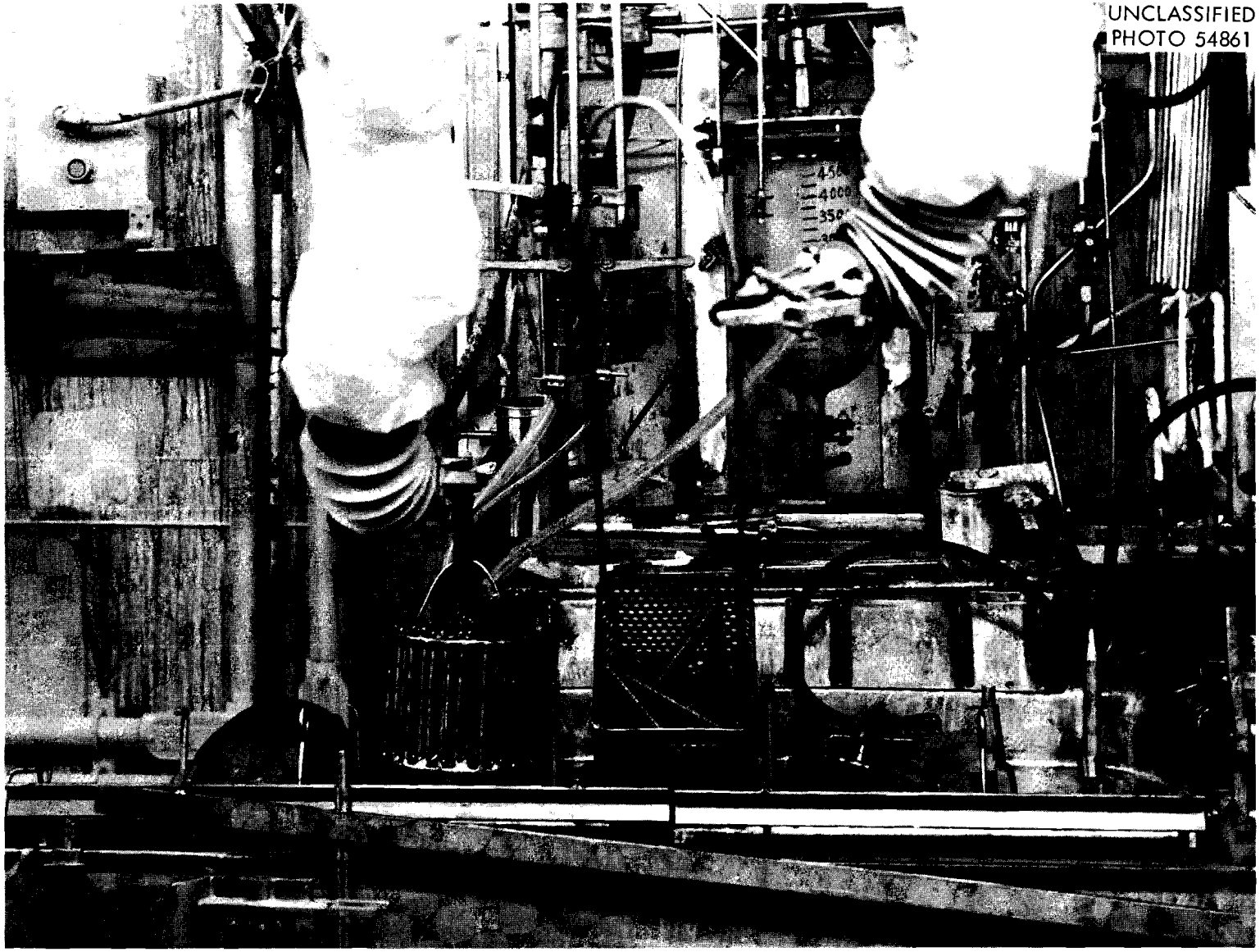

Fig. 5.15. Slugs (12) from one SRE core I fuel rod being transferred from dejacketer basket to steam cleaning basket. Slugs are 0.75 in. dia and 6 in. long. NaK reactor in background.

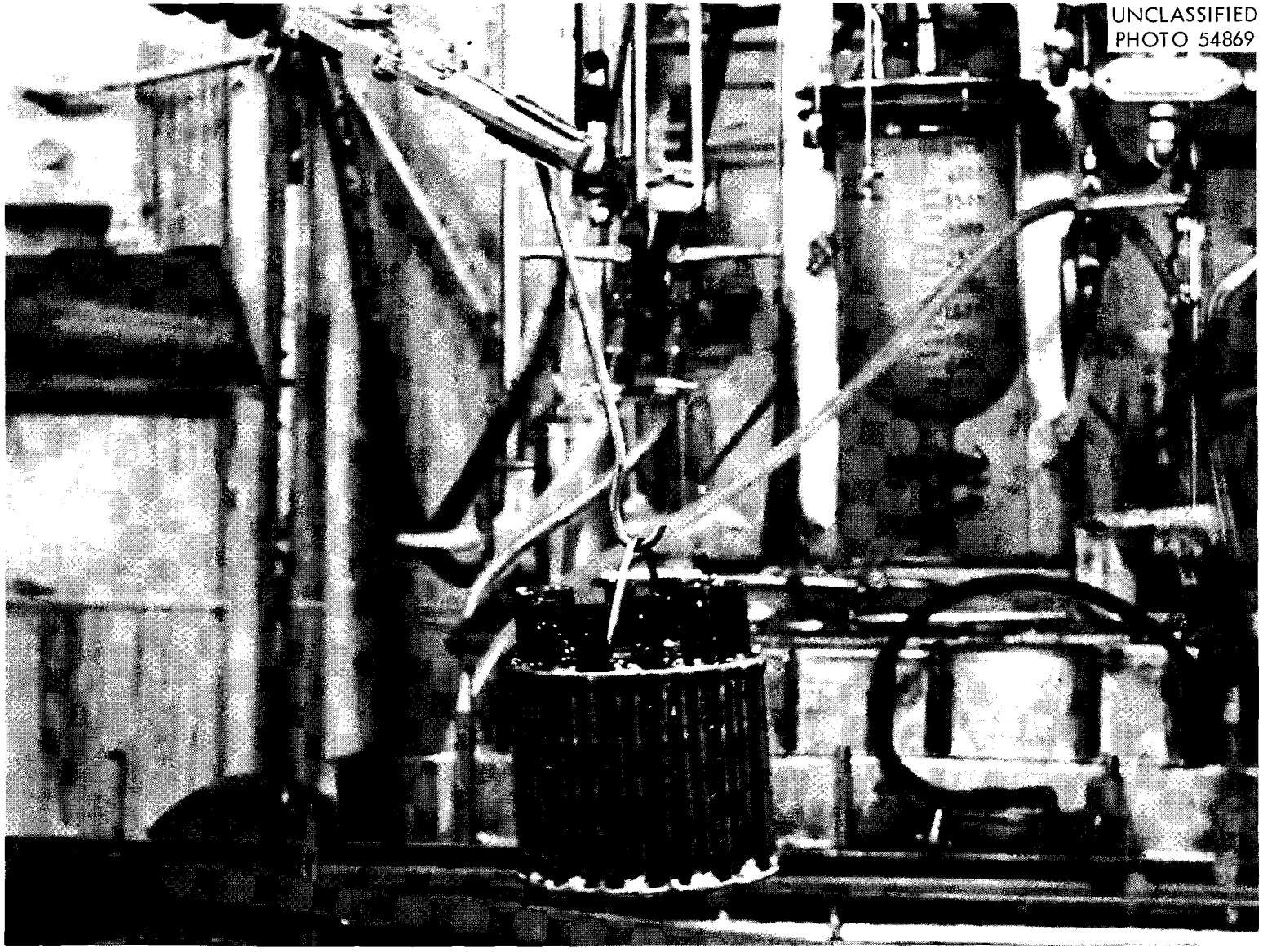

Fig. 5.16. Slugs from one SRE core I fuel rod being transferred to steam cleaner. Note: globules of NaK clinging to oily surfaces of uranium slugs.

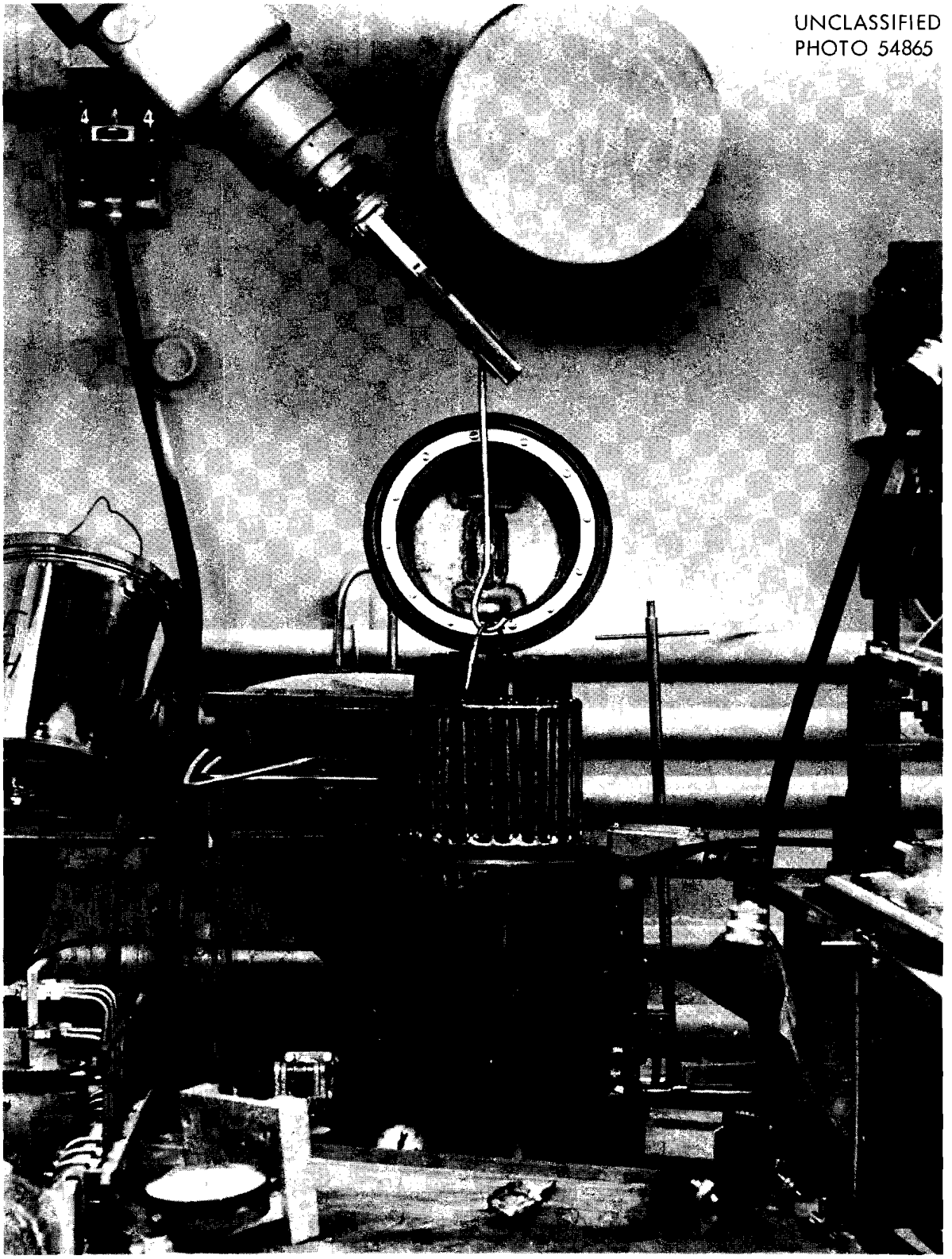

Fig. 5.17. Cleaned uranium slugs being withdrawn from steam cleaner.

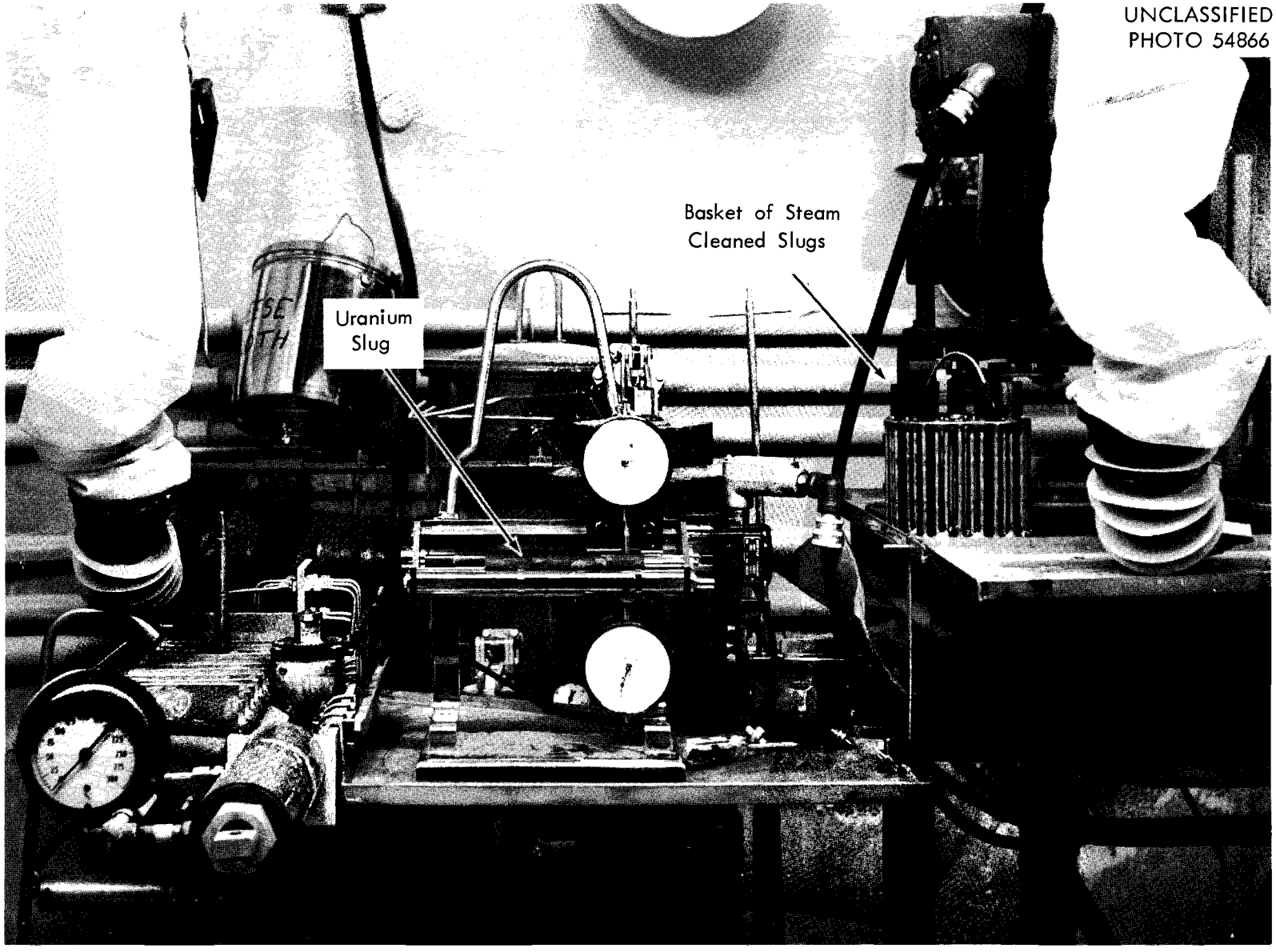

Fig. 5.18. Uranium slug in Profilometer for measurements of swelling and camber.

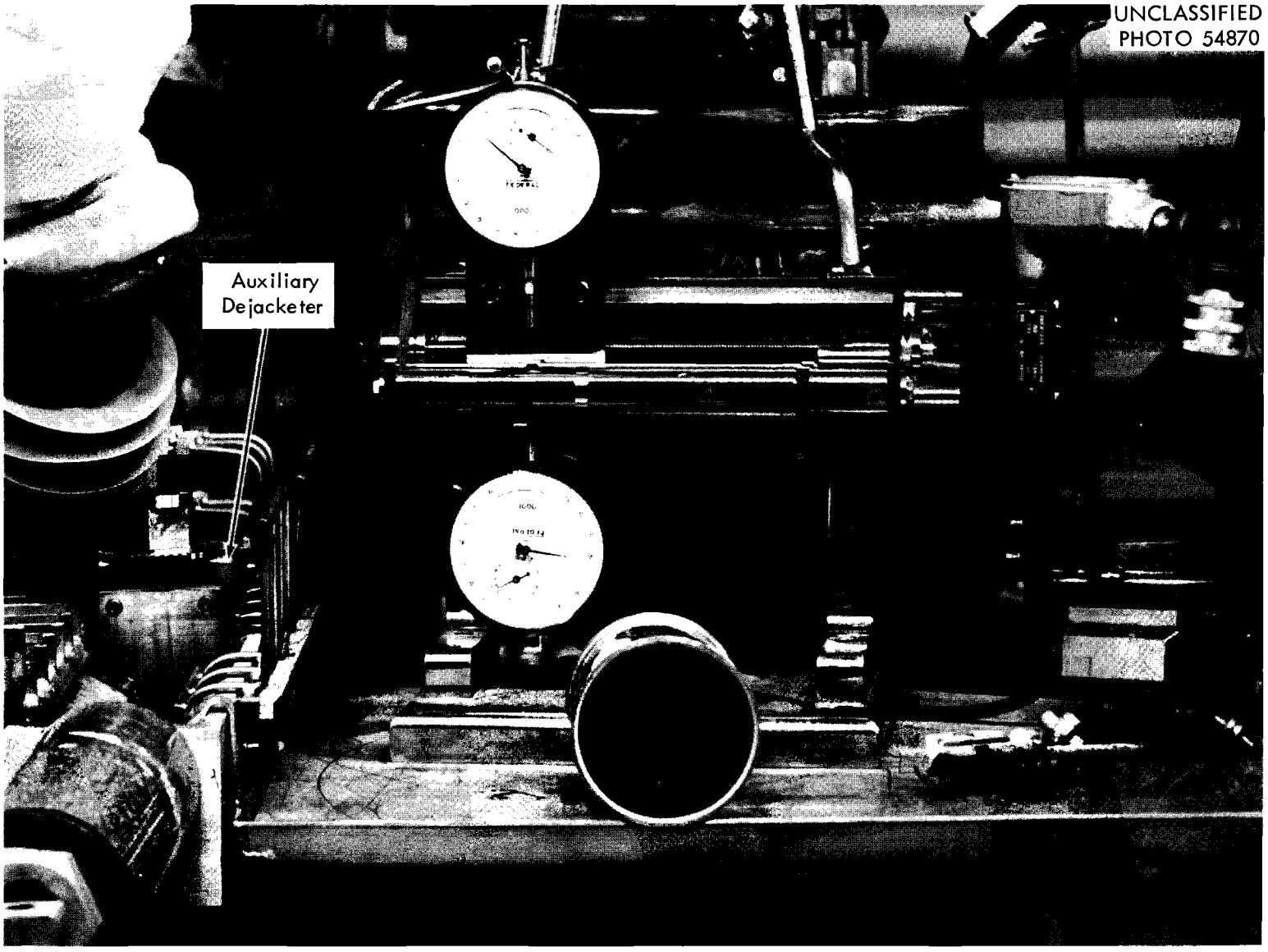

Fig. 5.19. Slugs (0.75 in. dia) from one SRE core I fuel rod in aluminum can preparatory to sealing of the lid Profilometer in background

UNCLASSIFIED
PHOTO 54859

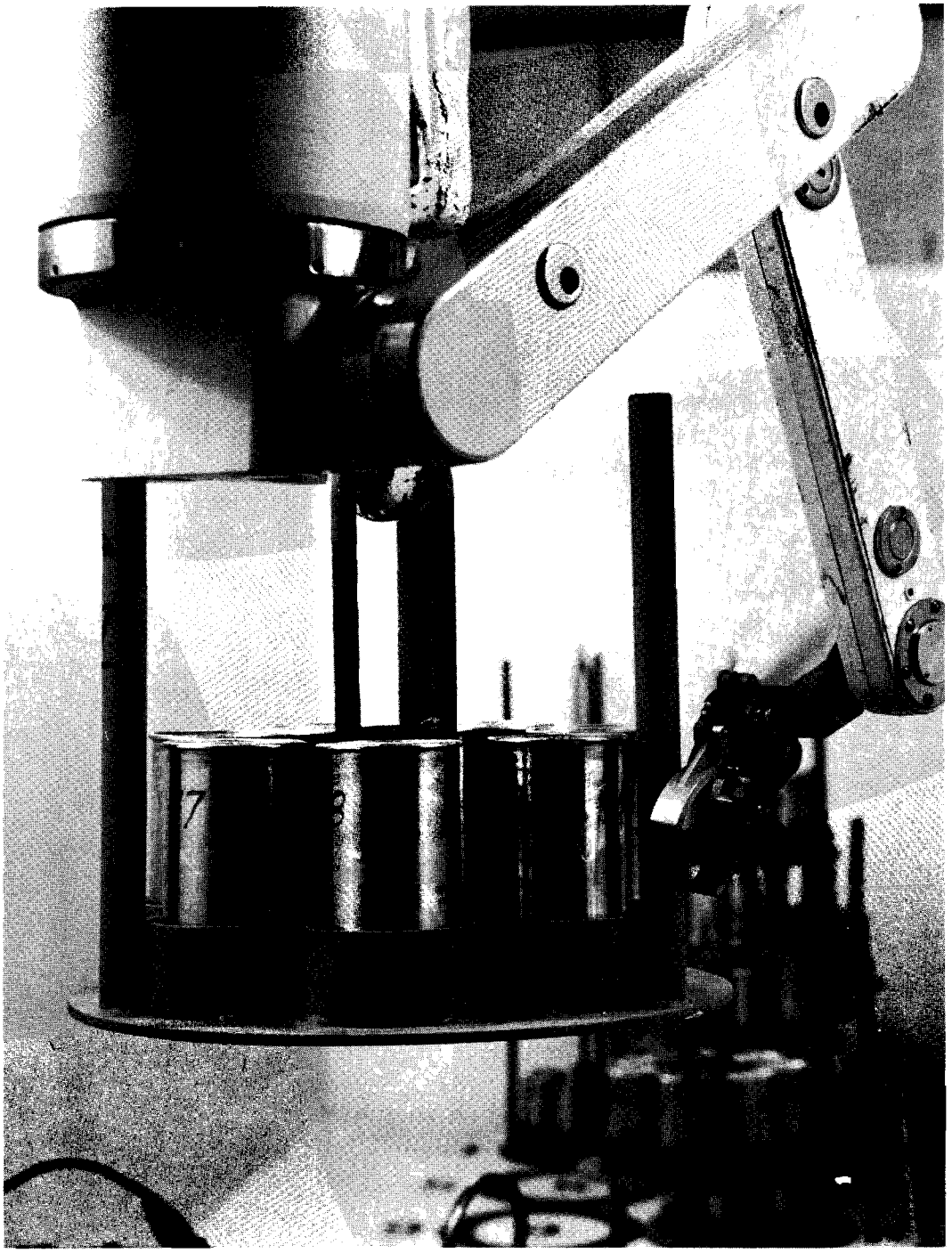

Fig. 5.20. Storage rack containing 7 aluminum cans filled with the contents of one SRE core I cluster (~70 kg U) in process of being stored in storage cell. Note other filled storage racks in background.

Measurements made on 5 of the 10 mil wall tubular jackets before and after applying 1500 psig internal hydraulic pressure show an expansion of 7 to 20 mils in diameter compared to 40 to 50 mils expansion exhibited on unirradiated jackets. One cluster of fuel jackets exhibited extreme hardness; there was no detectable expansion after pressurizing from 2400 to 2700 psig. This pressure applied on unirradiated jackets would result in rupturing and expansion of $>$ 300 mils as demonstrated in pre-operational tests.

The disposal of about 3,000 g of liquid metal NaK progressed without an incident or transfer difficulty. The NaK from 5 rods was coated on the slugs and bridged across the tube above the slugs in a waxy form so that it could not be disposed by vacuum transfer to the NaK reaction vessel. Disposal was accomplished in the slug cleaning vessel where steam was impinged against both the slugs and short sections of the NaK filled jackets.

Results of analysis of the liquid metal NaK from the center rod of 3 different clusters are as follows:

	Sample Number		
	A-18-1	A-19-2	A-23-3
U	none	none	none
Pu	none	none	none
Gross β (CPM/g)	3.59×10^7	8.14×10^6	5.45×10^6
Gross γ (CPM/g)	6.46×10^6	1.89×10^7	2.08×10^8
TRE, β (CPM/g)	$< 2 \times 10^4$	2.95×10^4	$< 3 \times 10^3$
Cs^{137} (CPM/g)	6.03×10^6	1.07×10^7	5.4×10^6
Na (%)	28	24	22
K (%)	72	76	78
O_2 (ppm)	2,890	16,600	3,270

6.0 REACTOR EVALUATION STUDIES

J. C. Suddath

6.1 Heat Transfer from Spent Reactor Fuels during Shipping. - J. S. Watson

Experimental measurements of temperature rises in mock fuel elements in a horizontal shipping carrier have been continued. The apparatus, which has been described previously (Unit Operations Monthly Report, March 1961) consisted of a 12-in.-dia SS container holding bundles of 5/16-in. electrically heated mock fuel tubes. Thus far bundles containing up to 64 tubes have been used. The results of some sample runs using this larger tube bundle are shown in Tables 6.1 through 6.6. Heat generation rates up to 0.0514 watts/tube-cm were employed by changing the voltage to the tubes, and the carrier wall temperature was varied by adding different layers of insulation to the container.

As in previous experiments using smaller tube bundles, the effects of both convection and radiation (and/or conduction) are evident. The convective flow of air through the bundles causes nonuniform carrier wall temperatures and higher tube temperatures near the top of the bundle than near the bottom. Radiation (and/or conduction) are probably largely responsible for the peak tube temperature being nearer the center than the top row of the bundle.

Along with the measured temperatures in Tables 6.1 through 6.6 calculated or predicted temperatures are shown based upon the relatively simple and supposingly conservative procedure described in the Unit Operations Monthly Report, June 1961. In general, the calculated and observed temperatures are in good agreement. The average difference between the temperatures is less than 15°C for all of these runs. (One should note that since all tube temperatures are not measured, this average is a function of which temperatures were and were not measured and used in the average. The measurements were made in scattered tubes throughout the bundle to minimize this effect.) The calculated results appeared to be closer to the measured temperatures near the center of the bundle. This is fortunate since this is where the peak temperature occurs and is the region of most interest. It is also fortunate that in this region the difference between the predicted and measured temperatures is always positive and the error in the predicted temperatures is on the safe side. However, it remains surprising that the predicted temperatures calculated with a supposingly conservative method are so close to the measured temperatures and very near the top of the bundle actually below the measured temperatures.

Table 6.1. Temperature Distribution in 64 Tube Bundle

1-1 87.78	1-2 101.61	1-3 128 109.07	1-4 129 112.37	1-5 130.5 112.37	1-6 128 109.07	1-7 112.5 101.61	1-8 106 87.79
2-1 101.61	2-2 121.81	2-3 132 132.78	2-4 135 137.58	2-5 134 137.58	2-6 132 132.78	2-7 114 121.81	2-8 101 101.61
3-1 109 109.07	3-2 124 132.78	3-3 137 145.72	3-4 143 151.40	3-5 151.40	3-6 145.72	3-7 132.79	3-8 109.08
4-1 108 112.37	4-2 121.5 137.58	4-3 136 151.40	4-4 157.49	4-5 157.50	4-6 151.40	4-7 137.58	4-8 112.37
5-1 112.37	5-2 137.58	5-3 129 151.40	5-4 132 157.50	5-5 135 157.50	5-6 130 151.40	5-7 137.58	5-8 104 112.37
6-1 109.07	6-2 132.78	6-3 123 145.72	6-4 126 151.40	6-5 130 151.40	6-6 125 145.72	6-7 110.5 132.79	6-8 103.5 109.08
7-1 101.61	7-2 121.81	7-3 132.79	7-4 137.58	7-5 113 137.58	7-6 107 132.79	7-7 100.5 121.81	7-8 94 101.62
8-1 87.79	8-2 101.61	8-3 109.08	8-4 112.37	8-5 105 112.37	8-6 103 109.08	8-7 89 101.62	8-8 86.5 87.79

Q = 0.002285 watts/cm
Av. wall temp. = 52.0°C
F_1 = 0.1031
F_2 = 0.0764
F_3 = 0.01878

Table 6.2. Temperature Distribution in a 64 Tube Bundle

1-1	1-2	1-3	1-4	1-5	1-6	1-7	1-8
		[56]	[56.5]	[57]	[56]	[52.5]	[51]
49.65	54.65	57.48	58.76	58.76	57.48	54.65	49.63
2-1	2-2	2-3	2-4	2-5	2-6	2-7	2-8
		[59]	[58]	[57]	[57]	[53.5]	[48]
54.65	62.53	67.09	69.15	69.15	67.09	62.53	54.65
3-1	3-2	3-3	3-4	3-5	3-6	3-7	3-8
[51.5]	[56]	[59]	[61]				
57.48	67.09	72.71	75.26	75.26	72.71	67.10	57.48
4-1	4-2	4-3	4-4	4-5	4-6	4-7	4-8
[51.5]	[54.5]	[60.5]					
58.76	69.15	75.26	78.04	78.04	75.26	69.15	58.76
5-1	5-2	5-3	5-4	5-5	5-6	5-7	5-8
		[57]	[59.5]	[58]	[58]		[48]
58.76	69.15	75.26	78.04	78.04	75.26	69.15	58.76
6-1	6-2	6-3	6-4	6-5	6-6	6-7	6-8
		[57]	[56]	[57]	[55.5]	[51]	[49]
57.48	67.09	72.71	75.26	75.26	72.72	67.10	57.48
7-1	7-2	7-3	7-4	7-5	7-6	7-7	7-8
				[52]	[51]	[48]	[46]
54.65	62.53	67.10	69.15	69.15	67.10	62.54	54.65
8-1	8-2	8-3	8-4	8-5	8-6	8-7	8-8
				[50]	[49]	[44.5]	[44]
49.65	54.65	57.48	58.76	58.76	57.48	54.65	49.65

Q = 0.005712 watts/cm
Av. wall temp. = 38.3°C
F_1 = 0.1031
F_2 = 0.0764
F_3 = 0.01878

Table 6.3. Temperature Distribution in a 64 Tube Bundle

1-1	1-2	1-3	1-4	1-5	1-6	1-7	1-8
		[91]	[92]	[93]	[91]	[81]	[75.5]
64.02	74.08	79.60	82.06	82.06	79.60	74.08	64.02
2-1	2-2	2-3	2-4	2-5	2-6	2-7	2-8
		[94]	[96]	[95]	[93]	[82]	[73]
74.08	89.18	97.56	101.26	101.26	97.56	89.18	74.08
3-1	3-2	3-3	3-4	3-5	3-6	3-7	3-8
[78]	[90]	[97]	[100.5]				
79.60	97.56	107.57	112.02	112.02	107.58	97.56	79.60
4-1	4-2	4-3	4-4	4-5	4-6	4-7	4-8
[78]	[85]						
82.06	101.26	112.02	116.81	116.81	112.02	101.26	82.06
5-1	5-2	5-3	5-4	5-5	5-6	5-7	5-8
		[91]	[93]	[94]	[92]		[73]
82.06	101.26	112.02	116.81	116.81	112.02	101.26	82.06
6-1	6-2	6-3	6-4	6-5	6-6	6-7	6-8
		[87.5]	[88]	[91]	[88]	[78]	[74]
79.60	97.56	107.58	112.02	112.02	107.58	97.56	79.60
7-1	7-2	7-3	7-4	7-5	7-6	7-7	7-8
				[80.5]	[75.5]	[72]	[69]
74.08	89.18	97.56	101.26	101.26	97.56	89.18	74.08
8-1	8-2	8-3	8-4	8-5	8-6	8-7	8-8
				[74]	[72]	[63]	[62]
64.02	74.08	79.60	82.06	82.06	79.60	74.08	64.02

Q = 0.01338 watts/cm
Av. wall temp. = 39.3°C
F_1 = 0.1031
F_2 = 0.0764
F_3 = 0.01878

Table 6.4. Temperature Distribution in a 64 Tube Bundle

1-1 109.26	1-2 127.90	1-3 166 137.74	1-4 167.5 142.04	1-5 170 142.05	1-6 166 137.74	1-7 146 127.90	1-8 135.5 109.26
2-1 127.90	2-2 154.26	2-3 174 168.25	2-4 178 174.31	2-5 175 174.31	2-6 173 168.25	2-7 148.5 154.26	2-8 127 127.90
3-1 142 137.74	3-2 163 168.25	3-3 183 184.51	3-4 190 191.58	3-5 191.58	3-6 184.51	3-7 168.25	3-8 137.74
4-1 140.5 142.04	4-2 160.5 174.31	4-3 180.5 191.58	4-4 199.12	4-5 199.12	4-6 191.58	4-7 174.31	4-8 142.05
5-1 142.05	5-2 174.31	5-3 170.5 191.58	5-4 174.5 199.12	5-5 179.5 199.13	5-6 172 191.58	5-7 108 174.31	5-8 132.5 142.05
6-1 137.74	6-2 168.25	6-3 162 184.51	6-4 167 191.58	6-5 170.5 191.58	6-6 165 184.51	6-7 144 168.26	6-8 132 137.75
7-1 127.90	7-2 154.26	7-3 168.25	7-4 174.31	7-5 148 174.31	7-6 139 168.26	7-7 126 154.26	7-8 117 127.90
8-1 109.26	8-2 127.90	8-3 137.74	8-4 142.05	8-5 135.5 142.05	8-6 132 137.74	8-7 111 127.90	8-8 107 109.26

Q = 0.0372 watts/cm
Av. wall temp. = 57.5°C
F_1 = 0.1031
F_2 = 0.0764
F_3 = 0.01878

Table 6.5. Temperature Distribution in a 64 Tube Bundle

1-1	1-2	1-3	1-4	1-5	1-6	1-7	1-8
		202	204	207	202	181	167
132.44	153.89	165.12	170.02	170.02	165.12	153.89	132.44
2-1	2-2	2-3	2-4	2-5	2-6	2-7	2-8
		213	218	215	211	184	157
153.89	183.86	199.63	206.44	206.44	199.63	183.86	153.89
3-1	3-2	3-3	3-4	3-5	3-6	3-7	3-8
178	203	225	234				
165.12	199.63	217.86	225.77	225.77	217.86	199.63	165.12
4-1	4-2	4-3	4-4	4-5	4-6	4-7	4-8
176	201	225.5					
170.02	206.44	225.77	234.18	234.18	225.77	206.44	170.02
5-1	5-2	5-3	5-4	5-5	5-6	5-7	5-8
		215	219	225	216	135	168
170.02	206.44	225.77	234.18	234.18	225.77	206.44	170.02
6-1	6-2	6-3	6-4	6-5	6-6	6-7	6-8
		204	210	216	208	183	168
165.12	199.63	217.86	225.77	225.77	217.87	199.63	165.12
7-1	7-2	7-3	7-4	7-5	7-6	7-7	7-8
				189	177	163	151
153.89	183.86	199.63	206.44	206.44	199.63	183.86	153.89
8-1	8-2	8-3	8-4	8-5	8-6	8-7	8-8
				172	168	143	137
132.44	153.89	165.12	170.02	170.02	165.12	153.89	132.44

Q = 0.0514 watts/cm
Av. wall temp. = 71.0°C
F_1 = 0.1031
F_2 = 0.0764
F_3 = 0.1878

Table 6.6. Temperature Distrubution in a 64 Tube Bundle

1-1 137.40	1-2 158.16	1-3 208.5 169.08	1-4 211 173.85	1-5 214 173.85	1-6 209.5 169.08	1-7 188 158.16	1-8 137.40
2-1 158.16	2-2 187.36	2-3 219 202.79	2-4 224 209.47	2-5 222 209.47	2-6 218 202.79	2-7 192 187.36	2-8 106 158.16
3-1 186 169.08	3-2 210.5 202.79	3-3 232.5 220.69	3-4 242 228.47	3-5 228.47	3-6 220.69	3-7 202.80	3-8 169.08
4-1 184.5 173.85	4-2 210.5 209.47	4-3 234 228.47	4-4 236.75	4-5 236.75	4-6 228.47	4-7 209.47	4-8 173.85
5-1 173.85	5-2 209.47	5-3 224 228.47	5-4 229 236.75	5-5 236 236.75	5-6 225 228.47	5-7 209.47	5-8 178 173.85
6-1 169.08	6-2 202.79	6-3 213 220.69	6-4 220 228.47	6-5 226.5 228.47	6-6 217.5 220.69	6-7 192 202.80	6-8 178 169.08
7-1 158.16	7-2 187.36	7-3 202.80	7-4 209.47	7-5 198 209.47	7-6 188 202.80	7-7 173 187.36	7-8 159.5 158.16
8-1 137.40	8-2 158.16	8-3 169.08	8-4 173.85	8-5 182 173.85	8-6 177.5 169.08	8-7 151.5 158.16	8-8 146 137.41

Q = 0.0514 watts/cm
Av. wall temp. = 79.0°C
F_1 = 0.1031
F_2 = 0.0764
F_3 = 0.01878

7.0 SOLVENT EXTRACTION STUDIES

A. D. Ryon

7.1 External Phase Separator for Light Phase Continuous Operation of a Pulse Column - A. N. Prasad

As an alternative to various methods of control of the interface at the bottom of a pulse column, the column was operated without an interface, a mixture containing all of the heavy phase (aqueous) plus some light phase (solvent) was withdrawn from the column to an external phase separator where the interface was simply controlled by a jackleg for the aqueous outlet. The solvent was recycled to the bottom of the column by an air lift. The surge capacity for solvent was designed to be minimized so that the flow in the column would not be upset. In fact, the solvent surge tank was built of 1-1/2-in.-dia glass pipe so the cross sectional area of it was less than 10% of the area of the 5-in.-dia pulse column. Automatic control of the system was attempted by operating the air lift with a constant air flow rate to recycle the solvent and using the solvent level in the 1-1/2-in.-dia surge tank (measured by an air bubbler) to control the pressure on a pressure pot used as a valve to regulate the flow rate of dispersion from the column to the phase separator (Figure 7.1).

The equipment consisted of a 5-in.-dia concatenated column (CF 61-1-72) modified with an extension on the top section to give the necessary head for flow out through pressure pot. The air pressure on the pressure pot was supplied from a 3:1 relay and was limited to a maximum of 4.5 psi to avoid blowing the seal leg. The height of the downstream side of the seal leg between the pressure pot and the phase separator was approximately 4-1/2 ft lower than the pressure pot so that it would not become locked with the aqueous phase. The phase separator was constructed of 6-in.-dia glass pipe to permit observation of the interface and the aqueous discharge port. The air lift was constructed of 1/2-in.-OD SS tubing (0.43-in.-ID), the air inlet was a standard tee and the air metering station was located about 50 ft away to simulate the distance involved in a shielded installation.

The pumping characteristics of the air lift are shown in Figure 7.2 which shows the typical relatively constant pumping rate for a wide range of air flow and in Figure 7.3 the nearly linear dependence of pumping rate on liquid head or submergence. Both of these characteristics are desirable in the present application where the air lift was operated with constant air flow, consequently the pumping rate tended to automatically maintain a constant level in the solvent surge tank. At the air flow required for maximum pumping, the air lift cycled at about 12 cycles per minute.

The circuit was tested with an aqueous phase composed of dilute nitric acid (sp. gr. 1.042) and TBP-Amsco solvent phase (sp. gr. 0.787) both of which were recycled. The pulse was maintained at 1 in. amplitude and 67 cpm frequency. The interface control system was tested by observing the external phase separator and recording the liquid level in the solvent surge tank during start up and step changes of the set point of the liquid level controller.

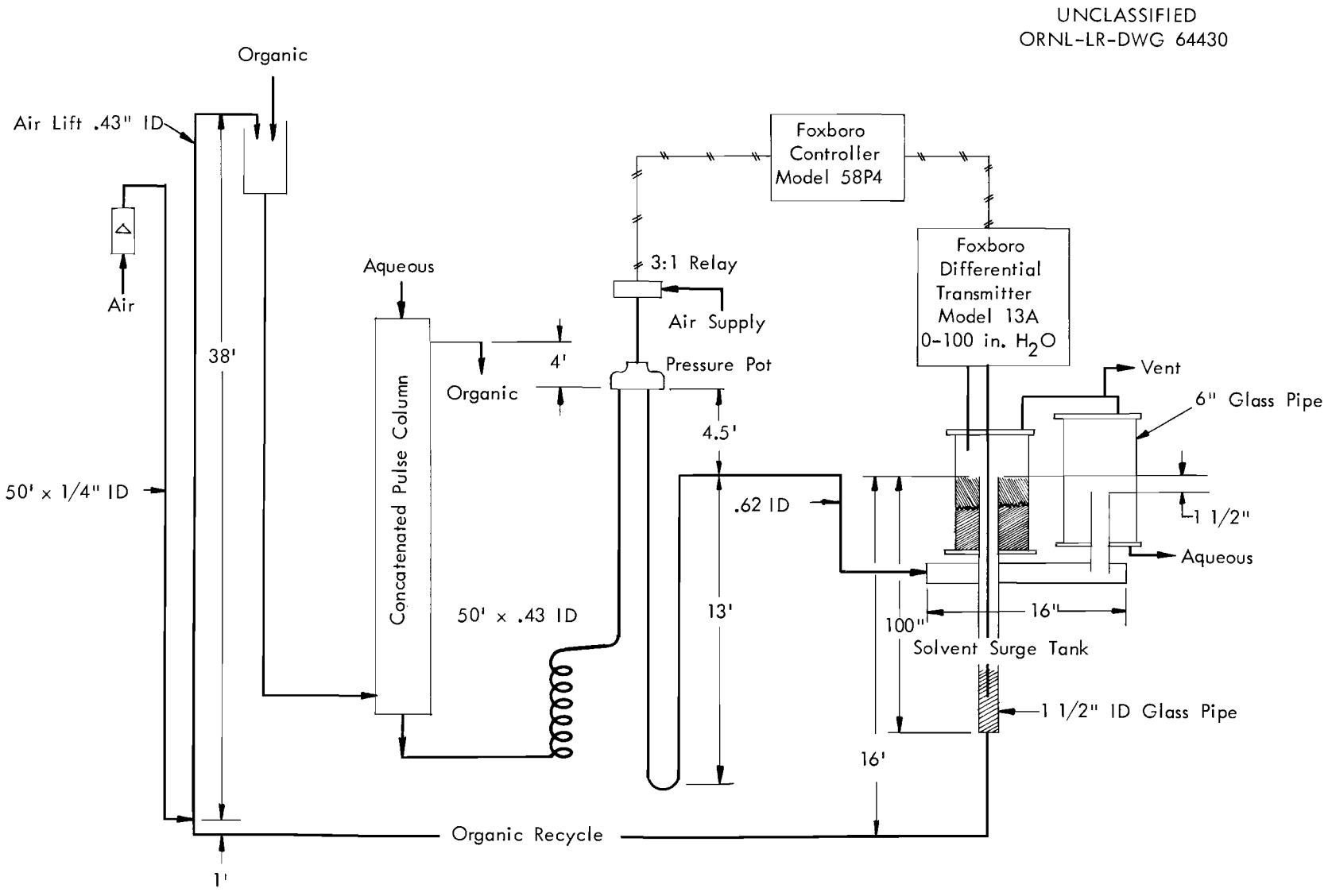

Fig. 7.1. Schematic diagram of interface control with external phase separator for a pulse column operated with organic continuous.

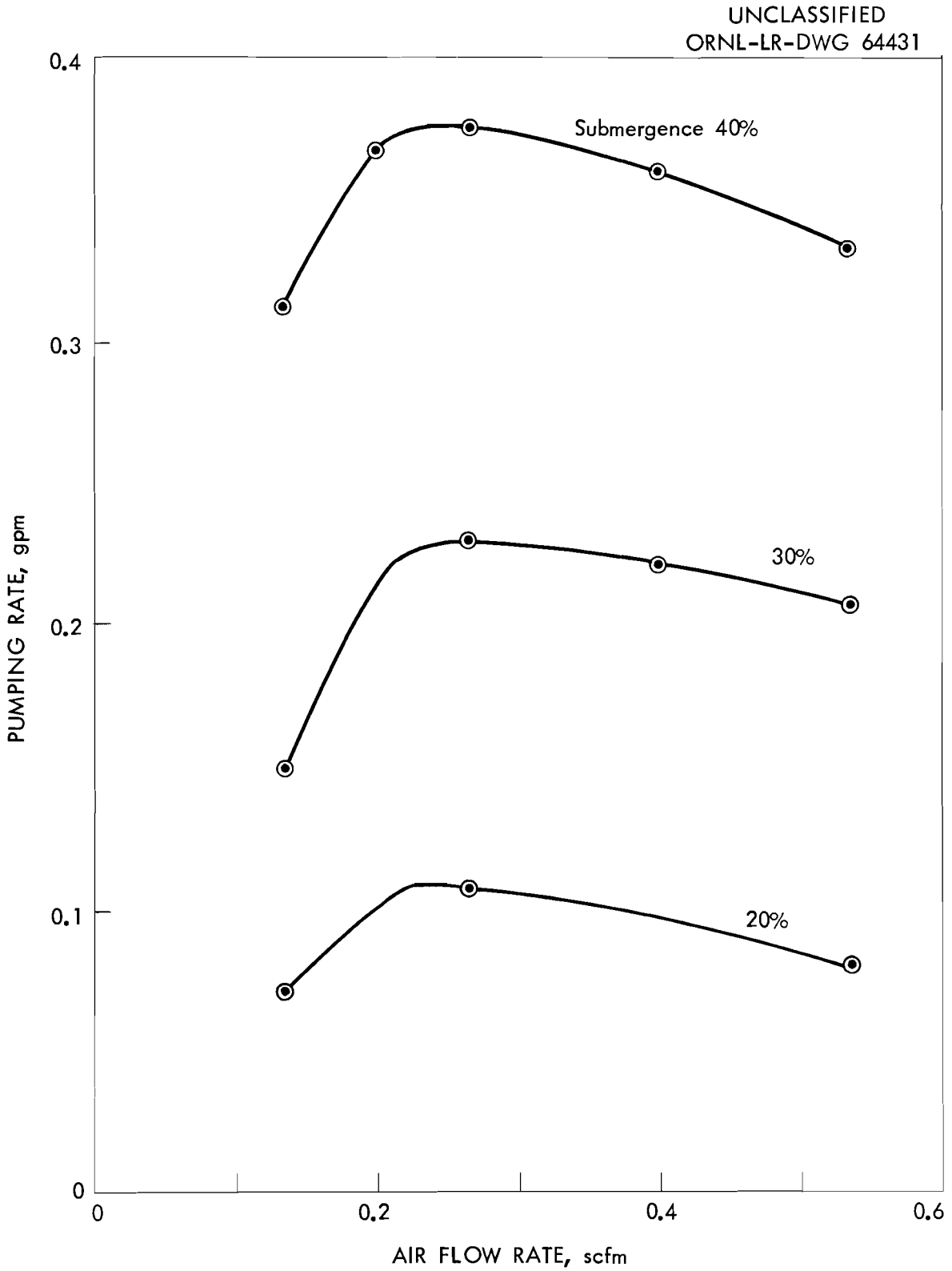

Fig. 7.2. Solvent pumping rate of air lift.

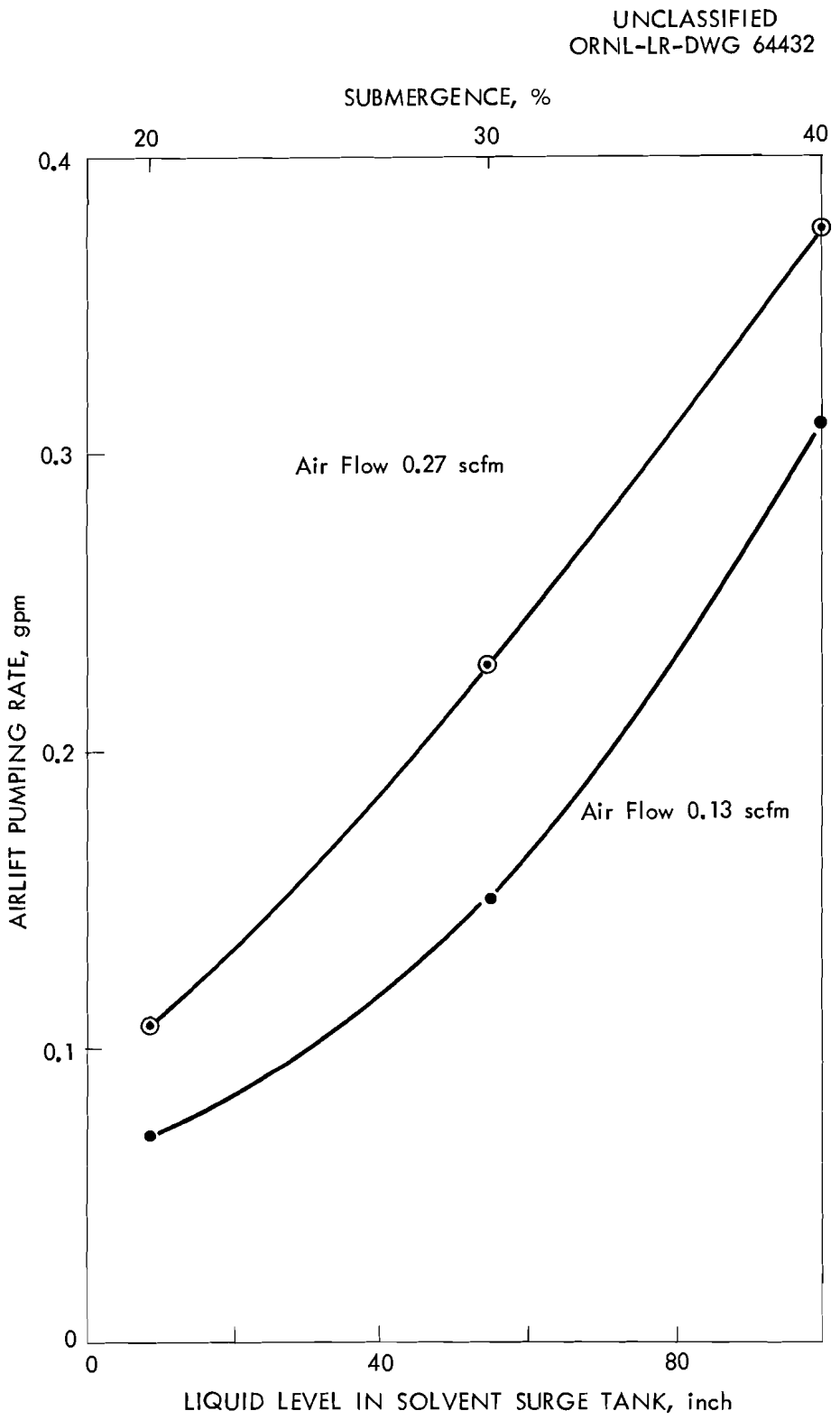

Fig. 7.3. Effect of head or submergence on airlift pumping rate at constant air flow rate.

The system was successfully demonstrated without loss of the interface, flooding, or overflow of solvent into the vent of the external phase separator. The main problem was a tendency for the flow rate of the dispersion to the phase separator to cycle as evidenced by visual slugs of separated phases entering the separator and fluctuations of solvent level in the surge tank. The frequency and amplitude were reduced to controllable values of 1 cycle per 10 min and an amplitude of 40 in. by using relatively sluggish control settings of 100% for gain and 10 min per reset on the controller. Further reduction of amplitude was obtained by decreasing the aqueous content of the dispersion flowing from the column either by decreasing the aqueous flow rate or by increasing the solvent recycle rate. The fluctuation of solvent level in the surge tank was 40 in. at 64% aqueous, 15 in. at 50% and 5 in. at 40%. The latter at a cycle time of 9 min results in a perturbation of less than 0.1 in. per min in the 5-in.-dia column.

The effect of changing solvent recycle rate was tested, either changing the air flow to the air lift, Figure 7.4, or by simply changing the set point of the level controller thereby changing the head and consequently the pumping rate of the air lift. As shown in Figure 7.5, the amplitude is significantly reduced by operating at the higher solvent recycle rate. The curves also demonstrate good control after either up or down step changes of the set point of the controller. A typical start up curve (Figure 7.6) shows a large surge of solvent flow into the surge tank caused by loading of aqueous in the column and insufficient pressure available in the pressure pot to control it. The pressure range could be readily increased by installing a second seal leg in series or by pressurizing the phase separator. In spite of the solvent surge the system was automatically controlled and leveled off after about 60 min.

The long term stability of the control circuit is demonstrated by three curves recorded over 5 hr periods (Figure 7.7). The average fluctuations of solvent level in the 1-1/2-in.-dia surge tank were less than 2 in. and the maximum was 5 in. with no indication of run away or loss of control.

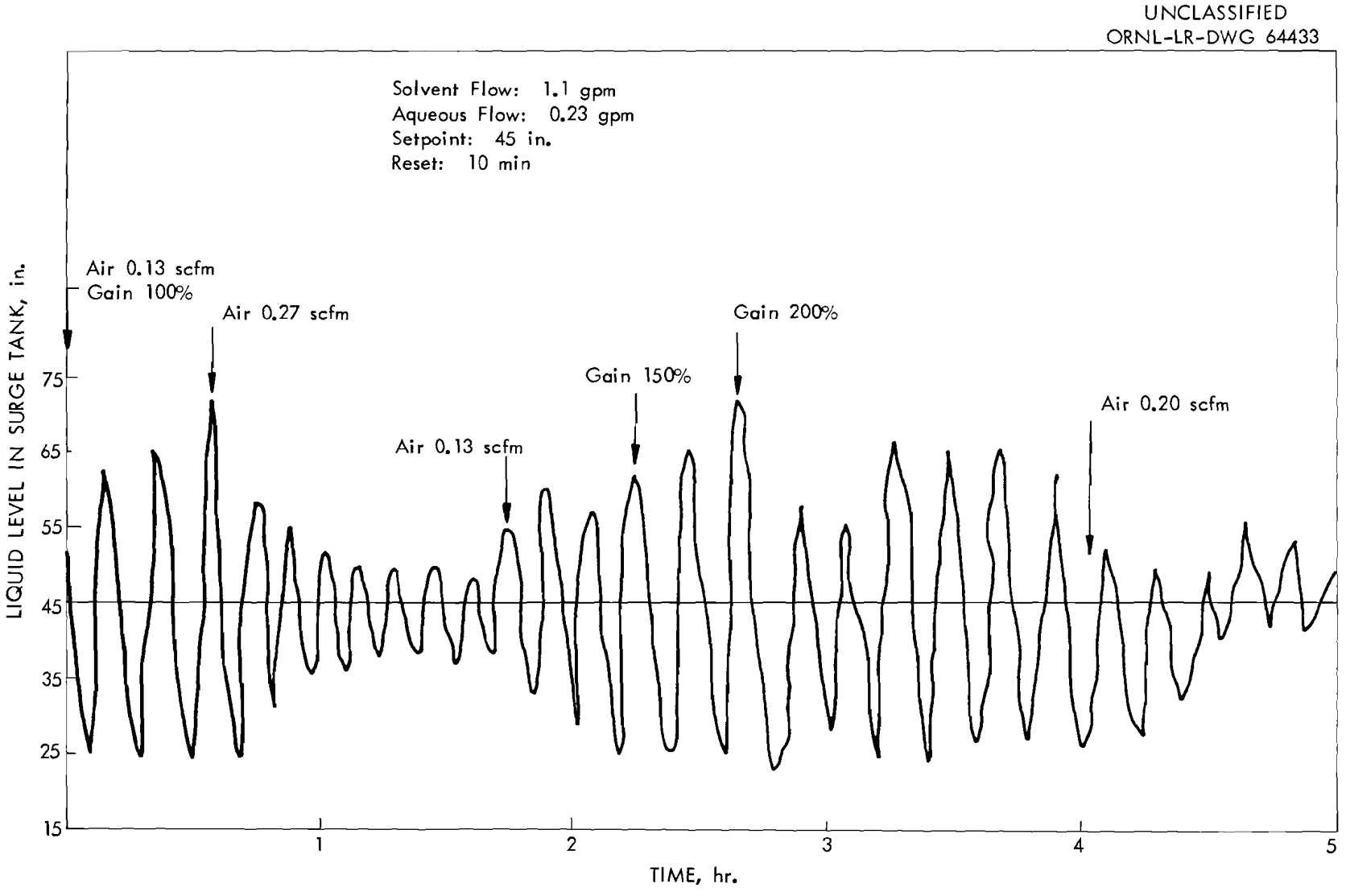

Fig. 7.4. Effect of air flow rate to air lift on control.

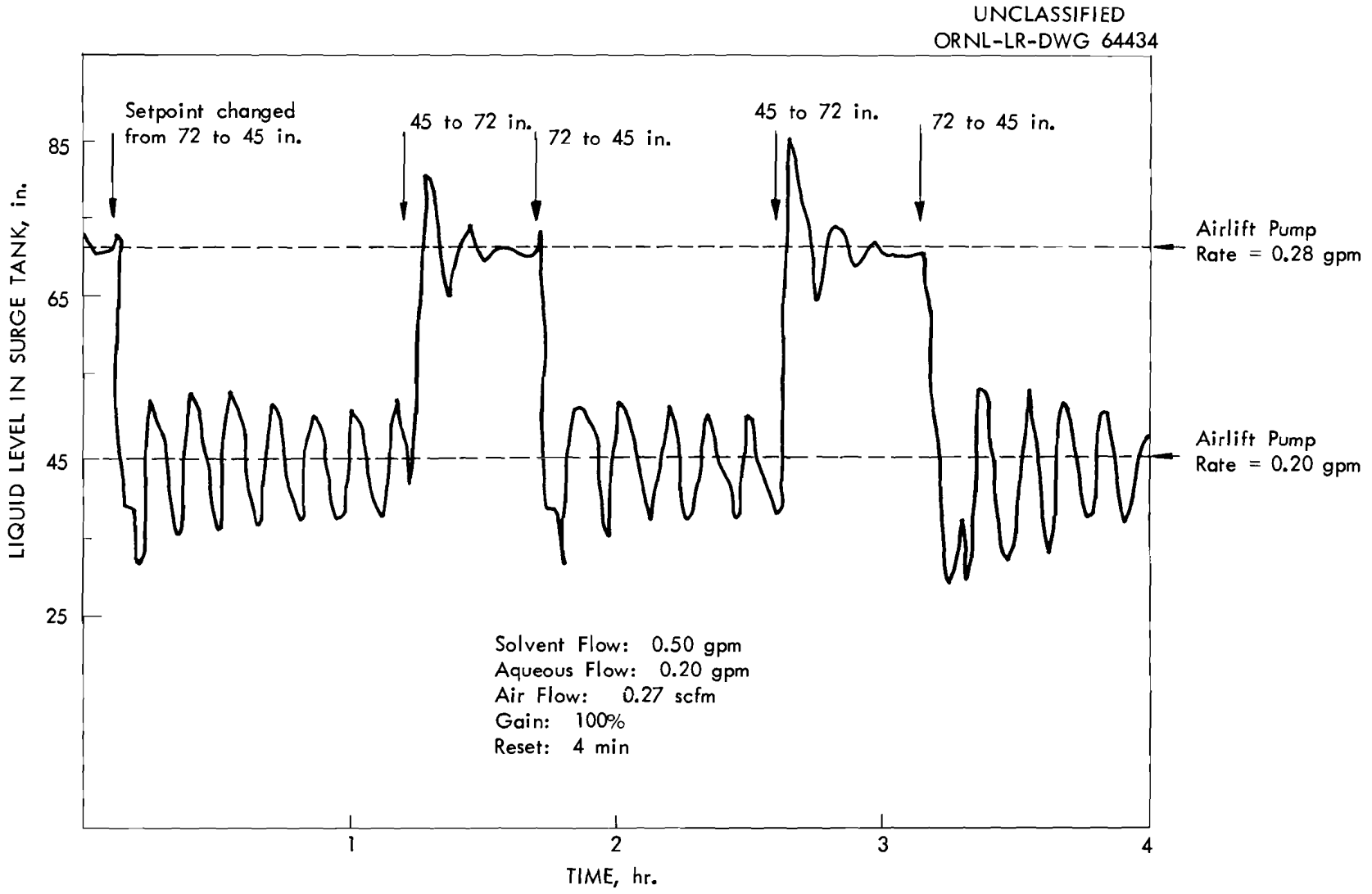

Fig. 7.5. Effect of liquid level in surge tank on control.

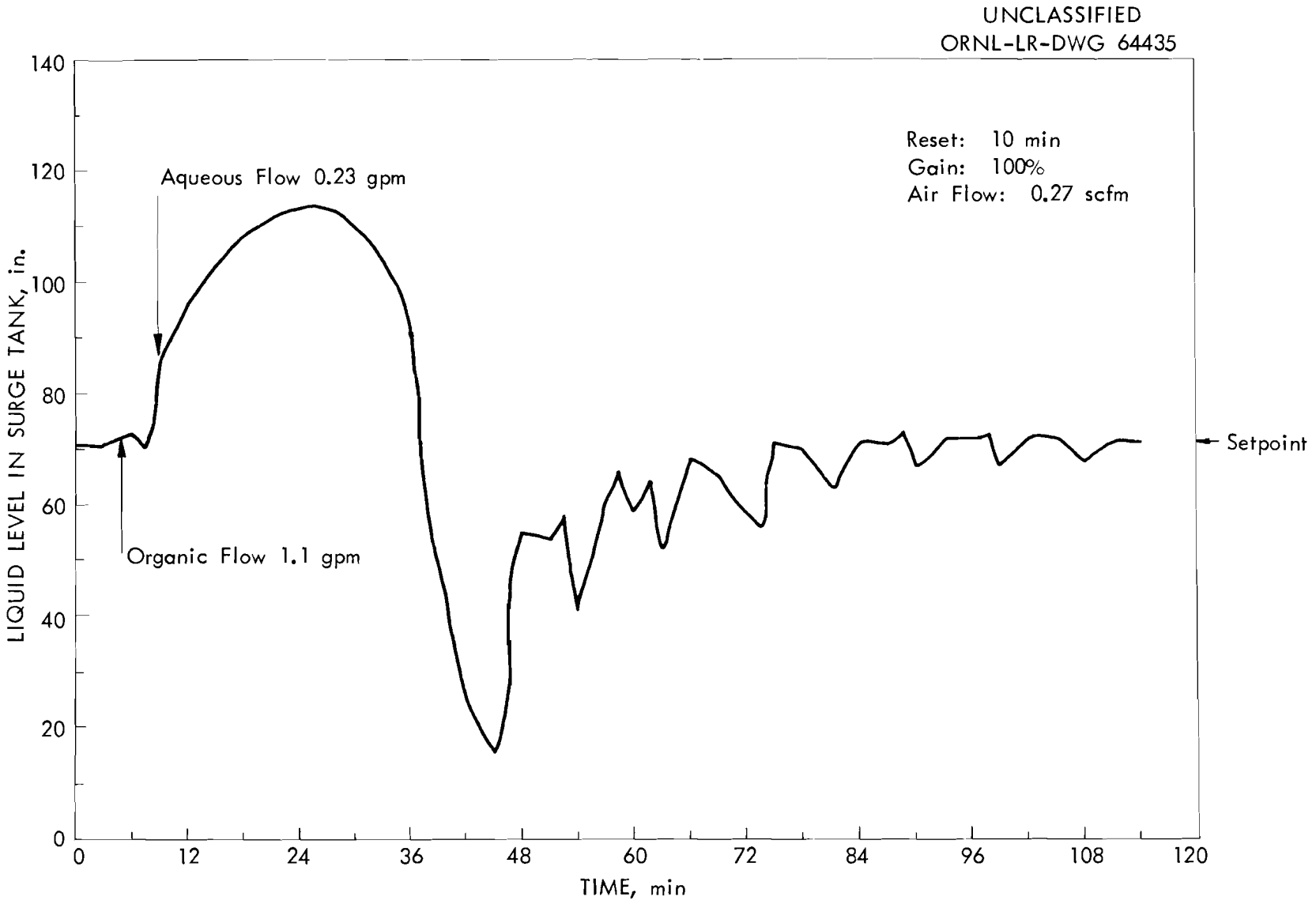

Fig. 7.6. Column startup.

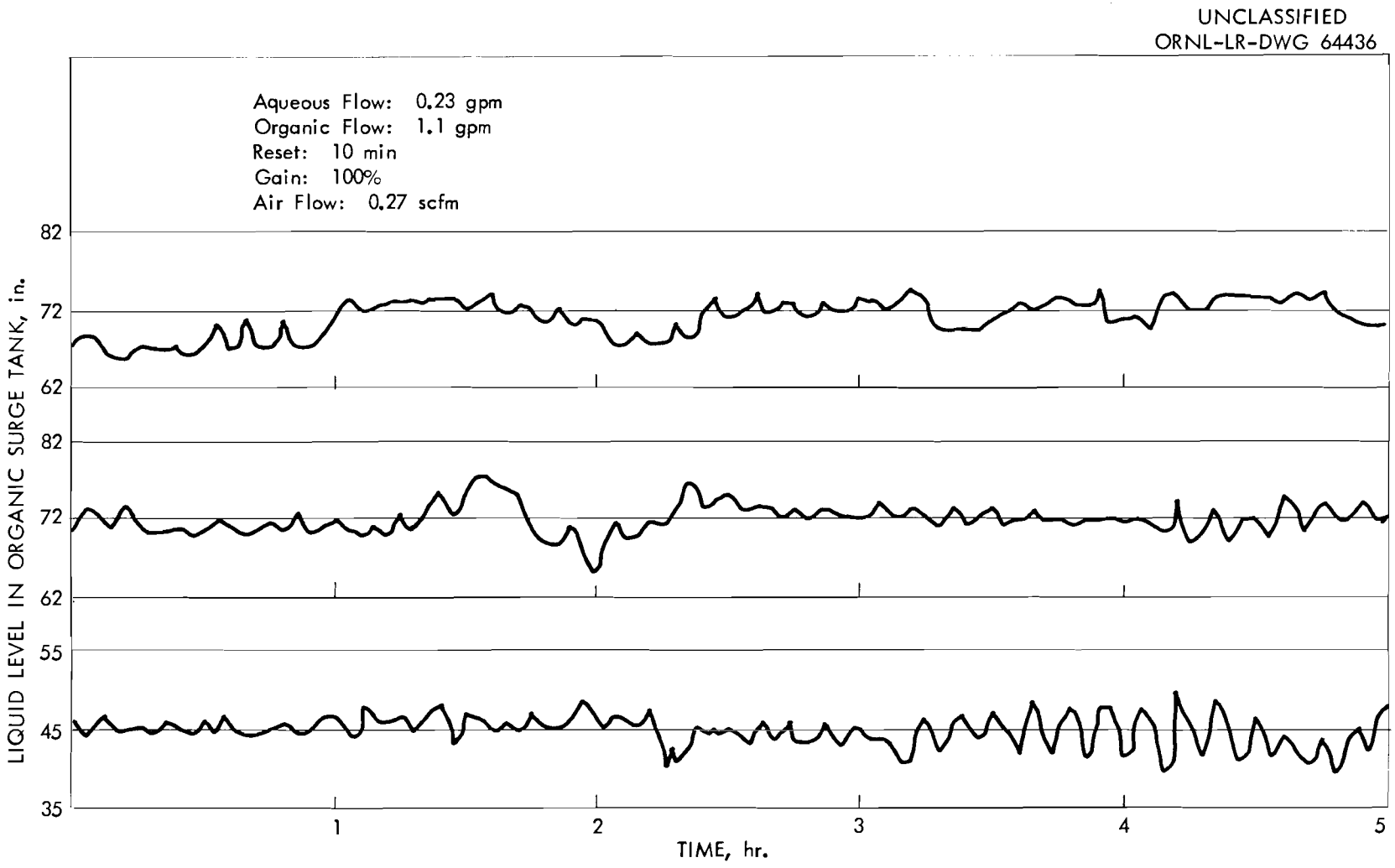

Fig. 7.7. Long term stability tests.

8.0 VOLATILITY

R. W. Horton

8.1 Hydrofluorination of ZrO_2 - J. D. Mottley

Dissolution studies of ZrO_2 slabs (2-in. x 4-in. x 1/4-in.) are being performed in an attempt to determine mechanisms of the dissolution reaction

$$ZrO_2 + 4HF \rightarrow ZrF_4 + 2H_2O$$

in molten salt. Rates twice as great as for metal dissolution were obtained in preliminary tests.

A hydrofluorination system was constructed which contained a 3.5-in.-ID x 13.5-in. dissolver pot, HF metering equipment, a condenser and sample collectors. INOR-8 corrosion specimens were placed into the dissolver to determine corrosion rates of this metal when contacted with molten salts containing HF and with HF and H_2O vapor.

A total of three runs were made, two with ZrO_2 specimens and one with a simulated zirconium fuel element. The purpose of the zirconium run was to compare dissolution data obtained from this system to data obtained under similar conditions from other systems. In all runs a salt of mole composition NaF = 26.1%, LiF = 42.6%, and ZrF_4 = 31.3% was used. The melting temperature of this salt is approximately 475°C.

For run DO-1 the reaction rate is plotted in Figure 8.1 as a function of run time. Cyclic changes in the rate reflect changes in the HF feed rate about the control point of 8.0 g per min. An average reaction rate of about 0.5 mg Zr/sq cm-min and an HF utilization of 6% was obtained. A summary of the operating conditions for this run is given in Table 8.1. The reaction rate of Zr was determined by H_2 evolution.

A comparison of the rate data from DO-1 with other data resulting from experiments in vessels of somewhat similar dimensions and under similar conditions is summarized in Table 8.2 and illustrated in Figure 8.2. The runs chosen have sufficient similarity to correlate well with HF velocity alone in the case of the copper-lined vessels. The lower rate obtained in DO-1 is probably due largely to corrosion product crud from the INOR-8 vessel and the rather massive INOR-8 corrosion specimens. It is also probable that the HF sparging device is less efficient in the DO vessel.

Two ZrO_2 runs were made; one at an HF flow rate of 11.5 g/min; the second at an HF flow rate of 1.75 g/min. Utilization of HF was determined periodically throughout the run by collecting condensed HF and water in polyethylene sampling bottles containing ice and analyzing for HF content by titration with standard NaOH.

Water formed by the dissolution reaction was determined by difference between the HF weight and total weight of the sample. Large differences in per cent utilization for a single run were calculated (Figures 8.3 and 8.4).

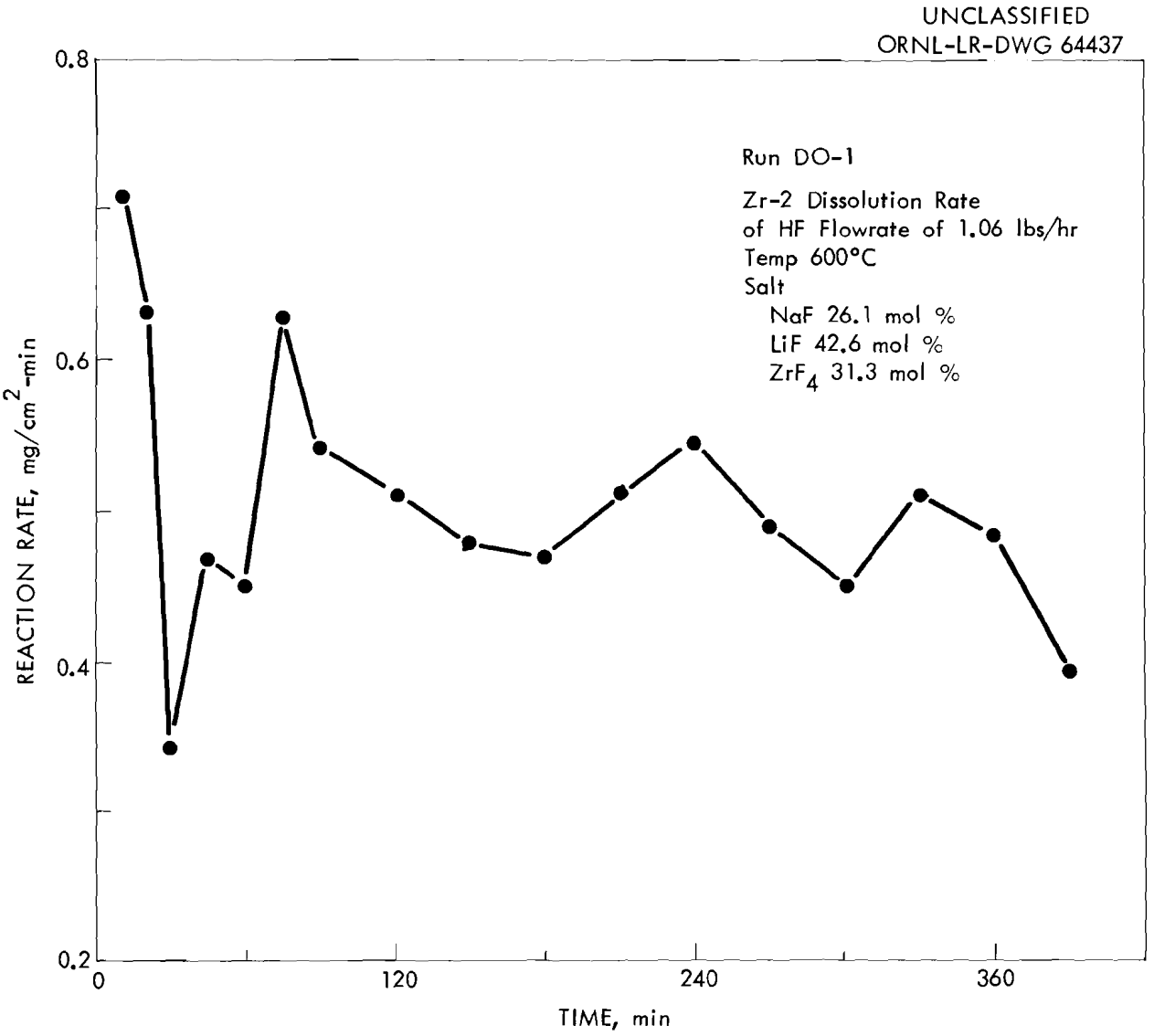

Fig. 8.1. Zr-2 dissolution rate during Run DO-1.

Table 8.1. Data Summary for Zr and ZrO_2 Runs

	Run Number		
	DO-1	DO-2	DO-3
Dissolution specimen	Zr metal	ZrO_2	ZrO_2
Area, sq cm	1290	490	490
Weight, g	806.37	616.40	642.65
Initial salt composition, mol %, NaF	26.1	26.1	26.1
LiF	42.6	42.6	42.6
ZrF_4	31.3	31.3	31.3
Temperature, °C	600	700	600
Length of run, hr	6.5	2	7
HF rate, g/min	8.0	11.4	1.75
% Utilization of HF	6.0	11	20
Reaction rate, mg/cm^2-min	~0.5	3.13	1.24

Table 8.2. Comparison of Zr-2 Dissolution Rate Data in Different Dissolvers

Elements: Fabricated from Zr-2 plates 0.1 in. or 0.125 in. thick, spacings 0.1 in. or 0.125 in.
Dissolution System: HF vapor sparged through the metallic element which is submerged in a molten salt containing ZrF_4 at concentrations stated.

Run No.	Dissolver Vessel Used	Cross Sectional Area, ft^2		HF Feed Rate		Temp. °C	Mol % ZrF_4	Dissolution Rate, mg/cm^2-min
		Dissolver	Element	lbs/hr	lbs/hr-ft^2			
D-2, P IV	Mark I Copper-Lined	0.179	0.0274	1.06	7	650	45	0.27
D-24	Mark I Copper-Lined, Modified	0.0935	0.0256	2.0	29	600	32	1.3
DS-6	Mark II Copper-Lined (with draft tube)	0.0451	0.0152	1.0	39	600	34	1.5
DO-1	INOR-8 Oxide Dissolver (3.5-in.-D x 13.5 in.)	0.0666	0.0152	1.06	20	600	31	0.5

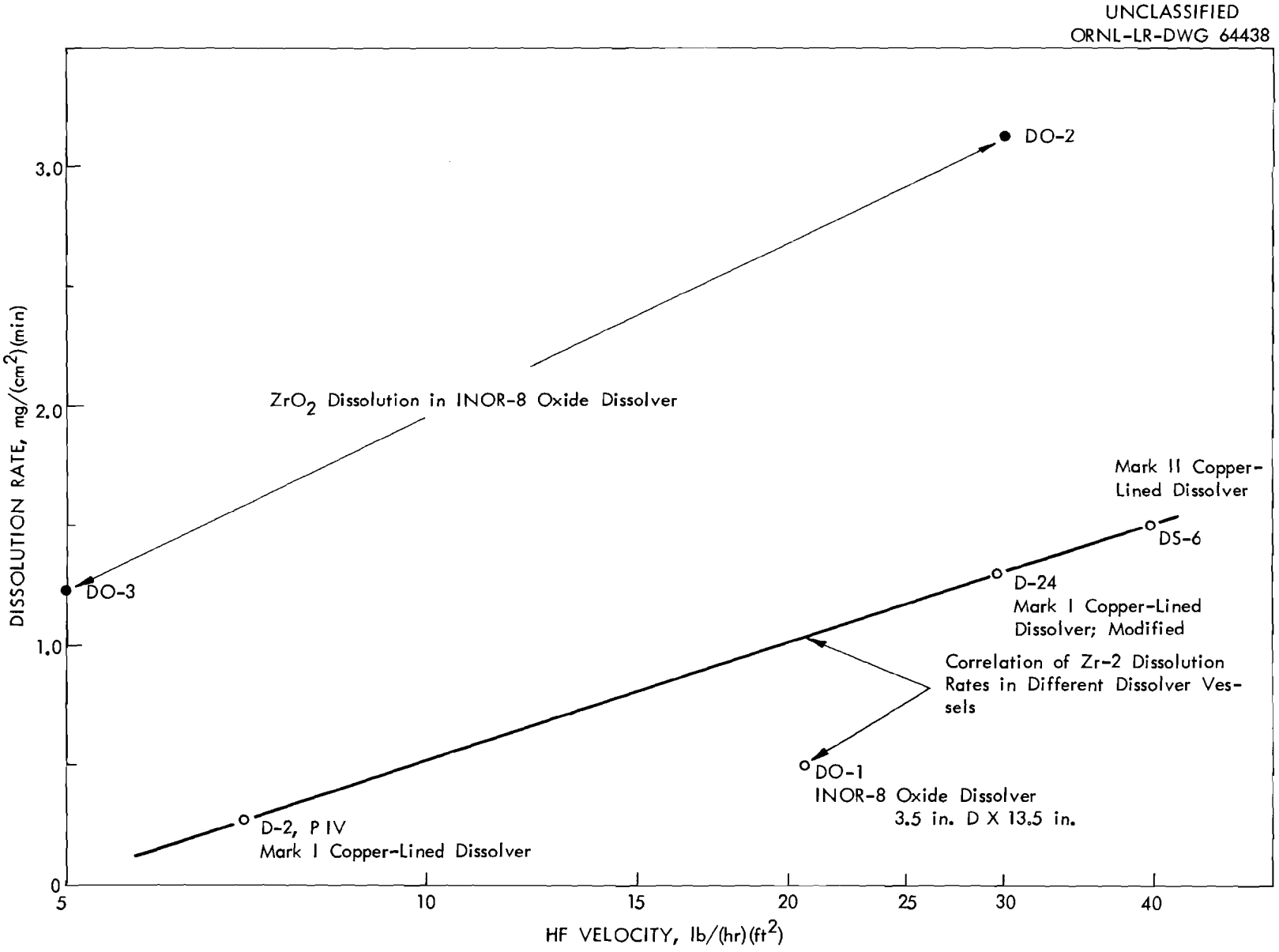

Fig. 8.2. Comparison of dissolution rates for Zr-2 and ZrO_2.

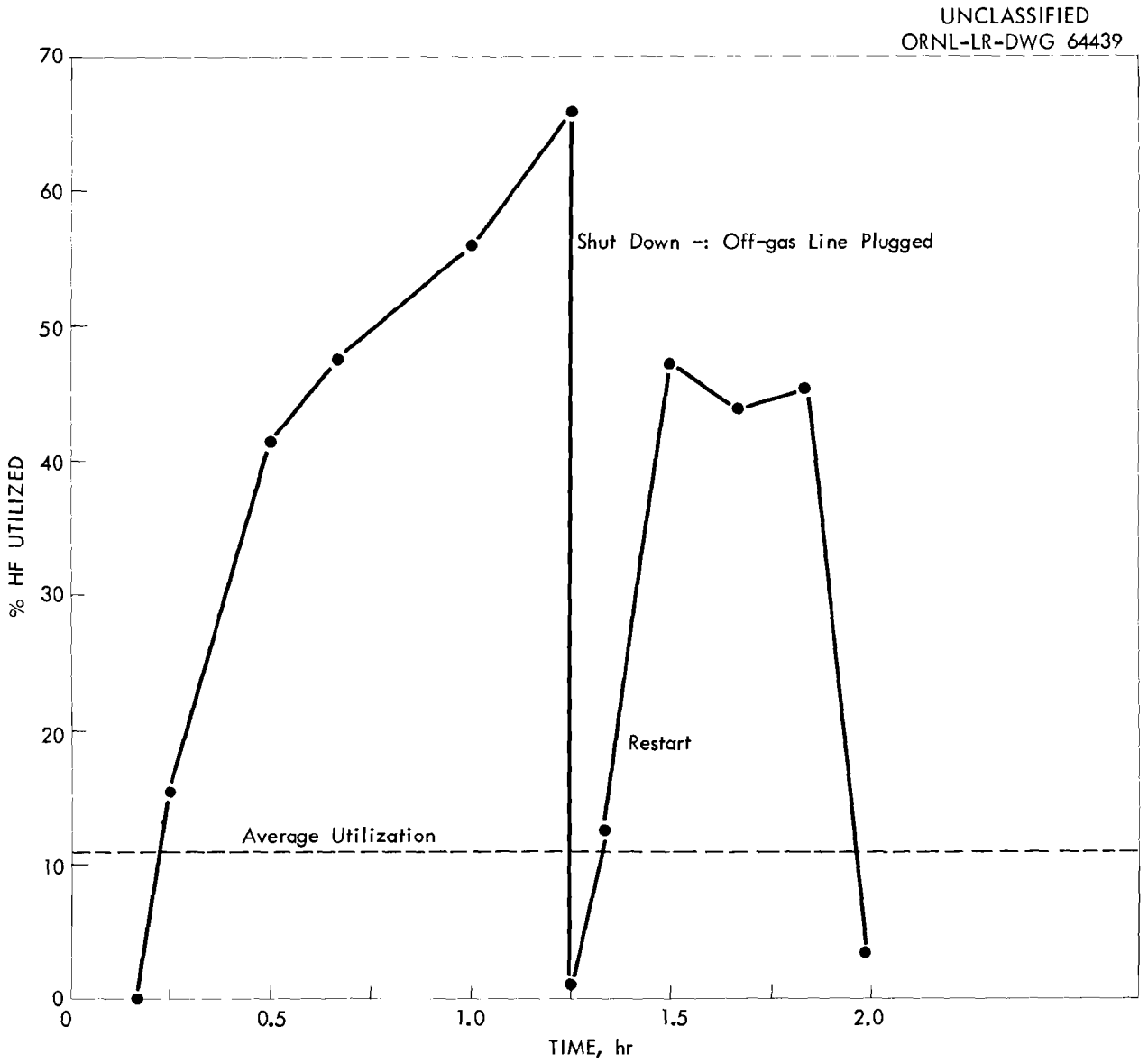

Fig. 8.3. HF utilization during ZrO_2 dissolution, Run DO-2.

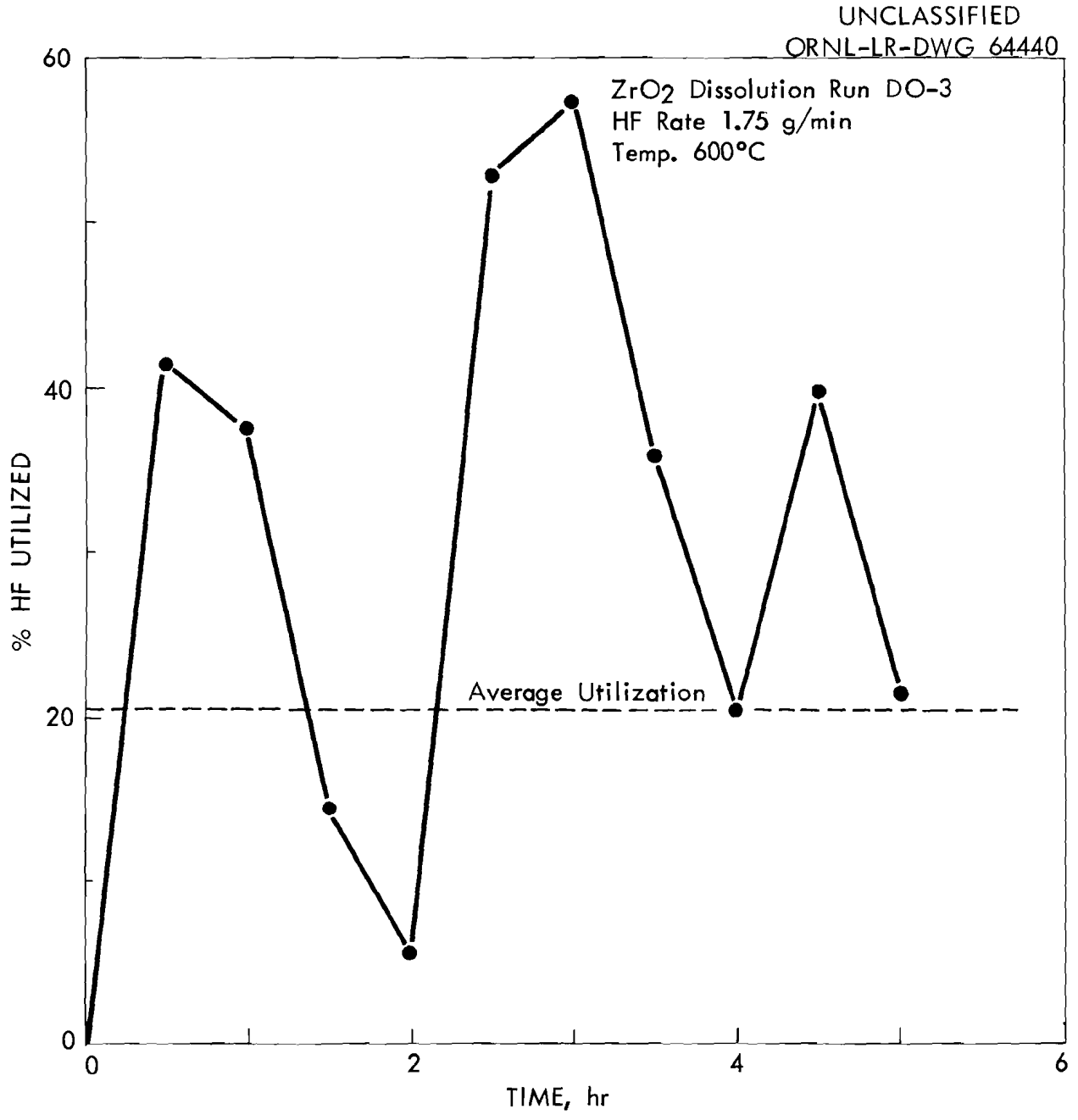

Fig. 8.4. HF utilization during ZrO_2 dissolution, Run DO-3.

When the ZrO_2 specimens were weighed after each run a much lower per cent utilization was obtained than the average of the individual samples. It is believed that off-gas solids present in the system accounted for the error in the individual sample calculations.

At an HF flow rate of 11.4 g/min HF an average reaction rate of 3.13 mg ZrO_2/sq cm-min and a 11% HF utilization were obtained. At an HF flow rate of 1.75 g/min an average reaction rate of 1.24 mg ZrO_2/sq cm-min and a 20% HF utilization were obtained. At the higher flow rate excessive plugging of off-gas lines with molten salt and off-gas solids occurred (probably due to mechanical carry-over). These dissolution rates are plotted in Figure 8.2 compared to the various Zircaloy-2 metal dissolution rates. The oxide rates cannc be correlated with HF velocity because the two runs were at different temperatures, however, it appears that the general relationship observed in metal dissolution might hold. The ZrO_2 dissolution proceeds at a considerably faster rate than metal dissolution.

X-ray diffraction of the ZrO_2 samples after hydrofluorination showed no deposition of any fluoride salts on the samples.

Analysis of the corrosion specimens will be performed when sufficient run time has occurred. Visual observation did not detect any corrosion roughening or pitting during the course of these two runs.

9.0 WASTE PROCESSING

J. C. Suddath

The purpose of the low volume close-coupled evaporator-calciner test is to determine the operating procedures and the conditions for the waste pot calcinating process so that a pilot plant can be designed. This test (R-40) is a purex calcination test with Mg and Na (0.2 M and 1.2 M) added to reduce sulfate volatility. Ruthenium was also added to study its behavior in this system.

9.1 Evaporator-Calciner Test R-40 - C. W. Hancher

Test R-40 was a repeat of test R-37 (Unit Operations Monthly Report, May 1961)(purex waste with 0.2 M Mg and 1.2 M Na, Table 9.1, was added to reduce sulfate volatility). Non-radioactive Ru was added to the feed in this test to determine its behavior during evaporation and calcination. The average feed rate for the test was 27 liters per hour (Tables 9.2 and 9.3).

The recovery balances were:

Nitrate	100.8%
Iron	117.0%
Ruthenium	98.1%
Sulfate	105.8%

The evaporator condensate was 1% in sulfate and below detectable limits (~1/2%) in Ru. The bulk density of the solid was 1.17 g/cc.

9.2 Evaporator-Calciner Control and Operation

Test R-40 started with the evaporator filled with room temperature purex waste, and the calciner empty at room temperature (Table 9.4). The control system for this test is shown in Figure 9.1. The evaporator is heated to operating temperature (113°C), then the calciner is filled while heating (calciner skin maximum 900°C).

As the control variables reached their set points they were switched to automatic control. The control settings for the five controlled streams are given on Tables 9.5 and 9.6.

The controller for the water addition failed to function properly, therefore, it was switched to manual early in the test. The manual set point of 38% was a lower temperature than desired but safe, Figures 9.2 and 9.3. The water to feed ratio was 5.6. The high water rate puts an extreme load on the evaporator, but assures a low Ru in the evaporator condensate by reducing the nitric acid concentration in the evaporator.

The evaporator liquid level control was satisfactory, Figure 9.4, except for the period when the calciner pot filled for the first time and the calciner demand suddenly decreased. The evaporator liquid level exceeded the "A" limit once, the "B" and "C" limits twice.

Table 9.1. Feed Concentrations, R-40

	H^+ M	Al g/ℓ	HNO_3 M	Fe g/ℓ	Na g/ℓ	Ni g/ℓ	Cr g/ℓ	SO_4 M
As made up	4.2	2.7	6.1	25.0	39.4	0.58	0.52	1.0
As analyzed								
Tank 1	4.03	2.4	5.94	26.5	41.3	0.531	0.356	0.94
Tank 2	4.03	2.2	5.97	27.5	42.6	0.500	0.430	1.06
Tank 3	4.03	2.4	5.71	26.3	39.8	0.451	0.342	0.93

Table 9.2. R-40 System Balances and Results

NO_3 Balance		
Input:	2462 g moles	
Recovery:		
Condensate	2310 g moles	93.8%
Solid	0.8 g moles	-
Evap.	90	3.7%
Off-gas	80	3.3%
		100.8%
Ru Balance		
Input:	0.429 g moles	
Recovery:		
Condensate	-	-
Solid	0.366 g moles	85.3%
Evap.	0.055 g moles	12.8%
		98.1%
Fe Balance		
Input:	178 g moles	
Recovery:		
Condensate	0.9 g moles	0.5%
Solid	203 g moles	114.0%
Evap.	4.5 g moles	2.5%
		117.0%
SO_4 Balance		
Input:	362 g moles	
Recovery:		
Condensate	3.0 g moles	0.9%
Solid	371 g moles	102.5%
Evap.	8.5 g moles	2.5%
		105.9%
Na Balance		
Input:	668 g moles	
Recovery:		
Condensate	? g moles	Small, ~0
Solid	593 g moles	88.8%
Evap.	12 g moles	1.8%
		90.6%
Al Balance		
Input:	31.7 g moles	
Recovery:		
Condensate	? g moles	Small, ~0
Solid	23.2 g moles	73.2%
Evap.	0.6 g moles	1.9%
		75.1%

Off-gas

1167 cu ft total
960 cu ft leakage and purge
207 cu ft non-condensable (139 cu ft oxygen)
207/373 = 0.554 cu ft/liter of system feed

Average Feed Rate

373/14 = 26.6 liter/hr average

Table 9.2. (Continued)

Water Feed Rate

2097 liters of water, water to feed ratio = 5.6

Calcined Solids

70.76 kg solid/60 liter = 1.17 g/cc bulk density

Table 9.3. Test Volumes and Concentrations

Test Time	Feed System	System Water Feed	Water To Feed Ratio	System Cond.	Evap. Press.	Mol NO_3 Input	Mol NO_3 Cond.	Evap. Density	Evap. Temp.	Evap. Na Conc.	Evap. Fe Conc.	Evap. Ru Conc.	Evap. H^+ Conc.	Evap. Steam Temp.	Evap. Steam Cond.	Evap. Al Conc.
hrs	liters	liters	ratio	liters	psig	g mole	g mole	g/cc	°C	g/ℓ	g/ℓ	g/ℓ	M	°C	liters	g/ℓ
1	86	0	0	64	-0.7	568	81	1.26	107.9	37.0	23.6	0.132	3.40	128	112	2.16
2	127	79	0.62	179	-0.6	838	426	1.32	110.2	42.0	24.9	0.141	4.65	130	306	3.43
3	148	132	0.89	308	-0.7	977	681	1.45	--	32.7	37.0	0.124	5.90	108	513	2.15
4	180	182	1.01	398	-0.8	1188	865	1.31	110.9	29.4	23.2	0.122	5.40	136	654	2.09
5	215	261	1.21	520	-0.7	1419	1093	1.32	110.5	28.3	20.8	0.116	5.75	133	847	1.88
6	248	341	1.38	641	-0.7	1637	1293	1.32	110.7	28.2	20.5	0.126	5.93	131	1036	1.86
7	275	394	1.43	760	-0.7	1815	1463	1.32	110.2	27.0	20.7	0.218	5.70	130	1223	1.76
8	301	473	1.57	875	-0.7	1987	1637	1.29	108.8	32.5	19.5	0.279	5.30	133	1402	2.45
9	323	556	1.72	992	-0.7	2132	1784	1.32	109.8	33.1	22.2	0.185	5.10	130	1585	2.15
10	339	640	1.89	1105	-0.7	2237	1902	1.32	109.0	36.7	24.2	0.251	4.40	128	1763	2.17
11	350	715	2.04	1215	-0.7	2310	1995	1.32	109.5	38.0	26.8	0.178	4.40	128	1935	2.44
12	359	799	2.23	1323	-0.7	2369	2074	1.32	108.8	39.4	28.7	0.283	3.85	127	2105	2.49
13	366	852	2.33	1430	-0.7	2416	2141	1.32	108.6	39.0	28.6	0.232	3.43	126	2270	2.58
14	373	935	2.51	1536	-0.7	2462	2163	1.32	108.1	30.4	31.1	0.154	3.20	124	2433	1.95
15		1014	2.72	1648	-0.7		2171	1.23	104.5	16.0	27.3	0.091	2.29	118	2595	1.03
16		1124	3.01	1746	-0.7		2175	1.13	101.9	9.7	12.5	0.061	1.55	115	2761	0.68
17		1166	3.13	1848	-0.7		2178	1.08	101.0	11.0	7.3	0.181	1.08	114	2918	0.69
18		1276	3.42	2043	-0.7		2182	1.09	101.0	10.9	9.8	0.184	1.13	114	3079	0.63
19		1355	3.63	2153	-0.7		2183	1.08	101.0	10.1	9.6	0.183	1.10	112	3246	0.66
20		1465	3.93	2306	-0.7		2184	1.08	101.0	10.1	9.5	0.176	0.82	112	3385	0.66
21		1544	4.14	2413	-0.7		2185	1.08	100.0	10.1	9.4	0.179	0.80	111	3547	0.66
22		1654	4.43	2519	-0.7		2186	1.07	100.0	10.9	9.4	0.189	0.68	112	3707	0.71
23		1734	4.65	2629	-0.7		2187	1.08	101.0	12.5	9.7	0.214	0.66	111	3867	0.76
24		1809	4.85	2721	-0.7		2188	1.08	101.0	13.8	10.9	0.220	0.71	110	4008	0.92
25		1889	5.06	2801	-0.7		2193	1.08	100.0	18.9	10.9	0.320	0.73	109	4136	0.93
26		1953	5.24	2863	-0.7		2203	1.11	103.3	15.3	16.7	0.262	1.56	111	4220	0.94
27		1976	5.30	2914	-0.7		2223	1.12	103.3	15.5	12.0	0.268	2.55	110	4307	0.90
28		1995	5.35	2996	-0.7		2275	1.15	106.0	17.8	13.4	0.328	3.35	111	4113	1.23
29		2017	5.41	3052	0		2293	1.19	104.0	15.5	16.1	0.305	4.11	114	4487	1.04
30		2070	5.55	3116	-0.1		2310	1.15	107.0	14.8	15.0	0.305	3.44	111	4566	0.87
31		2097	5.62	3159	-0.1									98	4639	

Table 9.3. (Continued)

Test Time	Calciner Heat Input	Calciner Temp. at Feed Point	Calciner Temp. at Mid-Section Center	System Off-gas	Off-gas Before Water Scrub						Off-gas After Water Scrub				
					N_2	O_2	Ar	N_2O + CO_2	NO_2	Air	N_2	O_2	Ar	N_2O + CO_2	NO_2
hrs	KWH	°C	°C	cu ft	Vol %	Vol %	Vol %	Vol %	Vol %	cu ft	Vol %	Vol %	Vol %	Vol %	Vol %
1	52	115	115	42	78.0	20.9	0.9	0.3	< 0.1	42.0	-	-	-	-	-
2	97	120	120	75	74.9	22.9	0.9	0.3	1.2	31.7	-	-	-	-	-
3	147	435	150	110	68.5	28.3	0.8	1.3	0.6	30.7	-	-	-	-	-
4	194	120	120	141	67.0	31.0	0.8	1.3	0.2	26.6	68.1	31.0	0.8	0.4	0.1
5	237	125	125	171	67.0	31.2	0.8	0.8	0.3	25.8	-	-	-	-	-
6	280	125	125	206	65.0	33.3	0.8	1.1	0.2	29.2	-	-	-	-	-
7	318	130	125	239	60.5	36.7	0.7	1.1	0.5	25.6	61.2	37.1	0.7	0.6	0.2
8	357	150	125	288	60.8	37.6	0.7	0.5	0.4	38.2	-	-	-	-	-
9	380	170	130	315	60.5	37.8	0.7	0.5	0.3	21.0	-	-	-	-	-
10	407	180	280	355	58.7	40.1	0.7	0.5	0.3	30.1	59.6	39.7	0.7	0.3	0.1
11	426	185	380	393	58.6	39.5	0.6	0.6	0.2	28.5	-	-	-	-	-
12	443	185	440	437	58.9	39.9	0.6	0.4	0.2	33.2	-	-	-	-	-
13	456	180	505	482	56.7	41.6	0.6	0.4	0.2	32.7	58.5	40.8	0.6	0.2	0.1
14	473	180	560	528	55.8	43.0	0.5	0.4	0.2	32.9	-	-	-	-	-
15	486	180	615	580	58.0	40.7	0.6	0.5	0.2	38.7	-	-	-	-	-
16	502	175	665	631	62.0	36.7	0.7	0.5	-	40.5	63.6	35.4	0.7	0.3	-
17	511	175	715	673	66.6	32.1	0.7	0.5	-	35.9	-	-	-	-	-
18	527	175	750	712	69.7	28.7	0.8	0.6	-	34.9	-	-	-	-	-
19	540	175	775	757	72.3	26.0	0.8	0.7	-	41.7	73.3	25.7	0.9	0.3	-
20	556	175	795	779	73.5	24.9	0.9	0.7	-	20.7	-	-	-	-	-
21	567	175	815	811	74.5	23.5	0.9	1.0	-	30.6	-	-	-	-	-
22	583	175	850	841	75.2	23.2	0.9	0.8	-	28.9	-	-	-	-	-
23	591	175	860	871	76.4	22.2	0.9	0.7	-	29.4	76.3	22.2	0.9	0.3	-
24	604	175	865	898	76.2	22.0	0.9	0.7	-	26.4	-	-	-	-	-
25	614	175	870	926	78.0	21.0	0.9	0.1	-	28.0	-	-	-	-	-
26	631	185	875	950	78.1	20.7	0.9	0.3	-	24.0	67.9	30.8	0.8	0.3	-
27	641	335	875	968	77.9	20.8	0.9	0.2	-	18.0	-	-	-	-	-
28	646	480	875	999	72.9	25.7	0.9	0.2	-	29.0	-	-	-	-	-
29	657	600	875	1048	74.6	24.2	0.9	0.2	-	46.8	-	-	-	-	-
30	664	655	875	1108	76.2	23.1	0.9	0.1	-	58.6	-	-	-	-	-
31	671	675	875	1167											
										960.3					

Table 9.4. Test R-40 Operation Log

Run Time		
0	9:00 a.m.	Start - Evap. full, cold, calciner empty - cool
0.5	9:30 a.m.	Calciner full, Evap. water on manual
2.75	11:45 a.m.	Calciner liquid level probes plugged, switched to secondary probe
7.50	4:30 p.m.	Calciner suddenly dropped from 70% to 20%, melting may have occurred
14.0	11:00 p.m.	Stopped system feed, began evaporator purge
16.0	1:00 a.m.	Stopped feeding calcining, evap. on standby, start calcining
25.0	10:00 a.m.	Evap. shut down
31.0	4:00 p.m.	End calcination

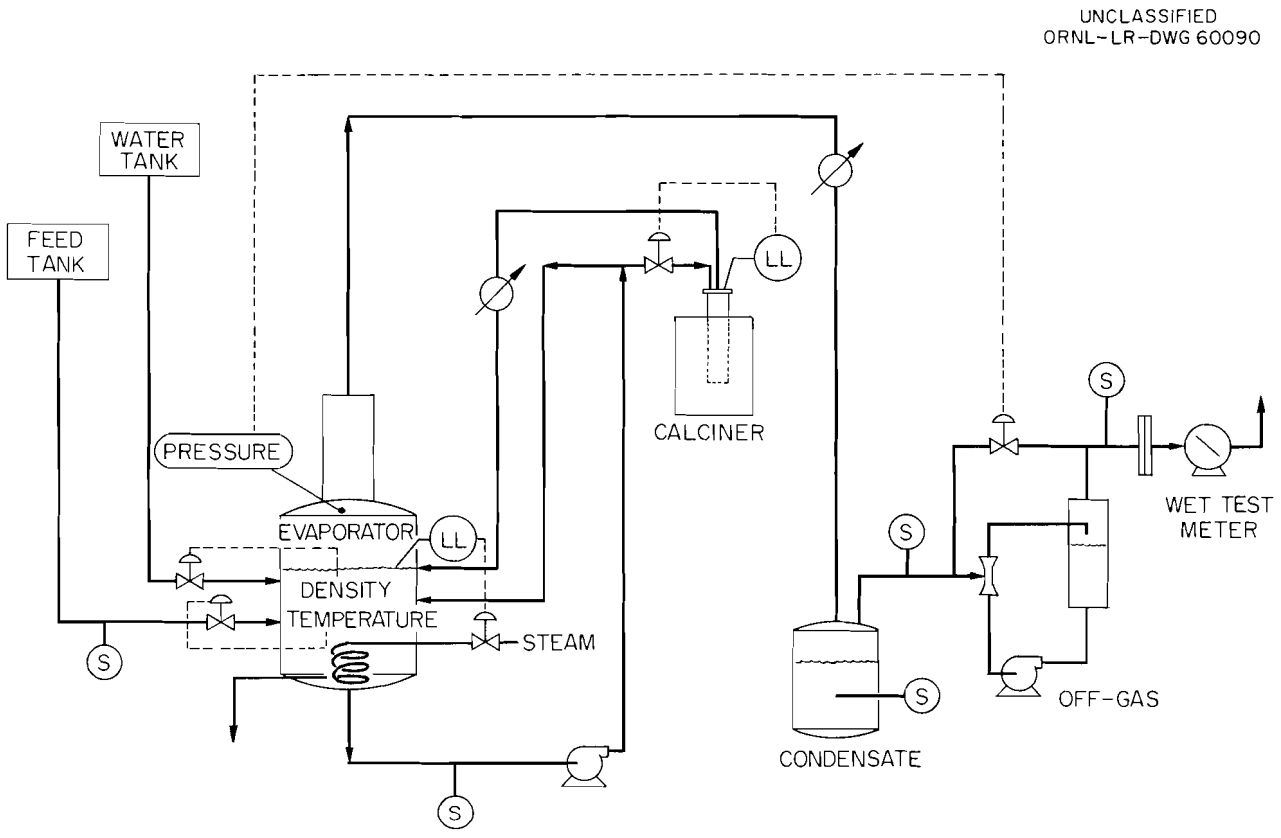

Fig. 9.1. Close-coupled evaporator and calciner test system.

Table 9.5. Control Ranges for Test R-40

Control Variable	Control Input	Control Ranges Full Scale	Prob Band %	Reset Rate min	Set Point Scale %
Evap. Liquid Level	Evap. Steam	7.4-55.0 liters	100	10	50
Evap. Density	Evap. Feed	1.0-1.5 g/cc	200	10	65
Evap. Temperature	Evap. Water	101-128°C	-	-	38 manual
Evap. Pressure	Jet Bypass	-5 to +5 psig	25	0.3	43
Cal. Liquid Level	Cal. Feed	54-62 liter	100	10	50

Table 9.6. Operational Limits for Test R-40

	Limit A	Limit B	Set Point	Limit C	Limit D	Hourly Readings min	Hourly Readings max
Evap. Liq Level							
Scale %	65	60	50	45	25	41[a]	100
liter	26.0	24.6	22.0	20.6	15.2	19.6	35.4
Evap. Density							
Scale %	80	75	65	50	40	46[b]	90
g/cc	1.40	1.375	1.325	1.25	1.20	1.23	1.45
Evap. Temperature							
Scale %	90	75	38 manual	30	0	0	40
°C	121.9	118.7	116.6	108.6	101.5	101.5	110.9
Evap. Pressure							
Scale %	47	45	43	40	38	44	43
psig	-0.25	-0.50	-0.70	-1.0	-1.35	-0.80	-0.70
Cal. Liq Level							
Scale %	30	40	50	60	70	43	100
liters	58	59	60	61	62	59	62

[a] Zero at startup

[b] Went to 17% during evap. purge

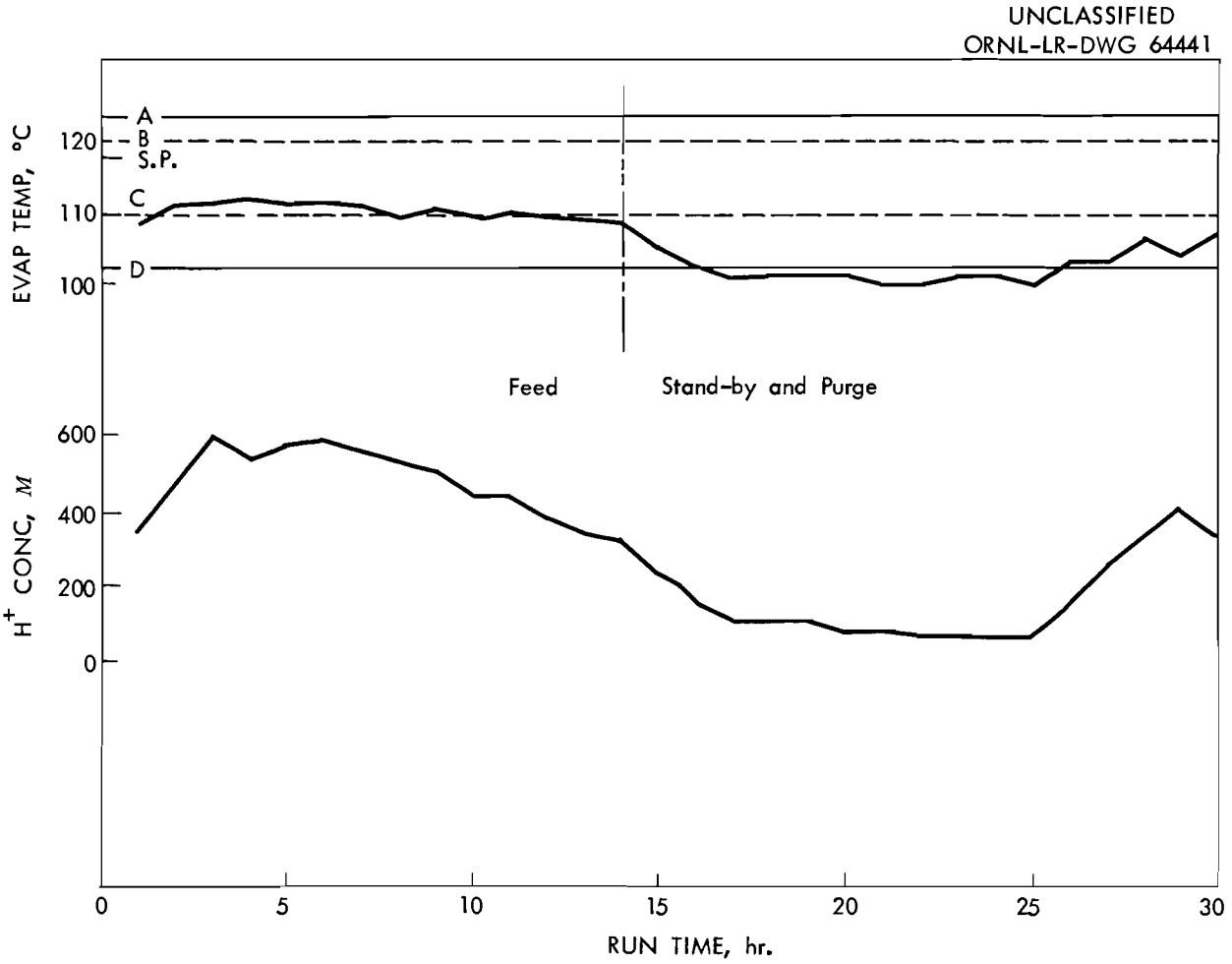

Fig. 9.2. Evaporator temperature control and acid concentration vs run time.

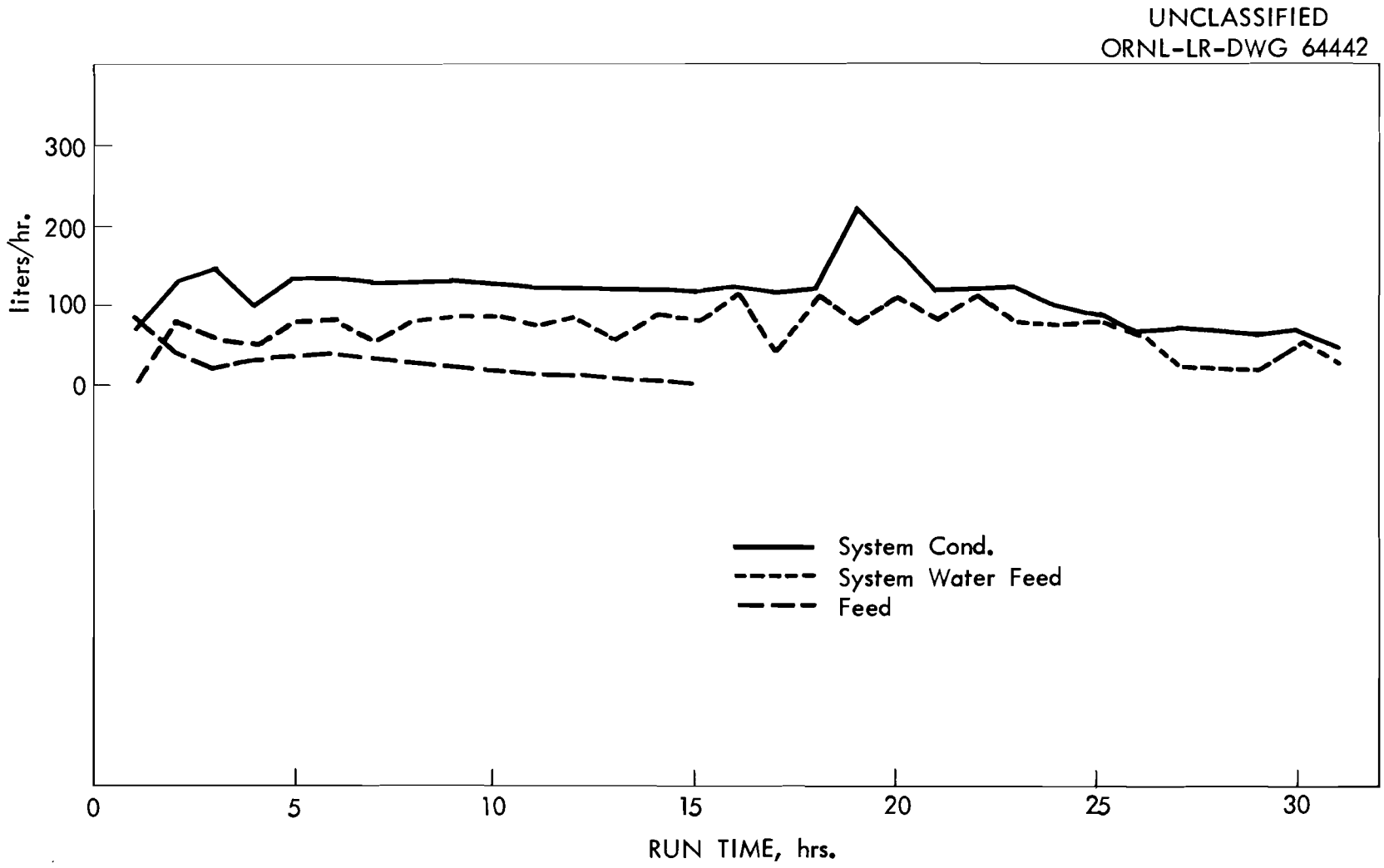

Fig. 9.3. System flow rates vs run time for Test R-40.

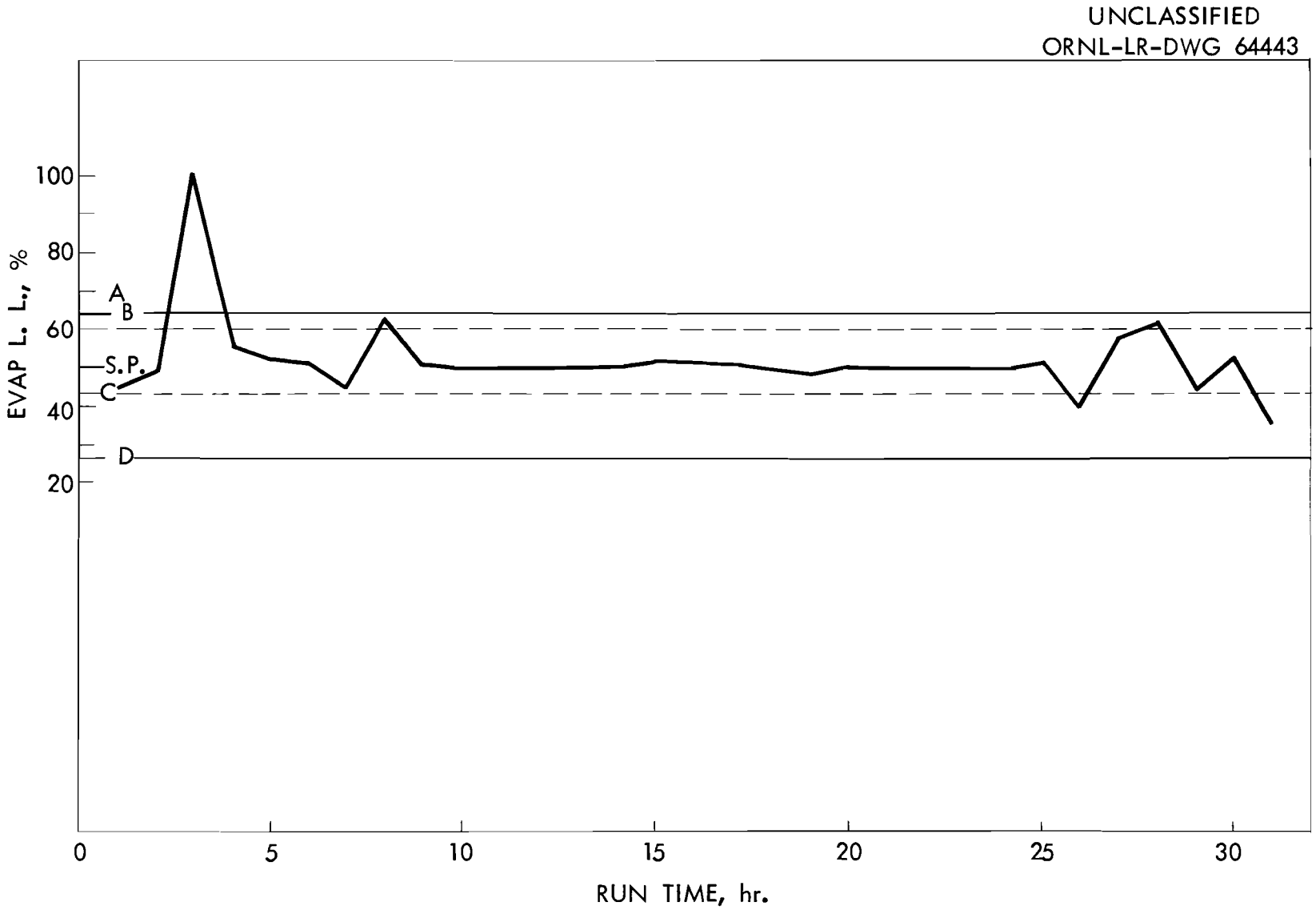

Fig. 9.4. Evaporator liquid level vs run time for Test R-40.

The control of the variables have been evaluated by the setting of limits.

Limit "A" Too high, out of control, dangerous

Limit "B" Upper limit of good control

Limit "C" Lower limit of good control

Limit "D" Too low, out of control, uneconomical or dangerous

The evaporator density control was good after the first start-up overshoot, Figure 9.5.

After the prepared feed was virtually all in the operating system, the feed to the evaporator was cut off and the calciner was fed from the evaporator which was diluted with water on liquid level demand, and allowed to purge its solids to calciner. By this method of operation very little solid or acid was held up in the evaporator for the next test cycle. The sulfate and Ru volatility should be at a minimum under these purge conditions.

Calcined Solids. The calcined solids had a bulk density of 1.17 g/cc (Tables 9.2 and 9.7), and had the appearance of a partial melt-down similar to test R-37.

Of the per cent of material recovered, the following amounts were in the solid and in the evaporator.

	Solid	Evaporator
Ru	87%	13% = 100%
SO_4	97%	2% = 99%
Iron	98%	2% = 100%

Table 9.7. Calcined Solid Analysis Test R-40

	Fe wt %	Na wt %	Al wt %	Ru mg/g	SO_4 wt %	NO_3 wt %
Wall:						
Top half	12.35	21.11	0.910	0.461	51.77	0.023
Bottom half	12.26	22.53	0.985	0.673	46.55	0.150
Center:						
Top half	19.12	19.92	0.793	0.512	50.03	0.110
Bottom half	20.45	13.50	0.840	0.840	53.25	0.010
Average	16.04	19.26	0.882	0.622	50.40	0.073

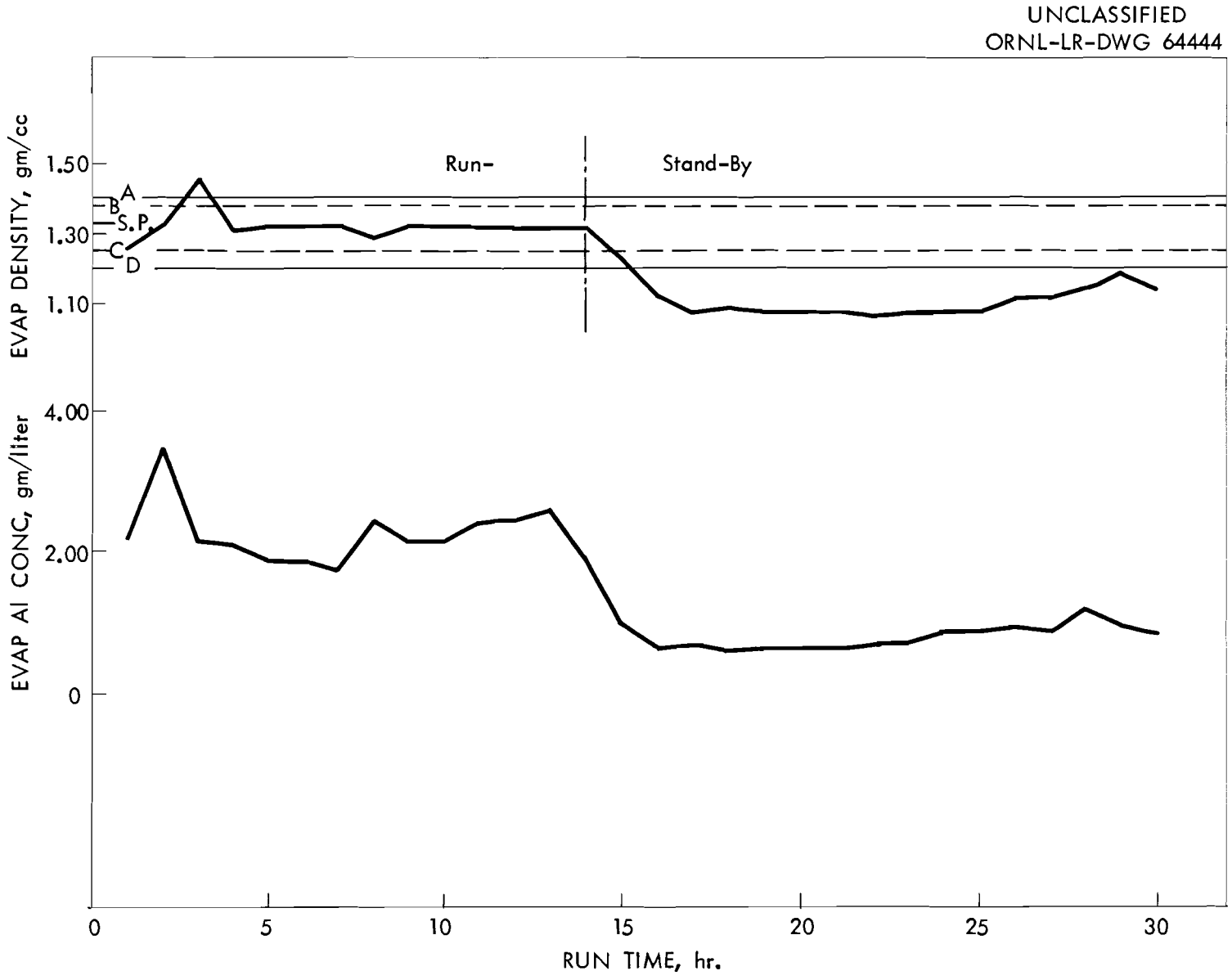

Fig. 9.5. Evaporator density and Al concentration vs run time for Test R-40.

DISTRIBUTION

1. E. L. Anderson (AEC Washington)
2. F. P. Baranowski (AEC Washington)
3. W. G. Belter (AEC Washington)
4. S. Bernstein (Paducah)
5. R. E. Blanco
6. J. O. Blomeke
7-10. J. C. Bresee
11. R. E. Brooksbank
12. K. B. Brown
13. F. R. Bruce
14. J. A. Buckham (ICPP)
15. L. P. Bupp (HAPO)
16. W. D. Burch
17. W. H. Carr
18. G. I. Cathers
19. J. T. Christy (HOO)
20. W. E. Clark
21. V. R. Cooper (HAPO)
22. K. E. Cowser
23. F. E. Croxton (Goodyear Atomic)
24. F. L. Culler, Jr.
25. W. Davis, Jr.
26. O. C. Dean
27. D. E. Ferguson
28. L. M. Ferris
29. R. J. Flanary
30. E. R. Gilliland (MIT)
31. H. E. Goeller
32. M. J. Googin (Y-12)
33. H. B. Graham
34. A. T. Gresky
35. P. A. Haas
36. M. J. Harmon (HAPO)
37. F. E. Harrington
38. L. P. Hatch (BNL)
39. O. F. Hill (HAPO)
40. J. M. Holmes
41. R. W. Horton
42. A. R. Irvin
43. G. Jasny (Y-12)
44. H. F. Johnson
45. W. H. Jordan
46. S. H. Jury
47. K. K. Kennedy (IDO)
48. B. B. Klima
49. E. Lamb
50. D. M. Lang
51. S. Lawroski (ANL)
52. R. E. Leuze
53. W. H. Lewis
54. J. A. Lieberman (AEC Washington)
55. R. B. Lindauer
56. A. P. Litman
57. J. T. Long
58. B. Manowitz (BNL)
59. J. L. Matherne
60. J. A. McBride (ICPP)
61. J. P. McBride
62. W. T. McDuffee
63. R. A. McGuire (ICPP)
64. R. A. McNees
65. R. P. Milford
66. J. W. Morris (SRP)
67. E. L. Nicholson
68. J. R. Parrott
69. F. S. Patton, Jr. (Y-12)
70. H. Pearlman (AI)
71. R. H. Rainey
72. J. T. Roberts
73. K. L. Rohde (ICPP)
74. C. A. Rohrmann (HAPO)
75. A. D. Ryon
76. W. F. Schaffer, Jr.
77-79. E. M. Shank
80. M. J. Skinner
81. C. M. Slansky (ICPP)
82. S. H. Smiley (ORGDP)
83. J. I. Stevens (ICPP)
84. C. E. Stevenson (ANL, Idaho)
85. K. G. Steyer (General Atomics)
86. E. G. Struxness
87. J. C. Suddath
88. J. A. Swartout
89. F. M. Tench (Y-12)
90. V. R. Thayer (duPont, Wilmington)
91. W. E. Unger
92. J. Vanderryn (AEC ORO)
93. F. M. Warzel (ICPP)
94. C. D. Watson
95-124. M. E. Whatley
125. G. C. Williams
126. R. H. Winget
127. C. E. Winters
128. R. G. Wymer
129-130. Central Research Library
131-134. Laboratory Records
135. Laboratory Records (RC)
136. Document Reference Section
137. Research and Development Division, ORO
138-152. DTIE